



**SAARLAND  
UNIVERSITY**

Department of Neuroanatomy,  
Institute for Anatomy and Cell Biology,  
Faculty of Medicine, Saarland University,  
Homburg / Saar, Germany.

**MOLECULAR AND FUNCTIONAL CHARACTERIZATION  
OF RIBEYE – GCAP2 INTERACTION IN THE  
PHOTORECEPTOR RIBBON SYNAPSE**

A thesis submitted to the Faculty of Medicine in fulfilment of  
the requirements for the degree of

**Doctor of Philosophy (Ph.D.)**

**JAGADEESH KUMAR VENKATESAN  
Germany 2010**

## Declaration

I hereby declare that the Ph.D. thesis entitled “Molecular and functional characterization of RIBEYE-GCAP2 interaction in the photoreceptor ribbon synapse” is a presentation of my original research work. Where other sources of information have been used, they have been acknowledged. No portion of work contained in this thesis has been submitted in support of any application for any other degree or qualification.

Homburg,

16.04.2010

JAGADEESH KUMAR VENKATESAN

Supervisor:

Co-supervisor:

## Acknowledgement

It is a pleasure to convey my gratitude to the contributors to this thesis and all of you in my humble acknowledgment.

In the first place I would like to record my gratitude to Prof. Frank Schmitz for his supervision, advice, and guidance from the very early stage of this research as well as giving me extraordinary experiences through out the work. Above all and the most needed, he provided me constant encouragement and support in various ways. His passions in science, which exceptionally inspire and enrich my growth as a student and a researcher.

I would also like to take this opportunity to thank Prof. Jens Rettig and Prof. Dieter Bruns for stimulating scientific discussions and inspiring atmosphere in the “Synapse club” seminar.

I would like to thank Dr. Karin Schwarz for her constant support and suggestion during my Ph.D thesis, I would like to thank Dr. Venkat Giri Magupalli, Dr. Kannan Alpadi, Dr. Josif Mirceski, Sivaraman Natarajan for their advice and their willingness to share their bright thoughts with me, which were very fruitful for shaping up my ideas and research.

I convey my special thanks to Silke Wahl and Anne Schuster for proof reading the “Zusammenfassung” of this thesis. I like to thank Shakil Ahmed, Rashmi Katiyar and Rizwana Anjum for creating pleasant and friendliest environment in the lab.

I would like to express my thanks to my colleagues and collaborators, who are shared the authorship in my publication: Dr. Sabine I. Mayer and Prof. Ching-Hwa Sung.

Many thanks to Sylvia Brundaler for her help in the scientific as well as personal life. Many thanks to Gerlinde Kühnreich, Gabi Kiefer, Franziska Markwart, Anne Rupp, Tamara Paul and Jennifer Neumann for their excellent technical assistance.

I would like to thank Dr. Lavanya Kannan and Dhanasekaran for their constructive comments on my thesis.

I would like to thank Nagaraj, Balachandar, Raspudin, P.S.Suresh Kumar, Jayachandran and Vasanth for the happiest moments in Germany.

I would also like to thank my parents Venkatesan Govindaswamy and Usha Venkatesan for creating an environment in which following this path seemed so natural. I thank my brother Yogesh Kumar Venkatesan and my sister Padmini Venkatesan for being supportive and caring.

The financial support from Sonderforschungsbereichs (SFB 530) and University of Saarland is gratefully acknowledged.

**Dedicated to my parents & my friends**

## SUMMARY

Ribbon synapses are tonically active, high-performance synapses found in the retina and inner ear. Morphologically, ribbon synapses are characterized by the presence of large electron-dense presynaptic specializations in the active zone, the synaptic ribbons. The synaptic ribbon is of particular importance for the physiology of ribbon synapses. But how the synaptic ribbon orchestrates ultra-fast synaptic transmission in ribbon synapses is still largely unknown. RIBEYE was identified by our group as a novel and major protein component of synaptic ribbons (Schmitz *et al.*, 2000). RIBEYE consists of a unique aminoterminal A-domain and a carboxy terminal B-domain which is identical to the protein CtBP2. RIBEYE(B)-domain consists of a NADH binding subdomain (NBD) and substrate-binding subdomain (SBD). SBD and NBD are connected by two flexible hinge regions, hinge 1 and hinge 2. From the identification and characterization of novel interaction partners of RIBEYE, we expect a better understanding of RIBEYE functions at ribbon synapse.

In my this work, I identified GCAP2 as a RIBEYE-interacting protein at photoreceptor ribbon synapses using various independent approaches. The guanylate cyclase activating protein 2 (GCAP2) is a recoverin-like neuronal  $\text{Ca}^{2+}$ -sensor protein highly expressed in photoreceptors. Three members of the GCAP family (GCAP1, 2 and 3) are known in the mammalian retina. GCAP2 contains four EF-hands from which the first EF-hand is non-functional and an aminoterminal myristoylation signal. GCAP2 is well known to modulate the activity of photoreceptor guanylate cyclases in a  $\text{Ca}^{2+}$ -dependent manner in photoreceptor outer segments. But GCAPs are not restricted to outer and inner segments but are also present in the presynaptic terminals of photoreceptors. In immunolabelling analyses of the bovine retina with GCAP2 antibodies, I showed the presence of GCAP2 in the presynaptic terminals at the ribbon sites as well as close to the synaptic ribbon. The significance of GCAP2 in the presynaptic terminals was initially unknown.

The GCAP2 prey clone that I obtained by the YTH screening with RIBEYE(B) as bait coded for the two carboxyterminal EF-hands (EF-hands 3 and 4) and the carboxyterminal region (CTR) of GCAP2. In the YTH system, I showed that the C-terminal region of GCAP2 is responsible for the interaction with hinge 2 region of RIBEYE. I corroborated the GCAP2-RIBEYE interaction using various

independent approaches. In bacterial GST pull-down assays, GCAP2 directly interacts with RIBEYE(B)-domain. In order to prove the GCAP2-RIBEYE interaction *in vivo*, I co-immunoprecipitated RIBEYE and GCAP2 from the bovine retina. Since RIBEYE is exclusively present at the synaptic ribbons in the mature retina, the co-immunoprecipitation experiments suggested that GCAP2 may be a component of synaptic ribbons. This hypothesis is further supported by biochemical assays, high resolution confocal microscopy and Proximity-Ligation Assays.

The hypothesis that hinge 2 region of RIBEYE(B) represents the core docking region for GCAP2 is further supported by point mutants of the hinge 2 region that completely abolished RIBEYE-GCAP2 interaction. Binding of NAD(H) to RIBEYE promotes RIBEYE/GCAP2 interaction. We suggest that binding of GCAP2 to the hinge 2 region requires the NAD(H)-induced, closed conformation of RIBEYE(B). The formation of the NAD(H)-induced closed conformation requires considerable structural rearrangements in the SBD and movement of both SBDa and SBDb. Based on the analyses of RIBEYE mutants we propose that an enhanced structural flexibility of the SBD in RE(B)C899S favors a conformation of the flexible hinge 2 region that is able to bind GCAP2 similar to the NAD(H)-bound conformation. Further investigations will be necessary to understand the complex regulation of GCAP2-RIBEYE interaction and how it is mediated by structural changes in the protein.

Synaptic ribbons are known to disassemble via spherical disassembly intermediates in response to illumination in the mouse retina when intracellular  $\text{Ca}^{2+}$  is low. Interestingly, photoreceptor terminals that were infected with GCAP2-EGFP virus typically displayed a loss of synaptic ribbons as analyzed by co-immunolabeling with anti-RIBEYE and at the electron microscopic level. GCAP2 overexpression in the synapse works similar on ribbon dynamics as chelating  $\text{Ca}^{2+}$  inducing a reduction in the number of synaptic ribbons. Therefore GCAP2 was ideal candidate to mediate these  $\text{Ca}^{2+}$ -dependent changes of synaptic ribbons.

Interesting, GCAP2 knockout mice have a disturbance in synaptic transmission as measured by reduced b-waves in ERG analyses. The above results will help to understand i) which synaptic mechanisms are targeted by RIBEYE-GCAP2 interaction, ii) what are the GCAP2 effector proteins, iii) how the GCAP2-effector interaction is affected by intracellular  $\text{Ca}^{2+}$  concentrations iv) how the recruitment of NADH to RIBEYE is regulated.

## ZUSAMMENFASSUNG

Ribbonsynapsen sind tonisch aktive Hochleistungssynapsen in der Retina und im Innenohr. Morphologisch sind Ribbonsynapsen durch die Anwesenheit von großen elektronendichten Strukturspezialisierungen in der aktiven Zone, den sogenannten Synaptic Ribbons, gekennzeichnet. Der Synaptic Ribbon ist von besonderer Bedeutung für die Physiologie der Ribbonsynapse. Aber wie genau der Synaptic Ribbon auf molekularer Ebene arbeitet, ist noch unbekannt. Das Protein RIBEYE wurde von unserer Gruppe als ein Hauptprotein der Synaptic Ribbons identifiziert (Schmitz et al., 2000). RIBEYE besteht aus einer aminoterminalen A-Domäne und einer carboxyterminalen B-Domäne, die identisch mit dem Protein CtBP2 ist. Die B-Domäne lässt sich wiederum weiter untergliedern in eine NAD(H)-bindende Subdomäne (NBD) sowie in die Substratbindungsdomäne (SBD). NBD und SBD sind durch zwei flexible Scharnierregionen, Scharnier 1 und Scharnier 2, miteinander verbunden. Von der Identifizierung und Charakterisierung von neuen Interaktionspartnern von RIBEYE erwarten wir ein besseres Verständnis vom Aufbau und der Rolle der Synaptic Ribbons in der Ribbonsynapse.

In meiner Dissertationsarbeit, identifizierte ich das Protein Guanylatcyclase-aktivierende Protein 2 (GCAP2) als ein RIBEYE-interagierendes Protein in der Photorezeptorsynapse. GCAP2 ist ein Recoverin-verwandtes  $\text{Ca}^{2+}$ -Sensorprotein, das in Photorezeptoren stark exprimiert wird. Drei Proteine aus der GCAP Familie sind bei Säugern bekannt (GCAP1, 2 und 3). GCAP2 enthält 4 EF-Hände, von denen die erste nicht-funktionell ist. GCAPs enthalten ein aminoterminales Myristoylierungssignal. Von GCAP2 ist bekannt, dass es in den Außensegmenten der Photorezeptoren auf eine  $\text{Ca}^{2+}$ -abhängige Weise die Aktivität membranständiger Guanylatcyclasen reguliert. GCAPs sind aber nicht nur auf das Außensegment beschränkt, sondern finden sich auch in der präsynaptischen Terminale von Photorezeptoren. In Immunfluoreszenzanalysen zeigte ich die Anwesenheit von GCAP2. Dort ko-lokalisiert GCAP2 mit RIBEYE und findet sich auch in der unmittelbaren Nachbarschaft von Synaptic Ribbons. Die funktionelle Bedeutung von GCAP2 in den präsynaptischen Terminalen war vor Beginn meiner Dissertationsarbeit noch komplett unbekannt.

In einem Hefe-Zwei-Hybridscreen (YTH) „fischte“ ich unter Verwendung von RIBEYE(B) als Köderprotein GCAP2 als potentiellen Interaktionspartner von RIBEYE. Der GCAP2 Beuteklon kodierte dabei für die beiden carboxyterminalen EF-Hände sowie den Carboxyterminus von GCAP2 (CTR). Im YTH System zeigte ich, dass die CTR Region von GCAP2 mit der Scharnierregion 2 von RIBEYE(B) interagiert. Diese Hefebefunde wurden mit verschiedenen anderen unabhängigen Untersuchungsmethoden weiter abgesichert und bestätigt. Unter Verwendung von bakteriell exprimierten und gereinigten Fusionsproteinen konnte ich zeigen, dass RIBEYE(B) und GCAP2 auch in-vitro interagieren. Um die Bedeutung dieser Interaktion auch in-situ zu zeigen, stellte ich Co-Immunopräzipitationsuntersuchungen an. Ich konnte RIBEYE mit GCAP2 ko-präzipitieren (und umgekehrt), was für die physiologische Relevanz der gefundenen Interaktion spricht. Da RIBEYE in der Retina praktisch ausschließlich an den Synaptic Ribbons vorhanden ist, sind diese Ko-Immunpräzipitationsdaten ein starker Hinweis darauf, dass GCAP2 eine Komponente der Synaptic Ribbons darstellt. Diese Hypothese wird weiter durch biochemische assays, hochauflösende konfokale Laserscanning-Untersuchungen sowie durch Proximity-Ligation-Assays unterstützt.

Die Scharnierregion 2 stellt die Hauptbindungsstelle für GCAP2 dar, was ich durch die Analyse entsprechender Punktmutanten weiter bestätigen konnte, die die Interaktion mit GCAP2 komplett unterbanden. Aufgrund Struktur-Funktions-Untersuchungen schlage ich vor, dass die Bindung von GCAP2 an die hochflexible Scharnierregion eine geschlossene Konformation der B-Domäne von RIBEYE benötigt. Die Bildung der NAD(H)-induzierten geschlossenen Konformation von RIBEYE erfordert umfassende Umstrukturierungen auch in der SBD sowie eine Rotation der SBD relativ zur NBD. Basierend auf der Analyse von RIBEYE Punktmutanten schlage ich vor, dass die erleichterte strukturelle Flexibilität einzelner RIBEYE-Punktmutanten (z.B. RIBEYEC667S und RIBEYE(C899S)) eine Konformation der Scharnierregion 2 erleichtert, die für die Bindung von GCAP2 benötigt wird. Weitere zukünftige Untersuchungen sind notwendig, um zu verstehen, wie diese Interaktion in-situ reguliert wird.

Synaptic Ribbons sind keine statischen Strukturen, sondern können sich in Abhängigkeit externer und interner Faktoren vergrößern oder verkleinern. Synaptic Ribbons können sich als Antwort auf verringertes intrazelluläres  $\text{Ca}^{2+}$  über sphärische Zwischenstufen (synaptic spheres) verkleinern. Interessanterweise konnten wir zeigen, dass die Infektion von Photorezeptoren mit GCAP2 ebenfalls zu einer Reduktion der Zahl der Synaptic Ribbons führen, so dass GCAP2 ein wichtiger Mediator dieser  $\text{Ca}^{2+}$ -abhängigen Plastizität der Synaptic Ribbons sein könnte.

Interessanterweise zeigen GCAP2 Knockout-Mäuse eine Störung in der synaptischen Transmission, die sich im ERG in einer Reduktion der b-Welle äussert. Diese Störung der synaptischen Transmission in den GCAP2 Knockout-Mäusen könnte auf eine gestörte Funktion der Synaptic Ribbons zurück zu führen sein. Die oben beschriebenen Daten werden helfen, weitere wichtige Fragestellungen zu beantworten: 1.) welche synaptische Prozesse werden durch die RIBEYE/GCAP2 Interaktion targetiert; 2.) was sind die GCAP2-Effektorproteine in der Synapse; 3.) Welche Rolle spielt  $\text{Ca}^{2+}$  bei der RIBEYE/GCAP2 Interaktion; 4.) wie wird *in-situ* die Bindung von GCAP2 an RIBEYE vermittelt?

## CONTENTS

<b>1.</b>	<b>INTRODUCTION</b>	
1.1.	Structure and function of retina	17
1.2.	Ribbon synapses of retina	19
1.3.	Synaptic vesicle cycle at ribbon synapses	21
1.4.	RIBEYE, the major component of synaptic ribbon	22
1.4.1.	The Domain structure of RIBEYE	22
1.4.2.	The structural model of RIBEYE (B) – domain	24
1.4.2.1.	Substrate binding domain of RIBEYE (B)	25
1.4.2.2.	NADH/NAD <sup>+</sup> binding domain of RIBEYE (B)	25
1.4.3.	The proposed functional role of RIBEYE in ribbon synapses	26
1.5.	GCAP2 - a photoreceptor enriched protein	27
1.6.	Mechanisms of GCAPs	28
1.7.	GCAP2 in visual cascade	29
1.8.	Working hypothesis	31
<b>2.</b>	<b>MATERIALS AND METHODS</b>	
2.1.	Bacterial strains	33
2.2.	Yeast strains	33
2.3.	Vectors	34
2.4.	Oligonucleotides	36
2.5.	Plasmid constructs	38
2.6.	Antibodies used for western blotting	45
2.7.	Antibodies used for immunolabeling	45
2.8.	Enzyme, proteins and molecular weight standards	46
2.9.	Chemicals	46
2.10.	Buffers and Media	47
2.11.	Instruments	51

2.12. Polymerase chain reaction (PCR)	53
2.13. Agarose gel electrophoresis	54
2.14. Agarose gel extraction	54
2.15. Restriction digest and ligations	54
2.16. Precipitation of ligation mixtures	55
2.17. Determination of DNA concentration	55
2.18. Bacterial Transformation	56
2.18.1. Preparation of competent bacterial cells	56
2.18.2. Transformation of electrocompetent bacteria <i>E.coli</i> DH10B	56
2.19. Isolation of plasmid DNA	56
2.19.1. Mini preparation	56
2.19.2. Maxi preparation	57
2.19.3. Purification of plasmid DNA for sequencing	57
2.20. Yeast Two- hybrid methods	57
2.20.1. Yeast cell transformation	58
2.20.1.1. Preparation of electro-competent yeast	58
2.20.1.2. Electroporation	58
2.20.2. Yeast mating	59
2.20.3. $\beta$ -Galactosidase assay	59
2.20.3.1. Colony lift filter assay	59
2.21. Site directed mutagenesis	60
2.22. Preparation of recombinant protein	61
2.22.1. Protein expression	61
2.22.2. Purification and elution of fusion proteins	61
2.22.3. Measurement of protein concentration	63

2.23. SDS-PAGE	63
2.24. Western blotting	63
2.25. GST-Pull down assays	64
2.26. Co-immunoprecipitation from the bovine retina	65
2.27. Purification of synaptic ribbon	66
2.27.1. Purification of photoreceptor synaptic complexes	66
2.27.2. Purification of synaptic ribbons from the OPL fraction	67
2.28. GST pull down assay in the presence of NAD <sup>+</sup> /NADH	68
2.29. Preabsorption for western blot Experiments	68
2.30. Preabsorption for immunofluorescence	68
2.31. Immunolabeling analyses	69
2.32. Double-labeling of cryostat sections of the bovine retina with GCAP2 antibodies and Peanut agglutinin	69
2.33. Generation of recombinant Semliki-Forest Virus	69
2.33.1. Cell Culture	69
2.33.2. Generation of recombinant SFV particles	70
2.33.3. Infection of mouse organotype retinal cultures	70
2.34. Organotypic culture of retinal explants	71
2.35. Whole mount immunostaining of organotypic retinal explants	71
2.36. 3D-reconstruction of immunolabeled structure in retinal explants	72
2.37. In-situ Proximity Ligation Assays (In-Situ PLA)	72

### **3. RESULTS**

3.1. Identification of GCAP2 as a RIBEYE interacting protein	75
3.2. RIBEYE interacts with myristoylation deficient protein full-length GCAP2	77
3.3. Mutations of the CTR of GCAP2 abolish interaction with RIBEYE(B)	77
3.4. GCAP2 does not interact with the SBD and NBD of RIBEYE(B)	78

3.5.	GCAP2 interacts with the flexible region of hinge2 region of RIBEYE(B)	79
3.6.	Point mutants of the hinge2 region of RIBEYE(B) disrupt interaction with GCAP2	80
3.7.	The A-domain of RIBEYE does not prevent GCAP2/RIBEYE(B) interaction	82
3.8.	GCAP2 binds to monomeric RIBEYE(B) and GCAP2 binding is independent upon RIBEYE(B) homodimerization	82
3.9.	GCAP2 interacts with RIBEYE(B) in fusion protein pull-down assays	83
3.10.	Characterization of GCAP2 antibodies	85
3.11.	Immunosignals of GCAP2 in the bovine retina can be blocked by GCAP2-GST preabsorption but not by GST preabsorption	86
3.12.	RIBEYE interacts with GCAP2 but not with GCAP1	86
3.13.	A monoclonal GCAP2 antibody that specific for GCAP2	88
3.14.	RIBEYE and GCAP2 can be co-immunoprecipitated from the bovine retina	88
3.15.	GCAP2 is present in purified synaptic ribbons	90
3.16.	GCAP2 co-localizes with synaptic ribbons in rod photoreceptor ribbon synapses	91
3.17.	GCAP2 is weakly expressed in cone photoreceptor ribbon synapses	92
3.18.	Labelling of presynaptic GCAP2 immunosignals can be blocked by pre-absorption with GCAP2-GST but not by GST	94
3.19.	RIBEYE and GCAP2 are localized very close to each other in photoreceptor synapses as judges by in-situ Proximity Ligation Assays	95
3.20.	Characterization of RIBEYE(B)/GCAP2 binding	97
3.21.	Mutations in SBD of RIEYE influence the binding of GCAP2 to RIBEYE(B)	99

3.22.	RIBEYE(B)/GCAP2 interaction is NAD(H)-dependent	100
3.23.	Low concentrations of NAD(H) promote RIBEYE/GCAP2 interaction	100
3.24.	NAD(H)- binding deficient RIBEYE(B)G730A mutant	102
3.25.	Viral overexpression of GCAP2 in presynaptic photoreceptor terminals promotes disassembly of photoreceptor synaptic ribbon	101
<b>4.</b>	<b>DISCUSSION</b>	
4.1.	RIBEYE-GCAP2 interaction requires structural rearrangements of RIBEYE(B)-domain.	106
4.2.	GCAP2, a candidate to mediate Ca <sup>2+</sup> and illumination dependent synaptic ribbon dynamics	108
<b>5.</b>	<b>REFERENCES</b>	
<b>6.</b>	<b>LIST OF FIGURES</b>	
<b>7.</b>	<b>ABBREVIATIONS</b>	
<b>8.</b>	<b>CURRICULUM VITAE</b>	

**CHAPTER 1**

---

**INTRODUCTION**

Vision is a highly complex task that involves several steps of parallel information processing in various areas of the central nervous system. The eye, a remarkable photo-sensor, can detect a single photon and transmit its signal to the higher brain center. Complex processing in the different classes of retinal neurons (photoreceptors, bipolar cells, horizontal cells, amacrine cells and ganglion cells) are the cellular substrates for visual signal processing. Conventional neurons encode information by changes in the rate of action potentials; this limits the amount of information transfer. However, sensory neurons such as photoreceptors in the retina and hair cells in the cochlea transmit light and sound signals, over a dynamic range of several orders of magnitude in intensity by graded changes in transmitter release. Graded synaptic output requires the release of several hundreds to several thousands of synaptic vesicles per second (for review, see Parsons and Sterling, 2003; Sterling and Matthews, 2005). To accomplish this high level of performance, the sensory neurons of the eye and cochlea maintain large pools of fast releasable synaptic vesicles and are equipped with a special type of chemical synapse, the ribbon synapse (for review, see Parsons and Sterling, 2003; Sterling and Matthews, 2005).

### **1. 1. Structure and function of retina**

The eye is a fluid-filled sphere enclosed by three layers of tissue. The outer layer is the sclera and this opaque layer is transformed into the cornea, a specialized transparent tissue that permits light rays to enter the eye. The middle layer of tissue includes three distinct but continuous structures: the iris, the ciliary body, and the choroid. The innermost layer of the eye, the retina, contains neurons that are sensitive to light and are capable of transmitting visual signals to higher brain centre via optic nerve. Despite its peripheral location, the retina or neural portion of the eye is actually part of the central nervous system (for review, see Purves *et al.*, 2001).

Although it has the same types of functional elements and neurotransmitters found in other parts of the central nervous system, the retina comprises only a few classes of neurons, and these are arranged in a manner that has been less difficult to unravel than the circuits in other areas of the brain. There are five main types of neurons in the retina: photoreceptors, bipolar cells, ganglion cells, horizontal cells, and amacrine cells. The cell bodies and processes of these neurons are stacked in five alternating layers, with the cell bodies located in the inner nuclear, outer nuclear, and ganglion

cell layers, and the processes and synaptic contacts located in the inner plexiform and outer plexiform layers. A direct three-neuron chain—photoreceptor cell to bipolar cell to ganglion cell—is the major route of information flow from photoreceptors to the optic nerve (for review, see Purves *et al.*, 2001).

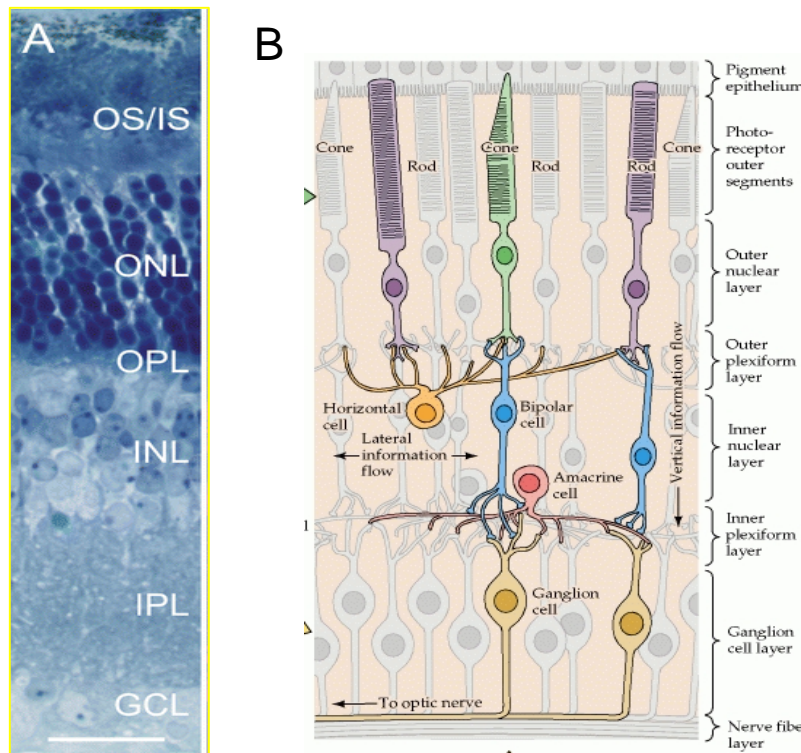


**Figure 1. Ribbon synapses of the mammalian retina**

**A.** Toluidine blue-stained vertical cryostat section of a mammalian retina showing the various retinal layers (*OS/IS* outer and inner segments of the rod and cone photoreceptors, *ONL* outer nuclear layer containing the somata of the photoreceptors, *OPL* outer plexiform layer or first synaptic region, *INL* inner nuclear layer containing the somata of the second order neurons, i.e. horizontal, bipolar and amacrine cells, *IPL* inner plexiform layer or second synaptic region, *GCL* ganglion cell layer containing the somata of the ganglion cells and of displaced amacrine cells) (Tom Dieck *et al.*, 2006). **(B)** Diagram of the basic circuitry of the retina (obtained from NCBI). A three-neuron chain—photoreceptor, bipolar cell, and ganglion cell—provides the most direct route for transmitting visual information to the brain. Horizontal cells and amacrine cells mediate lateral interactions in the outer and inner plexiform layers, respectively.

There are two types of light-sensitive elements in the retina: rods and cones. Both types of photoreceptors have an outer segment that is composed of membranous disks that contain photo-pigment and lies adjacent to the pigment epithelial layer and an inner segment that connects to the soma with the cell nucleus. The cell body gives rise to synaptic terminals that contact bipolar and horizontal cells. Absorption of light by the photo-pigment in the outer segment of the photoreceptors initiates a cascade of events that changes the membrane potential of the receptor, and therefore the amount of neurotransmitter released by the photoreceptor synapses on to the cells they contact. The synapses between photoreceptor terminals and bipolar cells (and horizontal cells) occur in the outer plexiform layer. More specifically, the cell bodies of photoreceptors make up the outer nuclear layer, whereas the cell bodies of bipolar cells lie in the inner nuclear layer. The axonal processes of bipolar cells make synaptic contacts in turn on the dendritic processes of ganglion cells and amacrine cells in the inner plexiform layer. The much larger axons of the ganglion cells form the optic nerve and carry the information about retinal stimulation to lateral geniculate nucleus of thalamus (for review, see Purves *et al.*, 2001). The other two types of neurons in the retina, horizontal cells and amacrine cells, have their cell bodies in the inner nuclear layer and are primarily responsible for lateral interactions within the retina. These lateral interactions between receptors, horizontal cells, and bipolar cells in the outer plexiform layer are mostly responsible for the visual system's sensitivity to luminance contrast over a wide range of light intensities (for review, see Purves *et al.*, 2001).

## **1.2. Ribbon synapse of retina**

Ribbon synapses of the vertebrate retina are unique chemical synapses characterized by pre-synaptic specializations, the synaptic ribbons. Synaptic ribbons are sheet-like organelles with a lamellar organization (Dowling, 1987; Sterling, 1998; Schmitz, 2009). The photoreceptor ribbon is a plate like, ~ 30nm thick structure, which extends perpendicular to the plasma membrane. The ribbon juts ~200nm into the cytoplasm, varies in length from 200-1000nm. Photoreceptor ribbons are usually longer than bipolar cells ribbons. The ribbon anchors along its base to an electron-dense structure (arciform density) that in turn anchors to the pre-synaptic membrane.

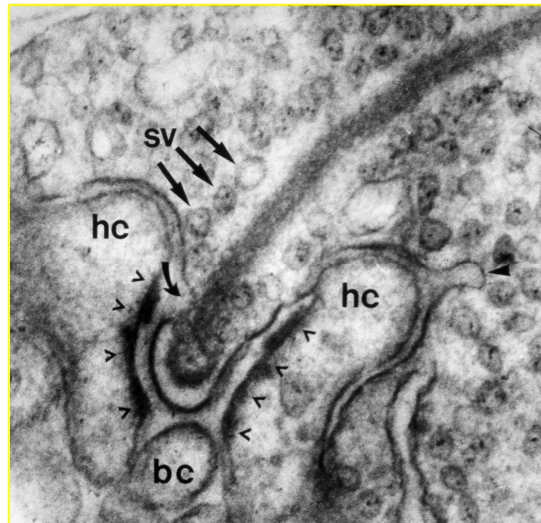


**Figure 2. Transmission electron micrograph of the photoreceptor ribbon synapse**

Abbreviations: sv, synaptic vesicle; bc, postsynaptic dendrites of bipolar cells; hc, postsynaptic dendrites of horizontal cells; black arrows-synaptic vesicle; bold arrow head- endocytosis; arrow head- postsynaptic density (Schmitz, 2009).

Physiologically ribbon synapses are characterized by a high rate of tonic neurotransmitter release mediated by continuous synaptic vesicle exocytosis (Dowling, 1987; Sterling, 1998). It is generally thought that ribbon synapses are specialized for rapid supply of synaptic vesicles for release and that this is achieved by fast delivery of synaptic vesicles to the active zone on the ribbon, analogous to a conveyor belt (for review, see Sterling and Matthews, 2005; tom Dieck *et al.*, 2006). The ribbon's surface is studded with small particles (~5nm diameter) to which synaptic vesicles tether via fine filaments (~5nm thick and ~40nm long). Usually there are several filaments per vesicle (Usukura *et al.*, 1987). Vesicles tethered along the base of the ribbon directly contact the presynaptic membrane and thus are considered 'docked'. Detailed studies of the distribution of various presynaptic proteins in ribbon synapses demonstrated that they generally contain the same proteins as conventional synapses (for review, see Sterling and Matthews, 2005; Schmitz, 2009). Only minor differences were observed, such as the use of syntaxin 3 instead of syntaxin 1 for fusion and of L-type  $Ca^{2+}$  channels instead of N-, P/Q-, or R-type channels for  $Ca^{2+}$  influx. Furthermore, rabphilin and synapsins are absent from ribbon synapses in some but not all species (for review, see Sterling and Mathews, 2005).

### 1.3. Synaptic vesicle cycle at ribbon synapses

Exocytosis at the bipolar ribbon synapse has been observed directly. The synaptic vesicles labelled by the dye FM1-43 are seen to pause at the membrane and then, upon opening of  $\text{Ca}^{2+}$  channels, all the dye released promptly within milliseconds. This process can be observed by total internal reflection microscopy (Zenisek *et al.*, 2000). The de-staining is consistent with full fusion (Zenisek *et al.*, 2000). The bipolar cell active zone can release neurotransmitter continuously for hundreds of milliseconds during strong stimulation. This release exhibits two kinetically distinct components: a small fast pool (20% of the total vesicle pool) is released in 1 ms, and a large sustained pool (80%) is released over several hundred milliseconds (for review, see Sterling and Matthews, 2005). The fast pool matches the number of vesicles docked at the base of the ribbon, and the sustained pool matches the number of vesicles tethered to the ribbon in higher rows, more distant from the plasma membrane (for review, see Sterling and Matthews, 2005). The neat correspondence between the pool of tethered vesicles and the pool for sustained release in both rods and bipolar cells suggests that the ribbon might serve as a platform where vesicles can be primed to allow sustained release (for review, see Sterling and Matthews, 2005)

The large amount of exocytosis during sustained vesicle exocytosis requires equally high-capacity endocytosis to retrieve the added membrane. In cone photoreceptors, fused membrane is directly recycled into small synaptic vesicles, without intermediate pooling into endosomes (Rea *et al.*, 2004). The recycled vesicles are mobile and, diffusing as fast as similarly sized microspheres and rapidly replenish the releasable pool (Rea *et al.*, 2004). Surprisingly, bipolar cells rely on a different mechanism for rapid retrieval, in which membrane is endocytosed in large bites that only later give rise to recycled synaptic vesicles (Paillart *et al.*, 2003). Unlike cones, where newly recycled vesicles rapidly appear in the pool tethered to ribbons, recycled vesicles make up only 10% of the vesicles on bipolar cell ribbons, even after 10 min of activity (Rea *et al.*, 2004). Thus, the bipolar cell relies on its large reserve of synaptic vesicles to replenish the releasable pool, whereas cone photoreceptors evidently have no large reserve pool and rely instead on rapid recycling. In this regard, the cone ribbon synapse resembles the conventional amacrine cell synapse,

where extensive labelling of recycled synaptic vesicles was observed, without significant labelling in larger endosomes (Paillart *et al.*, 2003).

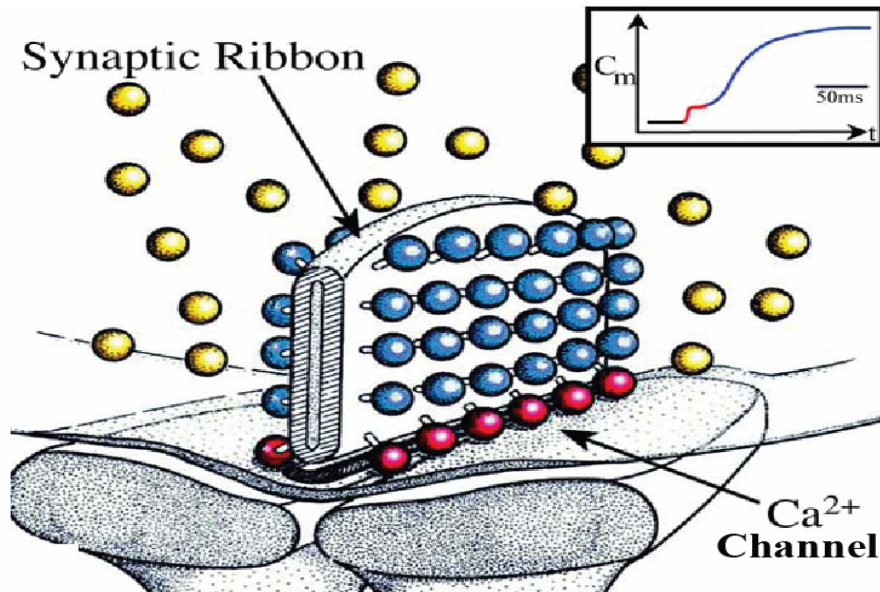


**Figure 3. 3D representation of synaptic ribbons** (Von Gersdorff *et al.*, 2001). Vesicles (yellow color) are reserve, vesicles (blue color) bound to synaptic ribbons are considered as tethered, vesicles tethered along the base of synaptic ribbon (red vesicles) are considered as docked (Sterling *et al.*, 2005). A typical bipolar contains 5-7 calcium channels in the preactive zone.

## 1. 4. RIBEYE- a major component of synaptic ribbon

### 1.4.1. The molecular structure of RIBEYE

The major component of synaptic ribbons from retina was identified as RIBEYE (Schmitz *et al.*, 2000). RIBEYE is composed of unique N-terminal A - domain specific for ribbons, mediates assembly of RIBEYE into large structures, and a B - domain identical with CtBP2, a transcriptional repressor that in turn is related to 2-hydroxyacid dehydrogenases. RIBEYE(B)-domain binds to NADH/NAD with high affinity (Schmitz *et al.*, 2000). The A-domain contains 563 aa residues and B-domain contains 425 aa residues. The A-domain is not significantly homologous to any of the currently described proteins and it contains abundance of serine and proline residues (Schmitz *et al.*, 2000). The B-domain is identical to CtBP2, a nuclear protein and together with CtBP1 constitutes a family of transcriptional co - repressors except to the first 20 amino terminal amino acids. CtBP1 was originally identified as “C terminal binding protein” for the adenovirus E1A protein (Schaeper *et al*, 1995), and CtBP2 was subsequently identified as close structural and functional homolog of

CtBP1(Katsanis *et al.*, 1998). The RIBEYE(A)-domain is not present in *D. melanogaster*, *C. elegans* and other lower vertebrates and invertebrates. This is supporting the notion that RIBEYE are an evolutionary innovation of vertebrates (Schmitz *et al.*, 2000).

The teleosts fish, *Fugu* and zebra fish have two *ribeye* genes, *ribeye a* and *RIBEYE(B)*. Depletion of RIBEYE in zebra fish (by the use of morpholino antisense oligonucleotides) has been shown to result in shorter synaptic ribbons (Wan *et al.*, 2005). Fish deficient in *ribeye a* lacks an optokinetic response. It has shorter synaptic ribbons in photoreceptors and fewer synaptic ribbons in bipolar cells (Wan *et al.*, 2005).

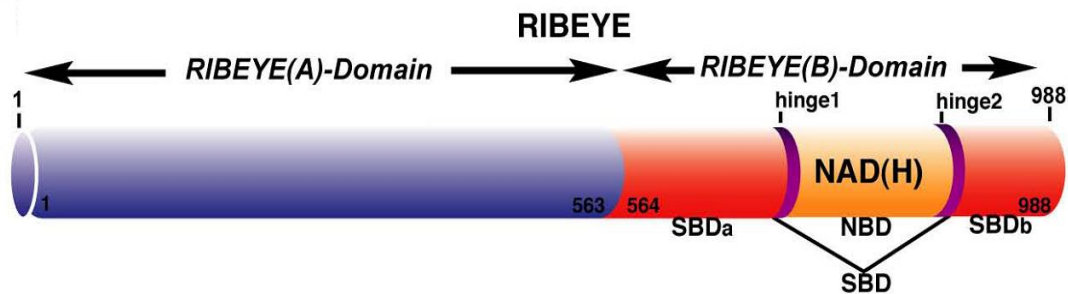


**Figure 4. Schematic domain structure of RIBEYE**

RIBEYE contains of a large amino-terminal A-domain and a carboxyterminal B-domain. The B-domain of RIBEYE contains the NADH-binding subdomain (NBD, depicted in yellow) and the substrate-binding subdomain (SBD, denoted in red).The A domain comprises of 563 aa and B domain comprises of 425 aa (adapted from Magupalli *et al.*, 2008).

The design of RIBEYE as a fusion protein of a novel domain with a pre-existing transcription factor suggests an intriguing evolutionary history, an accidental origin of RIBEYE in the vertebrate lineage by serendipitous addition of an exon encoding the A-domain to the pre-existing CtBP2 gene. However, further analyses indicate that the evolutionary history of RIBEYE may be even more complex and give a clue to the possible function of the B - domain (Schmitz *et al.*, 2000). CtBP1 and CtBP2 themselves are not novel in terms of sequence but are significantly homologous to enzymes of the family of  $\text{NAD}^+$ -dependent 2-hydroxyacid dehydrogenases (Schmitz *et al.*, 2000). In the nucleus the CtBP family protein plays a role in transcription repression and in the cytosol, they perform diverse functions associated with membrane trafficking, central nervous system synapses and in regulation of the microtubule cytoskeleton (for review, see Chinnadurai, 2003). Several studies indicated that RIBEYE is the major component of synaptic ribbons

(Schmitz *et al.*, 2000; Zenisek *et al.*, 2002; Wan *et al.*, 2005; Magupalli *et al.*, 2008; for review see Schmitz, 2009). Thus RIBEYE can be expected to exert a major influence on the function of synaptic ribbons.

#### 1.4.2. The structural model of RIBEYE(B) - domain

The RIBEYE(B)-domain contains two globular subdomains, the NADH-binding subdomain (NBD) and substrate-binding subdomain (SBD). The dinucleotide-binding domain with an evolutionarily conserved structure forms the core homology domain among these proteins (for review, see Chinnadurai, 2003). The NAD(H)-binding fold consists of two units of a mononucleotide-binding motif termed the Rossmann fold. The Rossmann fold is a conserved structural domain composed of three parallel  $\beta$  strands interconnected by  $\alpha$  helices, forming a parallel twisted  $\beta$  sheet flanked by  $\alpha$  helices with a  $\beta\alpha\beta\alpha\beta$  topology. In the dehydrogenase domain, each repeated  $\beta\alpha\beta\alpha\beta$  structural element binds a mononucleotide component of the NAD(H) coenzyme (for review, see Chinnadurai, 2003). Like other dehydrogenases, these structures demonstrate that CtBPs, CtBP1, CtBP2 and RIBEYE(B)-domain (Kumar *et al.*, 2002; Nardini *et al.*, 2003., Magupalli *et al.*, 2008) homodimerize through the dinucleotide-binding domain, forming an extensive, largely hydrophobic dimerization interface (for review, see Chinnadurai, 2003; Magupalli *et al.*, 2008).

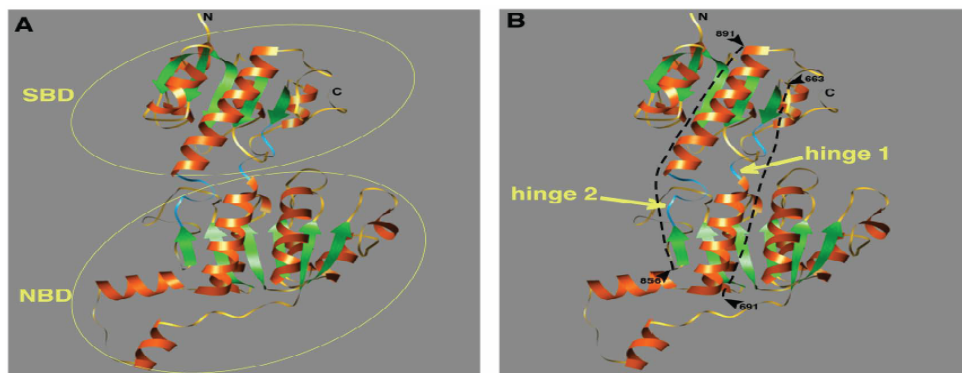


**Figure 5. Predicted RIBEYE(B) domain structure using homology modelling with CtBP1**  
**A,B)** Structure model of the B-domain of RIBEYE based on the crystal structure of tCtBP1 (Kumar *et al.*, 2002; Nardini *et al.*, 2003; see also Magupalli *et al.*, 2008; Alpadi *et al.*, 2008). The structure model covers large parts of the B-domain (RE(B)575-905). The B-domain of RIBEYE consists of a NAD(H)-binding subdomain (NBD) and a substrate-binding subdomain (SBD) which are connected by two flexible hinge regions, hinge 1 and hinge 2 (colored in blue). The dotted lines indicate the extensions of the hinge 1 and hinge 2 constructs tested in the YTH system.

#### **1.4.2.1. Substrate - binding domain of RIBEYE(B)**

In these structures, a deep cleft separates the SBD from the NBD, corresponding to a putative active site and the dinucleotide-binding pocket. For the D-2-hydroxyacid dehydrogenases, catalytic activity apparently proceeds through a “proton shuttle” between a histidine and a carboxylic acid residue (i.e., glutamate or aspartate) with the transfer of hydride ion between the substrate and coenzyme. An arginine residue located within proximity to the active site in 3PGDH interacts with the substrate carboxylic acid during catalysis. These residues are conserved in all D-2-hydroxyacid dehydrogenases (for review, see Chinnadurai, 2003 & 2005). All mammalian CtBP orthologues as well the *Drosophila* CtBP homologue also include these residues (hCtBP1 residues H315, E295, R266; corresponding residues in BARS/CtBP1 include H304, E284, and R255) indicating CtBP might retain oxo-reductase enzymatic activity (for review, see Chinnadurai, 2003 & 2005). Interestingly, most of the residues in the dehydrogenase consensus sequence are conserved in CtBPs and RIBEYE, including in particular the four residues that are involved in binding NAD<sup>+</sup> (GXGXXG-18-D) and the three amino acids that function in catalysis (R-30-E-19-H) (Schmitz *et al.*, 2000). This conservation suggests that RIBEYE and CtBPs may still be partly or completely enzymatically active (Schmitz *et al.*, 2000; Kumar *et al.*, 2002).

#### **1.4.2.2. NADH/NAD<sup>+</sup> - binding domain of RIBEYE(B)**

In addition to a central essential role in metabolism as a carrier of reducing equivalents, the nicotinamide adenine dinucleotide coenzymes (NAD and NADP) play a pivotal role in cellular signalling (for review, see Chinnadurai, 2003 & 2005). They also serve as substrates for covalent protein modifications as well as precursors to the synthesis of intracellular calcium mobilizing second messenger molecules i.e. cyclic - ADP ribose(cADPR) (for review, see Chinnadurai, 2003 & 2005). RIBEYE(B) - domain binds to NADH and NAD<sup>+</sup>(Schmitz *et al.*,2000). Strong and specific binding of <sup>14</sup>C-labeled NAD<sup>+</sup> was also observed. Scatchard analysis uncovered a single class of binding site in RIBEYE/CtBP2 with an affinity of 1.3 μM NAD<sup>+</sup>. <sup>14</sup>C-NAD<sup>+</sup> binding was completely inhibited by a 100-fold excess of unlabeled NAD<sup>+</sup> or by cibacron blue, which serves as a common ligand for NAD<sup>+</sup> binding site in many proteins but was unaffected by serine (Schmitz *et al.*,2000).

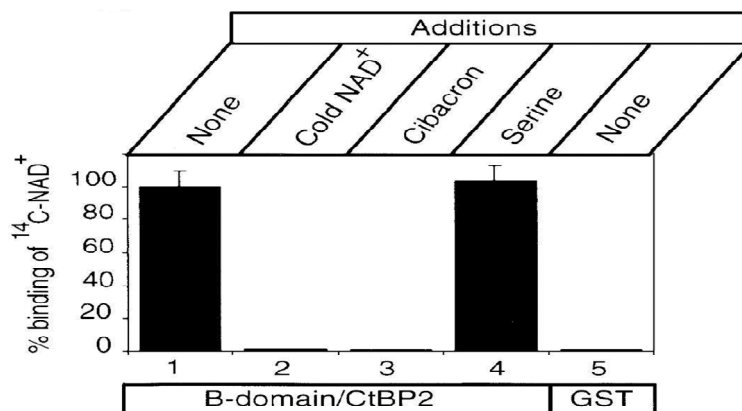


**Figure 6. Binding of NAD<sup>+</sup> to the B Domain of RIBEYE/CtBP2** The Specificity of NAD<sup>+</sup> binding to the B domain of RIBEYE. Binding of 10 μM <sup>14</sup>C-labeled NAD<sup>+</sup> in the absence of competitor (column 1, 100%) is displaced completely by 1 mM cold NAD<sup>+</sup> (column 2) or 1 mM Cibacron blue 3GA, an NAD<sup>+</sup> analog (column 3) but not by 1 mM serine (column 4). Column 5 shows binding to GST alone as background binding (Schmitz *et al.*, 2000).

These results suggest that the homology of the RIBEYE(B) domain/CtBP2 to NAD<sup>+</sup>-dependent 2-hydroxyacid dehydrogenases is functionally important, and that the domain may serve as an enzyme in synaptic vesicle priming on synaptic ribbons and in transcriptional repression (Schmitz *et al.*, 2000).

#### 1.4.3. The proposed functional role of RIBEYE in ribbon synapse

According to the model proposed by Schmitz *et al.*, 2000, the N-terminal A domain is involved in the formation of the synaptic ribbon. RIBEYE alone is not sufficient to organize bar shaped ribbons but requires at least one additional protein component indicated in the model as an inner-core protein. The presence of such a protein component is suggested by the finding of a second unique protein in the biochemically purified ribbon fraction, which has not yet been identified (Schmitz *et al.*, 2000). Recently we have demonstrated that RIBEYE is a scaffolding protein with ideal properties to explain the assembly of synaptic ribbons as well as its ultra-structural dynamics via the modular assembly mechanism (Magupalli *et al.*, 2008).

The RIBEYE(B) domain binds NAD<sup>+</sup> with high affinity indicating that its homology with NAD<sup>+</sup>-dependent dehydrogenases is functionally relevant and it may in fact serve as an enzyme. It is interesting that the CtBP1, a close homolog of CtBP2, was recently also suggested to function in membrane traffic under the name of “BARS” (brefeldin A-ADP ribosylated substrate) (Weigert *et al.*, 1999). CtBP1, as BARS, functioning as a lysophosphatidic acid coenzyme A acyltransferase in membrane fission in the Golgi complex (Weigert *et al.*, 1999). The structural

similarity of CtBPs with NAD<sup>+</sup>-dependent dehydrogenases well known that CtBP is ADP ribosylated in an NAD<sup>+</sup>-dependent reaction in parallel with GAPDH (another NAD<sup>+</sup>-dependent dehydrogenase (Girolama *et al.*, 1995). However, this assimilation also makes it difficult to judge how CtBP1 could function as a coenzyme A-dependent acyltransferases, since there is few similarity between the mechanisms of acyltransferases and dehydrogenases, raising questions about the precise enzymatic role of CtBP1 in Golgi membrane traffic (Schmitz *et al.*, 2000). In large number of organisms CtBPs are transcriptional repressors and it shows that their NAD<sup>+</sup> binding and enzymatic function may be enclose to perform this function (Schmitz *et al.*, 2000). PxDLS motif characterized as a consensus sequence which is the binding sequences for CtBPs in their target proteins . By analogy, Schmitz *et al.*, 2000 suggested on the surface of the ribbons array of B domain of RIBEYE (which is identical with CtBP2) is present. This RIBEYE is intend to interact with a target sequence containing the consensus motif PxDLS of CtBPs. This hypothesis shows that this interaction of synaptic vesicle protein which may contain target sequence and that may be involved in docking and/or translocation of vesicles and unnown enzymatic reaction of the B domain may be involved in priming. Identification of the binding partners for the B domain on the ribbon surface and the role of NAD<sup>+</sup> binding in their function will give valuable insight into how this domain might perform this proposed function (Schmitz *et al.*, 2000). In Recent shown that RIBEYE, the main component of synaptic ribbons, binds to Munc119, the mammalian ortholog of the *C. elegans* protein unc119 (Alpadi *et al.*, 2008). Munc119 in turn binds to CaBP4 which is an important regulator of L-type Ca<sup>2+</sup> channels (Haeseleer and others 2004; Haeseleer 2008). Data provided further evidence for a molecular link between the synaptic ribbons and presynaptic Ca<sup>2+</sup> channels. Ca<sup>2+</sup> - buffering systems in the presynaptic ribbon terminal have been recently reviewed (Thoreson 2007; Zanazzi and Matthews 2009).

### **1.5. GCAP2 - a photoreceptor enriched protein**

The guanylate cyclase activating protein 2 (GCAP2) is a recoverin-like neuronal Ca<sup>2+</sup>-sensor protein highly expressed in photoreceptors (for review, see Koch *et al.*, 2002; Palczewski *et al.*, 2004). Three members of the GCAP family (GCAP1, 2 and 3) are known in the mammalian retina: GCAP 1 and 2 are expressed both in rod and cone photoreceptors whereas GCAP3 is exclusively found in cone

photoreceptors (Imanishi et al., 2002). GCAP2 contains four EF-hands from which the first EF-hand is non-functional. GCAP2 contains an aminoterminal myristoylation signal and is myristoylated *in-situ* (Olshevskaya et al., 1997). GCAP2 is well known to modulate the activity of photoreceptor guanylate cyclases in a  $\text{Ca}^{2+}$ -dependent manner (for review, see Koch et al., 2002). GCAPs are not restricted to outer and inner segments of photoreceptors but are also present in the presynaptic terminals (Otto-Bruc et al., 1997; Duda et al., 2002, Pennesi et al., 2003; Makino et al., 2008). The significance of GCAP2 in the presynaptic terminals is unknown.

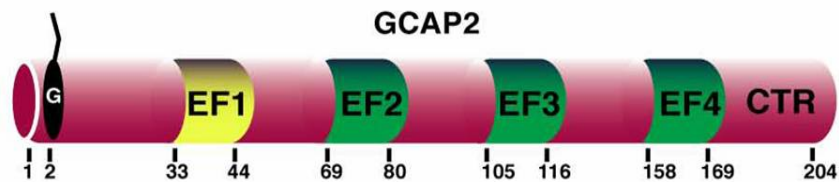


**Figure 7.** The schematic drawing of GCAP2(aa1-204). The 4 EF- hands of GCAP2 are indicated in color. EF-hand 1 (colored in yellow) is non-functional and does not bind  $\text{Ca}^{2+}$ ; EF-hands 2-4 (colored in green) are functional and bind  $\text{Ca}^{2+}$ . Glycine G2 is myristoylated *in-situ*.

### 1.6. Mechanisms of GCAP

The mechanism of modulation of retinal Guanylate cyclases (RetGCs) by GCAPs is now better understood, less is known about the significance of multiple RetGCs and GCAPs. *In vitro*, GCAPs display some preferences toward RetGCs. For example, GCAP1 stimulates RetGC1 more efficiently than RetGC2, while GCAP2 and GCAP3 effectively stimulate both RetGC1 and RetGC2. RetGC1 and GCAP1 are important for cone and rod function in humans. Mutations in the RetGC1 gene have been linked to Leber's congenital amaurosis type I (Perrault et al., 1996) and to autosomal dominant cone rod dystrophy (adCORD)(Kelsell et al., 1998) and defects in the GCAP1 gene have been linked to adCORD (Downes et al., 2001). A naturally occurring null mutation in RetGC1 in chickens, which have cone dominated retinas, leads to the loss of cones and rods. However, disruption of RetGC1 expression in mice leads to the degeneration of cones primarily (Yang et., 1999) indicating that RetGC2 may substitute for the loss of RetGC1 in murine rods. It is not clear why photoreceptors express two GCAP proteins with very similar biochemical behavior. The ratio of GCAP1 to GCAP2 in bovine retinas has been estimated at between 3:1 and 4:1 (OttoBruc et al., 1997) and the GC activity stimulation attributable to GCAP2

has been estimated at about 30%. Based on this data, the question was raised of whether GCAP2 would have a physiological role in phototransduction (OttoBruc et al., 1997). The compartmentalization of GCAP2 differs from that of GCAP1 in rods and cones of retinas from higher species (OttoBruc A et al., 1997). GCAP1 appears to be more abundantly expressed in the cone outer segments of human, monkey and bovine retinas.

### **1.7. GCAP2 in visual cascade**

Visual excitation in retinal photoreceptor cells is mediated by a cascade that leads to the enzymatic hydrolysis of cGMP and the subsequent closure of cGMP-gated channels in the plasma membrane. Recovery of the dark state requires the resynthesis of cGMP, which is catalyzed by particulate (membrane-associated) guanylate cyclases (RetGCs). RetGC activity has long been known to be stimulated with high cooperativity by the decrease in cytosolic  $[Ca^{2+}]$  that follows light exposure (Koch et al., 1998). This cyclase stimulation has been proposed to be the major mechanism by which photoreceptors adjust their sensitivity according to background illumination (Koutalos et al., 1996). The soluble regulators that confer  $Ca^{2+}$ -sensitivity to RetGCs have been cloned and identified as 23kDa  $Ca^{2+}$ -binding proteins from the calmodulin superfamily (Koutalos et al., 1995) the guanylate cyclase-activating proteins (GCAPs). Two isoforms of RetGCs are expressed in mammalian retinas, RetGC1 and RetGC2 (Shyjan et al., 1992). RetGC1 localizes to the outer segments and synaptic terminals of rods and cones, (Liu et al., 1994) whereas the distribution of RetGC2 within photoreceptors is less well known. Three isoforms of mammalian GCAPs, namely GCAP1, GCAP2 and GCAP3 have been isolated (Haeseleer et al., 1999). GCAP1 and GCAP2 have both been localized to photoreceptors in numerous studies, (Howes et al., 1998) although reports of the distribution of GCAPs between rods and cones in different species have been more ambiguous (Howes et al., 1998). In the human, monkey and bovine species, GCAP1 immunoreactivity appears stronger in the cone outer segments, whereas GCAP2 immunostaining is seen in the entire region of rods and cones (Kachi et al., 1999). GCAP3 expression seems to be limited to humans (Haeseleer et al., 1999) and zebrafish (Imanishi et al., 2002) localizing to all cone types in human retinas (Imanishi et al., 2002). Whether individual GCAPs might play distinct roles in phototransduction is not known.

In photoreceptor cells, photoactivation of rhodopsin or cone visual pigment results in a transient decrease in the concentrations of  $\text{Ca}^{2+}$  and cGMP. These receptors and second messengers are linked through a cascade of specific activation/inactivation reactions in phototransduction. The levels of  $\text{Ca}^{2+}$  and cGMP are strictly controlled and interconnected. cGMP is a gating ligand of the plasma membrane cation channels that are permeable to  $\text{Ca}^{2+}$  ions. After cGMP is hydrolyzed, the efflux of  $\text{Ca}^{2+}$  exceeds the influx, resulting in decreased  $[\text{Ca}^{2+}]$  within the cell. The lowering of  $[\text{Ca}^{2+}]$  triggers production of cGMP through activation of a photoreceptor-specific particulate guanylate cyclase (GC).

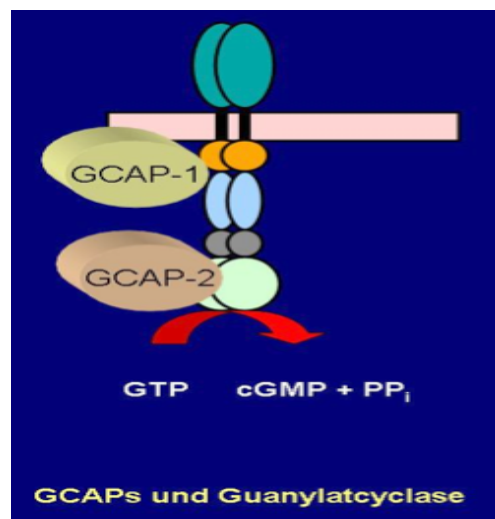


**Figure 8.** Domain structure of Guanylate Cyclase and their interaction with GCAP proteins (image from homepage of Prof.Dr. KW Koch; University of Oldenburg)

The  $\text{Ca}^{2+}$  sensitivity of GC (e.g., the higher activity at low levels of  $[\text{Ca}^{2+}]$ ) is mediated by guanylate cyclase-activating proteins (GCAPs). When  $\text{Ca}^{2+}$  is low, GCAP proteins activate GC activity, when  $\text{Ca}^{2+}$  is high GCAP proteins inactivate GC activity. Light sensitivity of vertebrate photoreceptor cells is controlled by multiple feedback loops that  $\text{Ca}^{2+}$  independent mechanisms (Dizhoor *et al.*, 1996).

### **1.8. Working hypothesis**

In the biological system most of the protein, function with other proteins to build a functional cellular task depending upon certain external stimuli and stage of the cell. Synaptic vesicle cycles are orchestrated by protein-protein interactions in every step of exocytosis and endocytosis. In order to better understand the function of synaptic ribbons at a molecular level I performed a YTH screen using RIBEYE(B) as a bait and obtained the neuronal  $\text{Ca}^{2+}$ - sensor protein GCAP2 as a potential prey. This interaction has been analyzed at the molecular and functional level in the following Ph.D. thesis work.

## **CHAPTER 2**

---

### **MATERIALS AND METHODS**

## 2.1. Bacterial strains

Strain	Genotype	Source & Reference
DH10B	F- <i>mcrA</i> $\Delta(mrr-hsdRMS-mcrBC)$ $\phi 80lacZ\Delta M15$ $\Delta lacX74$ <i>recA1</i> <i>endA1</i> <i>araD139</i> $\Delta(ara, leu)7697$ <i>galU</i> <i>galK</i> $\lambda$ - <i>rpsL</i> <i>nupG</i>	Invitrogen, Grant, S. <i>et al.</i> (1990)
BL21(DE3)	F' <i>ompT</i> <i>hsdS<sub>B</sub></i> ( <i>r<sub>B</sub><sup>-</sup>m<sub>B</sub><sup>-</sup></i> ) <i>gal</i> <i>dcm</i> (DE3)	Invitrogen , Grodberg und Dunn, (1988)

## 2.2. Yeast strains

Strain	Genotype	Source & Reference
AH109	MAT $\alpha$ , <i>trp1-901</i> , <i>leu2-3, 112</i> , <i>ura3-52</i> , <i>his3-200</i> , <i>Gal4</i> $\Delta$ , <i>gal80</i> $\Delta$ , <i>LYS2::GAL1<sub>UAS</sub>-GAL1<sub>TATA</sub>-</i> <i>HIS3</i> , <i>GAL2<sub>UAS</sub>-GAL2<sub>TATA</sub>-ADE2</i> , <i>URA3::MEL1<sub>UAS</sub>-</i> <i>MEL1<sub>TATA</sub>-lacZ</i>	Clontech, James <i>et al.</i> 1996
Y187	MAT $\alpha$ , <i>ura3-52</i> , <i>his3-200</i> , <i>ade2-101</i> , <i>trp1-901</i> , <i>leu2-3, 112</i> , <i>gal4</i> $\Delta$ , <i>met</i> , <i>gal80</i> $\Delta$ , <i>URA3::GAL1<sub>UAS</sub>-GAL1<sub>TATA</sub>-lacZ</i>	Clontech, Harper <i>et al.</i> 1993

### 2.3. Vectors

Vectors	Description	References
pACT2	<p>The pACT2 vector expresses a hybrid protein by a fusion of the GAL4-activation domain (AD), at high levels in yeast host cells from the constitutive ADH1 promoter (<i>P</i>); transcription is terminated at the ADH1 transcription termination signal. It also contains an HA epitope tag and a MCS. The protein is targeted to the yeast nucleus by the nuclear localization sequence from SV40 T-antigen. It is a shuttle vector that replicates autonomously in both <i>E. coli</i> and <i>S. cerevisiae</i> and carries the <i>bla</i> gene, which confers ampicillin resistance in <i>E. coli</i>. It also contains the <i>LEU2</i> nutritional gene that allows yeast auxotrophs to grow on limiting synthetic media.</p>	Clontech Laboratories Inc.
pGBKT7	<p>The pGBKT7 vector expresses proteins fused to GAL4 DNA binding domain (DNA-BD). In yeast, fusion proteins are expressed at high levels from the constitutive <i>ADH1</i> promoter (<i>PADH1</i>); transcription is terminated by the T7 and <i>ADH1</i> transcription termination signals (<i>TT7</i> &amp; <i>ADH1</i>). It also contains the T7 promoter and a c-Myc epitope tag. It is a shuttle vector replicates autonomously in both <i>E. coli</i> and <i>S. cerevisiae</i> from the pUC and 2 μ ori, respectively. It the Kan<sup>r</sup> for selection in <i>E. coli</i> and the <i>TRP1</i> nutritional marker for selection in yeast.</p>	Clontech Laboratories Inc.

pSE1111	The pSE1111 vector expresses proteins fused to GAL4 activation domain. It used as negative control vector (prey vector) for checking auto-activation of prey constructs.	Bai & Elledge, 1996
pSE1112	The pSE1112 vector expresses proteins fused to GAL4 DNA binding domain. It used as negative control vector (bait vector) for checking auto-activation of bait constructs	Bai & Elledge, 1996
pGEX-KG	The pGEX-KG vector contains coding sequence for Glutathione S Transferase (GST), MCS, pBR322 origin, and ampicillin resistance, Ptac is transcription promoter for the expression of the GST or GST Fusions proteins, chemically inducible by IPTG, high-level expression. An internal lac I <sup>q</sup> gene for use in any E. coli host. Very mild elution conditions for release of fusion proteins from the affinity matrix, thus minimizing effects on antigenicity and functional activity. PreScission™, thrombin, or Factor Xa protease recognition sites for cleaving the desired protein from the fusion product.	Basal-vector from Pharmacia and pGEX-KG gifted from T.C.Sudhof lab.
pMAL-C2	The pMAL-C2 vector facilitates the expression and purification of foreign proteins/peptides in Escherichia coli by fusion to maltose-binding protein. It contains E.Coli male gene , Lac I and tac promoter. It has ampicillin resistance gene.	Clontech laboratories Inc.

pSFV1	The pSFV1 eukaryotic expression vector is a novel DNA expression system based on the Semliki Forest virus (SFV) Ashery <i>et al.</i> 1999. It's replicon has a broad host range and a high level of expression efficiency. It offers a proper glycosylation of the recombinant protein. The DNA of interest is cloned into the pSFV1 plasmid vector which serves as a template for <i>in vitro</i> synthesis of recombinant RNA. The recombinant RNA in the cells drives its own replication and capping, results in production of large amounts of heterologous protein in host cells while inhibiting host protein synthesis. The pSFV1 plamid has a ampicillin resistance gene	Invitrogen life technology
-------	---	----------------------------

#### 2.4. Oligonucleotides

Name	Primer No	Sequence	Restriction site
GCAP2aa3-aa204 for	657	TTTTGGATCCTACAGCAGTTC AGCTGGGAG	BamHI
GCAP2aa3-aa204rev	633	TTTTTCTCGAGTCAGAACATG GCACTTTTCC	XhoI
GCAP2aa105-aa204for	677	TTTTTGGATCCTAGGTGGCAG CGACAAGGACCGCAATCGC	BamHI
GCAP2aa105-aa204rev	633	TTTTTCTCGAGTCAGAACATG GCACTTTTCC	XhoI
GCAP2aa118-aa204for	678	TTTTTGGATCCTAGGTGGCAG CCTGGACATCGTGGAGTCC	BamHI
GCAP2aa118-aa204rev	633	TTTTTCTCGAGTCAGAACATG GCACTTTTCC	XhoI
GCAP2aa158-aa204for	679	TTTTTGGATCCTAGGTGGCAG CGATGAAAATGGAGATGGTC AG	BamHI

GCAP2aa158-aa204rev	633	TTTTTCTCGAGTCAGAACATGGC ACTTTTCC	XhoI
GCAP2aa171-aa204for	681	TTTTTGGATCCTAGGTGGCAGCG TTGAAGGT GCCCGTCGT	BamHI
GCAP2aa171-aa204rev	633	TTTTTCTCGAGTCAGAACATGGC ACTTTTCC	XhoI
RE(B)hinge1 for	749	TTTTCCATGGTAGGCGGTAGTGG AATCGCCGTGTGAAC	NcoI
RE(B)hinge1 rev	750	TTTTGGATCCCCGCCGATACAGA TTGAG	BamHI
RE(B)hinge2for	751	TTTTCCATGGTAGGCGGTAGTGC TCCAAATCTCATCTGGCA	NcoI
RE(B)hinge2rev	752	TTTTGGATCCGCGACCTGTGATT GCTCG	BamHI
RE(B)hinge2forT865S	822	TGCACACCACACAGTGGCTGGT ACAGC	
RE(B)hinge2revT865S	823	GCTGTACCAGCCACTGTGTGGTG TGCA	
RE(B)hinge2forW867E	826	CCACACACAGCCGAATACAGCG AACAAG	
RE(B)hinge2revW867E	827	CTTGTTTCGCTGTATTCGGCTGTG TGTGG	
B-DOM for pACT2/pGBKT7	406	TTTTCCATGGTTATCCGCCCCCA GATCATGA	NcoI
B-DOM rev pACT2/pGBKT7	405	TTTTTCTCGAGCTATTGCTCGTTG GGGTGCT	XhoI
NBD-RE(B) for	508	TTTTGAATTCTTATCCCATCTGC TGCAGT	EcoRI
NBD-RE(B) rev	509	TTTTTCTCGAGGCTGTACCAGGCT GTGT	XhoI
Moazed outward for	353	GTTCCATGGAGATCCGCCCCCA GATCAT	NcoI

Moazed outward rev	354	GTTCTCGAGCTATTGCTCGTTGGGGT	XhoI
SBD-RE(B) for	523	AACATCCCATCTGCTGCAGGAGGATCTT ACAGCGAACAAGCATCA	
SBD-RE(B) rev	522	TGATGCTTGTTTCGCTGTTAGATCCTCTG CAGCAGATGGGATGTT	
RE(B) D758N for	866	TACTTACAGAACGGGATAGAGCGG	
RE(B) D758N rev	867	CCGCTCTATCCCGTTCTGTAAGTA	
RE(B) E844Q for	868	CATGAGTCTCAGCCCTTCAGCTTT	
RE(B) E844Q rev	869	AAAGCTGAAGGGCTGAGACTCG	
RE(B) F848W for	870	CCCTTCAGCTGGGCTCAGGGCCCA	
RE(B) F848W rev	871	TGGGCCCTGAGCCCAGCTGAAGGG	
RE(B) $\Delta$ CTR for	406	TTTTCCATGGTTATCCGCCCCAGATCAT GA	NcoI
RE(B) $\Delta$ CTR rev	467	TTTTCTCGAGCCAAGGAGTTGAAGTAAC AA	XhoI

## 2.5. Plasmid Constructs

**GCAP2(95-204)pACT2.** This YTH prey clone (encoding EF3, EF4 and CTR of GCAP2) was obtained by yeast two hybrid screening using RIBEYE(B) as bait (Alpadi et al., 2008).

**GCAP2(1-204)pACT2,** encoding full-length GCAP2 cDNA. Full-length GCAP2 was amplified by PCR with the following primers: forward primer (632): TTTTGGATCCTAATGGGGCAGCAGTTCAGC); reverse primer (633): TTTTCTCGAGTCAGAACATGGCACTTTTCC) and retinal bovine cDNA as template. The PCR product was cloned into the BamHI/XhoI sites of pACT2.

**GCAP2(1-204)G2ApACT2,** encoding full-length GCAP2 with a point-mutated myristoylation signal. The insert was amplified by PCR using following primers: point mutant-encoding forward primer (1072): TTTTGGATCCTAATGGCCCAGCAGTTCAGC, reverse primer (633): TTTTCTCGAGTCAGAACATGGCAC TTTTCC and full-length GCAP2pGEX as template. The PCR product was digested with BamHI/XhoI and cloned into the respective sites of pACT2.

**GCAP2(3-204)pACT2**, encoding full-length GCAP2 from which the first two amino acids are deleted. The insert of GCAP2(3-204)pACT2 was amplified by PCR with the following primers: forward primer (657): TTTTGGATCCTACAGCAGTTCAGCTGGGAG); reverse primer (633): TTTTCTCGAGTCAGAACATGGCACTTTTCC) and full-length GCAP2 cDNA as template. The PCR product was cloned into the BamHI/XhoI sites of pACT2.

**GCAP2(105-204)pACT2**. The insert was amplified by PCR with the following primers: forward primer (677): TTTTGGATCCTAGGTGGCAGCGACAAGGACCGCAATCGC); reverse primer (633): TTTTCTCGAGTCAGAACATGGCACTTTTCC) and full-length GCAP2 cDNA as template. The PCR product was cloned into the BamHI/XhoI sites of pACT2.

**GCAP2(118-204)pACT2**. The insert was amplified by PCR with the following primers: forward primer (678): TTTTGGATCCTAGGTGGCAGCCTGGACATCGTGGAGTCC); reverse primer (633): TTTTCTCGAGTCAGAACATGGCACTTTTCC) and full-length GCAP2 cDNA as template. The PCR product was cloned into the BamHI/XhoI sites of pACT2.

**GCAP2(158-204)pACT2**. The GCAP2 (aa158-204) pACT2 was amplified by PCR with the following primers: forward primer (679): TTTTGGATCCTAGGTGGCAGCGATGAAAATGGAGATGGTCAG); reverse primer (633): TTTTCTCGAGTCAGAACATGGCACTTTTCC) and full-length GCAP2 cDNA as template. The PCR product was cloned into the BamHI/XhoI sites of pACT2.

**GCAP2(171-204)pACT2**. The insert was amplified by PCR with the following primers: forward primer (681): TTTTGGATCCTAGGTGGCAGCGTTGAAGGTGCCGTCGT); reverse primer(633): TTTTCTCGAGTCAGAACATGGCACTTTTCC) and full-length GCAP2 cDNA as template. The PCR product was cloned into the BamHI/XhoI sites of pACT2.

**GCAP2(1-204)pGEX.** Full-length GCAP2 was excised from GCAP2(1-204)pACT2 with NcoI/XhoI and cloned into the respective sites of pGEX-KG.

**GCAP2(171-204)E172DpACT2.** The insert was generated by PCR with forward primer (1032): TTTTGGATCCTAGTTGATGGTGCCCGTCGT; reverse primer (633): TTTTCTCGAGTCAGAACATGGCACTTTTCC using GCAP2(171-204)pACT2 as template and cloned into the BamHI/XhoI sites of pACT2.

**GCAP1pMalC2.** The insert was amplified by PCR using the following primers: forward primer (961): TTTTGAATTCATGGGGAACATTATGGACG); reverse primer (962): TTTTCTAGATCAGCCGTCGGCCTCC and bovine retina cDNA library as template. The PCR product was cloned into the EcoRI/XbaI sites of pMal-C2.

**GCAP1(156-205)pACT2.** The insert was amplified by PCR using following primers: forward primer (968): TTTTCCATGGAGATGGAGGGCGTCCAGAAG; reverse primer (969): TTTTCTCGAGTCAGCCGTCGGCCTCC and GCAP1pMalC2 as template. The PCR product was cloned into the NcoI/XhoI sites of pACT2.

**RE(B)pGBKT7 encoding full-length RIBEYE (B )domain**

The full length Ribeye(B) domain was amplified by PCR with forward primer(406): TTTTCCATGGTTATCCGCCCCCAGATCATGA, reverse primer(405): TTTTCTCGAGCTATTGCTCGTTGGGGTGCT and bRIBEYE(B) cDNA as template. The PCR product was subsequently digested with NcoI/XhoI and cloned into the NcoI/salI sites of pGBKT7.

**RE(B)pMal-C2 encoding full-length RIBEYE B domain.** The insert was generated via PCR with forward primer(96):TTCACAATTGATCCGCCCCCAGATCATG, reverse primer(979):TTCAGTAGTCTATTGCTCGTTGGGGTGCT and using rRE(B)pGEX(Schmitz et al,2000) as a template, digested with MunI/SpeI and subsequently cloned into the EcoRI/XbaI sites of pMAL-C2.

**RE(B)hinge1pGBKT7; RE(B)663-691pGBKT7.** The insert was generated via PCR with forward primer (749): TTTTCCATGGTAGGCGGTAGTGGAATCGCCGTGTGCAAC; reverse primer (750): TTTTGGATCCCCGCCGATACAGATTGAG using rRE(B) pMalC2 as template. The PCR product was cloned into the NcoI/BamHI sites of pGBKT7.

**RE(B)hinge2pGBKT7; RE(B)856-891pGBKT7.** The insert was generated via PCR with forward primer (751): TTTTCCATGGTAGGCGGTAGTGCTCCAAATCTCATCTGCA; reverse primer (752): TTTTGGATCCGCGACCTGTGATTGCTCG using rRE(B) pMalC2 as template. The PCR product was cloned into the NcoI/BamHI sites of pGBKT7.

**RE(B)E844QpGEX,**

The insert was generated via PCR with outward forward primer (353): GTTCCATGGAGATCCGCCCCCAGATCAT, mutated forward primer (868): CATGAGTCTCAGCCCTTCAGCTTT; mutated reverse primer (869): AAAGCTGAAGGGCTGAGACTCATG, outward reverse primer (354) GTTCTCGAGCTATTGCTCGTTGGGGT using rRE(B)pSK as template.

**RE(B)E844QpGBKT7,** was cloned by inserting the amplified mutated PCR product (see above) into the NcoI/SalI site of pGBKT7 (Alpadi et al., 2008).

**RE(B)F848WpGEX,**

The insert was generated via PCR with outward forward primer (353): GTTCCATGGAGATCCGCCCCCAGATCAT; mutated forward primer (870): CCCTTCAGCTGGGCTCAGGGCCCA; mutated reverse primer (871): TGGGCCCTGAGCCCAGCTGAAGGG; outward reverse primer (354): GTTCTCGAGCTATTGCTCGTTGGGGT using RE(B)pGEX as template.

**RE(B)F848WpGBKT7,** was cloned by inserting the amplified mutated PCR product (see above) into the NcoI/SalI site of pGBKT7 (Alpadi et al., 2008).

**RE(B)D758NpGEX.**

The insert was generated via PCR with outward forward primer (353): GTTCCATGGAGATCCGCCCCAGATCAT; mutated forward primer (866): TACTTACAGAACGGGATAGAGCGG; mutated reverse primer (867): CCGCTCTATCCCGTTCTGTAAGTA; outward reverse primer (354): GTTCTCGAGCTATTGCTCGTTGGGGT using RE(B)pGEX as template.

**RE(B)D758NpGBKT7**, was cloned by inserting the amplified mutated PCR product (see above) into the NcoI/SalI site of pGBKT7(Alpadi et al., 2008).

**RE(B)G730ApGBKT7.**

Full-length RE(B)G730A was excised from RE(B)G730A pGEX with NcoI/XhoI and cloned into the NcoI/SalI sites of pGBKT7 (Alpadi et al. 2008).

**RE(B)C683SpGEX.** The point mutant was generated with the QuikChange site-directed mutagenesis kit (Stratagene) using using RE(B)pGEX (862) as template and the following primers: forward primer (816): CGACAGTCTCCCATATCCTC; reverse primer (817): GAGGATATGGGAGACTGTTCG according to the manufacturers instructions.

**RE(B)C683SpMalC2.** The insert was generated via PCR using following primers: forward (856): TTTTAGATCTATCCGCCCCAGATCATG; reverse (857): TTTTGTCGACCTATTGCTCGTTGGGGTG and RE(B)C683SpGEX as template. The PCR product was cloned into the BglII/SalI sites of pMalC2

**RE(B)C899SpGEX.** This construct was generated by a site-directed mutagenesis kit (QuikChange, Stratagene) using RE(B)pGEX (862) as template and the following primers: forward primer (810): TACGAAACTCTGTCAACAAAG; reverse primer (811): CTTTGTTGACAGAGTTTCGTA according to the manufacturer's instructions.

**RE(B)C899SpMalC2.** The insert was generated via PCR using following primers: forward (856): TTTTAGATCTATCCGCCCCCAGATCATG; reverse (857): TTTTGTCTGACCTATTGCTCGTTGGGGTG and RE(B)C899SpGEX as template. The PCR product was cloned into the BglII/SalI sites of pMalC2.

**RE(B)F904WpGBKT7** (Magupalli et al., 2008).

**RE(B) $\Delta$ HDLpGBKT7.** The insert was generated via overlapping PCR using the following primers PCR1: outward forward primer (353): GTTCCATGGAGATCCGCCCCCAGATCAT; reverse primer (504): GGATCCGAGCAGCTCCTCCTCCAGATTGAGGATATGGCA. PCR2: forward primer (505): TGCCATATCCTCAATCTGGGAGGAGGAGCTGCTCGGATCC; outward reverse primer (354): GTTCTCGAGCTATTGCTCGTTGGGGT using ratRIBEYE in pSK (Schmitz et al., 2000) as template. The PCR product digested with NcoI/XhoI and cloned into the NcoI/SalI sites of pGBKT7.

**RE(B) $\Delta$ CTRpGBKT7.** In this RIBEYE(B) construct, the hydrophobic carboxyterminal region of RIBEYE(B) (aa912-988) is deleted. The insert was generated via PCR using the following primers: forward (406): TTTTCCATGGTTATCCGCCCCCAGATCATGA, reverse (467): TTTTCTCGAGCCAAGGAGTTGAAGTAACAA and RE(B)pGEX (864) as template. The PCR product was digested with NcoI/XhoI and cloned into the NcoI/SalI sites of pGBKT7.

**RE(B)NBDpGEX-KG encoding NAD (H)-binding domain of RIBEYE B domain** (Magupalli et al., 2008). The NAD(H)-binding sub domain of RIBEYE(B) was amplified by PCR using rRIBEYE in pSK (Schmitz et al., 2000) as a template and the following primers Globular RE(B) FOR(508; TTTTGAATTCTTATCCCATCTGCTGCAGT), Globular RE(B) REV(509; TTTTCTCGAGGCTGTACCAGGCTGTGT); and cloned in frame with the GST-encoding cDNA of pGEX-KG using the EcoRI and XhoI sites.

**RE (B) NBDpGBKT7** (Magupalli et al., 2008).

The NBD-cDNA was cut out from pRE (B) NBD-GEX by EcoRI, XhoI and cloned into pGBKT7 vector in frame with GAL4-BD of pGBKT7 at the EcoRI and Sall site.

**RE(B)SBDpGBKT7 encoding substrate binding domain of RIBEYE(B) domain**

The two parts of substrate binding domain of Ribeye B domain was amplified by PCR using two sets of primers: outward forward (353):GTTCCATGGAGATCCGCCCCCAGATCAT; internal rev (522):TGATGCTTGTTCGCTGTTAGATCCTCCTGCAGCAGATGGGATGTT; Internal forward(523):AACATCCCATCTGCTGCAGGAGGATCTTACAGCGAACAAAGCA TCA outward reverse (354):GTTCTCGAGCTATTGCTCGTTGGGGT Then these two products were joined by Combo PCR using the outward forward (353) and outward reverse (354) primers and subsequently cloned into the NcoI/SalI sites of pGBKT7.

**RE(B)hinge2T865SpGBKT7.** The insert was generated with the QuikChange site directed mutagenesis kit (Stratagene) according to the manufacturer's instructions using the following primers: forward primer (822): TGCACACCACACAGTGGCTGGTACAGC; reverse primer (823): GCTGTACCAGCCACTGTGTGGTGTGCA using RE(B)856-891pGBKT7 as template.

**RE(B)hinge2W867EpGBKT7.** This construct was generated with the QuikChange site directed mutagenesis kit (Stratagene) via PCR with forward primer (826): CCACACACAGCCGAATACAGCGAACAAAG; reverse primer (827): CTTGTTCGCTGTATTCCGGCTGTGTGTGG using RE(B)856-891pGBKT7 as template.

**RE(AB)pGBKT7 encoding full-length RIBEYE (A- and B- domain)** (Magupalli et al., 2008).

## 2.6. Antibodies used for western blotting

Antibody	Source	Dilution used	Secondary antibody	Dilution used
GCAP2 6th immune serum	Rabbit polyclonal	1:1,000	Goat anti-rabbit (GAR)-POX (SIGMA) Cat.No: A6154	1:10,000
GCAP2(A1) (Santa Cruz) Cat.No: SC-59543	Mouse monoclonal	1:1,000	Goat anti-mouse (GAM) POX (SIGMA) Cat.No: A3673	1:10,000
U2656 ( Schmitz et al., 2000)	Rabbit polyclonal	1:10,000	GAR POX (SIGMA) Cat.No: A6154	1:10,000
RIBEYE/CtBP2 (BD Transduction Laboratories) Cat.No: 612044	Mouse monoclonal	1:10,000	GAM POX (SIGMA) Cat.No: A3673	1:10,000

## 2.7. Antibodies used for Immunolabeling

Antibody	Source	Dilution used	Secondary antibody	Dilution used
GCAP2 6th immune serum	Rabbit polyclonal	1:500	GAR Cy3 (ZYMED) Cat.No: 81-6115	1:1,000
GCAP2(A1) (Santa Cruz) Cat.No: SC-59543	Mouse monoclonal	1:1,000	GAM Cy3-(ROCKLAND) Cat.No: 610-104-121	1:1,000
U2656 (Schmitz et al., 2000)	Rabbit polyclonal	1:1000	GAR Cy2 (ROCKLAND) Cat.No: 611-111-122	1:1,000
RIBEYE/CtBP2 (BD Transduction Laboratories) Cat.No: 612044	Mouse monoclonal	1:500	GAM Cy2(Jackson ImmunoResearch) Cat.No:115-096-146	1:1,000
Gat1(K-20) (Santa Cruz) Cat.No: SC-389	Rabbit polyclonal	1:500	GAR Cy3 (ZYMED) Cat.No: 81-6115	1:1,000
Visual Arrestin (E-12) (Santa Cruz) Cat.No: SC-3457	Goat Polyclonal	1:500	RAG Cy3 (SIGMA) Cat.No.: C 2821	1:1,000
SV2 A (Synaptic Systems) Cat.No: 119 00 2	Rabbit polyclonal	1:500	GAR Cy2 (ROCKLAND) Cat.No: 611-111-122	1:1,000
Synaptophysin (Sigma) Cat.No: S5768	Mouse monoclonal	1:500	GAM Cy2 (Jackson ImmunoResearch) Cat.No:115-096-146	1:1,000

## 2.8. Enzyme, Proteins and molecular weight standards

Bovine serum albumin	Sigma
100 bp DNA-Leiter Roti® Mark	Roth
T4 DNA ligase	Roche Diagnostics
Low range protein standarRoti® Mark	Roth
Lysozyme	Roth
Restriction enzymes	New England Biolabs
Taq polymerase	PeQLab

## 2.9. Chemicals

Agar-Agar	Roth
Agarose	Roth
3-Amino-1,2,4-triazol	Sigma
Ampicillin	Roth
BSA	Sigma
Chloroquine	Sigma
Coomassie Brilliant Blue R 250	Roth
DEAE-Dextran	Sigma
N,N-Dimethylformamide	Roth
Disodium hydrogen phosphate	Roth
Dithiothreitol (DTT)	Sigma
EDTA	Roth
Ethidiumbromide	Roth
Glucose	Roth
Glutathione-Sepharose	Sigma
Glycerol	Roth
Glycine	Roth
IPTG	Roth

Potassium chloride	Roth
Potassium hydrogen phosphate	Roth
Lithiumacetate	Sigma
Magnesiumchloride Hexahydrate	Roth
$\beta$ -Mercaptoethanol	Roth
Sodium azide	Sigma
Sodium carbonate	Roth
Sodium chloride	Roth
Sodium dihydrogenphosphate	Roth
NPG (n-Propylgallate)	Sigma
ONPG (o-Nitrophenyl- $\beta$ -D-galactoside)	Sigma
Phenylmethylsulfonylfluoride (PMSF)	Roth
Ponceau-S	Roth
Saccharose	Roth
Sorbitol	Roth
Tris	Roth
Triton X-100	Fluka
X-GaL(5-Brom-4-Chlor-3-indoyl- $\beta$ -galactoside)	Roth

## 2.10. Buffers & Media

Acetate buffer (P3)	3 M Potassium acetate, pH 5.5
3-Amino-1,2,4-triazol	10 mM in a dd H <sub>2</sub> O
Ampicillin	50 mg/ml A.dest, steril filtered
Bradford-Reagent Roti®-Quant	Carl Roth,
Breaking –buffer	100 mM Tris-HCl pH 8.0 1 mM $\beta$ -Mercaptoethanol 20 % Glycerol

100 x BSA 10 mg/ml (Restriction digestion)	New England Bio labs
Coomassie-Brilliant blue stain	600 ml Isopropanol 1560 ml dd H <sub>2</sub> O 240 ml acetic acid 0,6 g Coomassie Brilliant Blue R 250
OPTIMEM/GlutaMax™ medium	10% (v/v) tryptose phosphate broth, 20 mM HEPES, 2.5% FCS
ECL-solution	1:1 obtained with ECL 1 & ECL2 (ECL1) 5.0ml 1M Tris-HCl , pH: 8.5 500µl luminol 220µl PCA Made up to 50ml with dd H <sub>2</sub> O (ECL2) 5.0ml 1 M Tris-HCl , pH 8.5 32µl Hydrogen peroxide (30%) Made up to 50.0 ml with dd H <sub>2</sub> O
De-staining solution for coomassie stain gel	100 ml acetic acid 300 ml Ethanol Make up to 1 litre with dd H <sub>2</sub> O
Loading buffer for Agarose gel	10 µl 100 mM EDTA 490 µl dd H <sub>2</sub> O 500 µl Glycerol
LiAc/TE/DTT	20 ml 1 M Lithium acetate 10 ml 200mM DTT 20 ml TE (0.1M Tris- HCL, 10mM EDTA) - made up to 200 ml with ddH <sub>2</sub> O - Filter sterilized
IPTG	0.1 M in PBS

Lysis buffer for <i>E. coli</i> (P2)	200 mM NaOH 1% SDS
LB Nutrient medium for Bacteria	Invitrogen GmbH, Karlsruhe
Na <sub>2</sub> CO <sub>3</sub>	1 M in dd H <sub>2</sub> O.
ONPG-Stock solution	4 mg/ml in Z-Puffer
5x PBS	40 g NaCl 1 g KCl 7.2 g Na <sub>2</sub> HPO <sub>4</sub> 1.2 g KH <sub>2</sub> PO <sub>4</sub> Make up to 1 litre with dd H <sub>2</sub> O
PMSF-Stock solution	40mM in 100% Isopropanol
Polyacrylamidgel 10% (minigel)	1 ml ddH <sub>2</sub> O, 1.27 ml 1 M Tris pH 8.8 1.67 ml 30% Acrylamide 50 µl 10% SDS 1 ml 50% Glycerol 3.3 µl TEMED 25 µl 10% APS
Ponceau S-stain	30 g Trichloroaceticacid 5 g Ponceau S Make up to 1 litre with dd H <sub>2</sub> O
10x restriction enzyme buffer	New England Bio Labs ®Inc.; Frankfurt/Main
Resuspensions buffer (P1)	50 mM Tris-HCL, pH 8.0 10 mM EDTA 100 µg/ml RNase A

SD-Dropout-Medium (Minimalmedium)	BD biosciences 26.7 g/l
-L SD Dropout-liquid medium -W SD Dropout-liquid medium -LW SD Dropout-liquid medium -ALWH SD Dropout- liquid medium	+0.69 g -Leu-DO Supplement (BD) +0.74 g -TRP-DO Supplement (BD) +0.64 g-Leu-TRP-DO Supplement(BD) +0.6 g-Ala-Leu-Trp- HIS-Supplement (BD) All medium was make up to 1 litre with dd H <sub>2</sub> O Adjusted pH 5.8
SDS-PAGE- Electrophoresis buffer	3.03 g Tris 14.4 g Glycine 1.0 g SDS Make up to 1 litre with dd H <sub>2</sub> O
SDS-loading buffer 4 x	1.6 g SDS 4 ml β-Mercaptoethanol 2 ml Glycerol 2 ml 1M Tris pH 7.0 4 mg Bromo phenol blue 2 ml of dd H <sub>2</sub> O.
Taq-Puffer	Peqlab
2 x TBS	28 ml 5 M NaCl 3 ml 1 M KCl 1 ml 1 M CaCl <sub>2</sub> 0.5 ml MgCl <sub>2</sub> 4.5 ml 200 mM Na <sub>2</sub> PO <sub>4</sub> , pH 7.4 20 ml 1 M Tris-HCl, pH 7.9 Make up to 500 ml of filter dd H <sub>2</sub> O.
1xTAE-Puffer	40 mM Tris pH 7.8 10 mM Sodium acetate, 1 mM EDTA

Transfer Buffer (Western Blot)	TRIS 15.125 g Glycine 72.05 g Methanol 1 litre Make up to 5 litres with dd H <sub>2</sub> O.
X-Gal solution	20 mg/ml in N,N-Dimethylformamid (DMF)
X-Gal detection solution	340µl X-Gal solution 54 µl β-Mercaptoethanol Make up to 20 ml with Z-Puffer
YPD-Medium	Clontech 50g YPD dissolved in 1 litre of ddH <sub>2</sub> O. Autoclave
Z-buffer	<b>Z-Buffer:</b> 60mM Na <sub>2</sub> HPO <sub>4</sub> 40mM NaH <sub>2</sub> PO <sub>4</sub> 10mM KCl 1mM MgSO <sub>4</sub> 50mM β-mercaptoethanol pH7.0 Do not autoclave

### 2.11. Instruments

Biofuge fresco	Heraeus
Biofuge primo R	Heraeus
Biofuge stratos	Heraeus
Chemidoc XRS System	Bio-Rad
Elektrophoretic apparatus –Agarosegel	Bio-Rad
Elektroporator ECM 399	BTX

Flourescence microscope Axiovert 200M Camera AxioCam MRm	Carl – Zeiss
Incubator Bacteria/Yeast	Memmert
Incubator cell culture Sterile cycle CO <sub>2</sub> Incubator	Thermo
Multifuge1 S-R	Heraeus
PCR- Mastercyclergradient	Eppendorf
pH-Meter	Inolab
SDS-PAGE electrophoresis apparatus Mini-Protean II 2D Cell	Bio-Rad
Power Supply EPS 301	Amersham Biosciences
Shaker Incubator Innova 4230	New Brunswick Scientific
Rotator	NeoLab
Rotor for Ultracentrifuge, 70Ti	Beckmann
Sterilbank, Lamin Air Modell 1,2	Holten
Thermomixer compact	Eppendorf
Ultracentrifuge	Beckmann
Vortex	VWR International
Microtome-cryostat, Cryo-Star HM560MV	Microm Int. GmbH, Walldorf

SW40 rotor	Beckman
Rotator centrifuge, JA20	Beckman

## 2.12. Polymerase chain reaction

The following criteria were changed according to need. Primers were designed manually according to some basic principles. The  $T_m$  value of primer was kept around 50-55°C. Primer length was usually not more than 20-22 bases. The restriction sites were added to the primers along with overhang ends for efficient digestion of PCR products and cloning into the specific vectors. Primers were diluted in sterile ddH<sub>2</sub>O to get a 100µM concentration. 100-200 ng of DNA was used as a template.

### PCR master mix

10x PCR buffer-5µl

10mM dNTPs-1µl

Template DNA-100ng

100µM Forward primer-0.5µl

100µM Reverse primer-0.5µl

Taq Polymerase (5U/µl)-1µl

Sterile water to make up to 50µl

### PCR cycling conditions

Initial Denaturation- 95°C for 2 mins

8 cycles

Denaturation - 95°C for 30 sec

Annealing - 55°C for 30 sec

Extension - 72°C (approximately 1 min for 1000bp)

30 cycles

Denaturation - 95°C for 30 sec

Annealing - 65°C for 30 sec

Extension - 72°C (approximately 1 min for 1000bp)

Final extension - 72°C for 7 mins

### **2.13. Agarose gel electrophoresis**

Agarose gel electrophoresis is used for separation, purification and identification of plasmid DNA and DNA fragments. The size of a DNA fragment was determined by comparison with standard DNA marker. A Rough estimation of the DNA concentration can be made by comparing the band intensity of the sample and a reference marker DNA band upon staining with ethidium bromide. Depending on the size of the DNA molecules, the agarose concentration chosen was between 0.8 % and 1.2 % (w/v). DNA-samples were mixed with 10x DNA loading buffer and applied into the wells of the gel. In parallel, a marker was loaded. 1X TAE buffer was used for agarose solution and as electrophoresis buffer. The electrophoretic separation was done at 5Volts/cm. DNA fragments were visualized by UV-light and documented using BIO-RAD Gel Doc machine.

### **2.14. Agarose gel extraction**

The DNA fragments were extracted from agarose gel using the QIA®quick gel extraction kit. The specific DNA band was cut out from the gel. 1 ml of QX1 buffer and 5µl of QX1 suspension were added to the excised gel band. This mixture was kept at 55°C shakers for 30 mins. Then the mixture was centrifuged at 13,000 rpm for 1 mins and the supernatant was removed and to the pellet 1 ml of QX1 buffer was added and mixed. The centrifugation step was repeated. To the pellet 1 ml PE wash buffer was added and mixed. The mixture was centrifuged at 13,000 rpm for 1 min and the supernatant was removed. This step was repeated and the pellet was dried at room temp for 15 mins. Then 30 ml of pre-warmed 1mM Tris HCl pH8.4 was added and kept at 55°C in thermal shaker for 10 mins. This mixture was centrifuged at 13,000 rpm for 2 mins and the supernatant which contains DNA was taken and used for further experiment.

### **2.15. RESTRICTION DIGESTION & LIGATION (CLONING)**

#### **Restriction Digestion mixture**

Plasmid	10.0µl
10X buffer	3.0µl
10X BSA	3.0µl
Enzyme I	0.5µl

Enzyme II 0.5 $\mu$ l

Sterile dd H<sub>2</sub>O to make up 30 $\mu$ l

The insert and vector were digested with appropriate enzymes for 2 to 3 hours at 37°C. The digested products were fractionated by agarose gel electrophoresis. Then appropriate band excised from the gel and eluted using Qiagen gel extraction method. The concentration of eluted insert and vector DNA was measured. The insert to vector concentration used for ligation is 3:1 weight ratio.

#### **Ligation mixture**

Insert 12 $\mu$ l (approx.400ng)

Vector 4 $\mu$ l (approx.100ng)

10X ligase buffer 2 $\mu$ l

T4 DNA ligase 1 $\mu$ l

Sterile water to make up 20 $\mu$ l

The ligation mixture was incubated at room temp for over night. The amounts of restriction enzyme and DNA, the buffer and ionic concentrations, and the temperature and duration of the reaction varies depending upon the specific application. Then 2  $\mu$ l of ligation mixture was electroporated to *E.Coli* DH10B bacteria. The colonies were selected on respective antibiotic plates and plasmids were isolated from mini culture and the insert was checked by restriction digestion and confirmed by sequencing.

#### **2.16. Precipitation of ligation mixtures**

The DNA was purified from high salt concentrations for an efficient transformation into *E. coli* DH10B by electroporation. It is done with 3mM sodium acetate. (1 volume ligation mixture, 1/10 volume 3M sodium acetate (pH 5.0) and 10 volumes of ice cold ethanol). The DNA pellet was washed once with 70 % ethanol and resuspended in a suitable volume of dd H<sub>2</sub>O.

#### **2.17. Determination of DNA concentration**

The DNA molecules in solution can absorb UV-light and this absorption can be measured by a spectrophotometer. The higher the concentration, the greater optical density at 260nm. The following relationship exists between the optical density (OD) and the DNA concentration:

Double stranded DNA:  $1 \text{ OD}_{260} = 50\mu\text{g/ml}$

## **2.18. BACTERIAL TRANSFORMATION**

### **2.18.1. Preparation of electrocompetent bacterial cells**

All procedures were carried out in sterile and aseptic environment. Glycerol stock of *E.coli* cells was freshly streaked on LB plate and incubated overnight at 37°C. Overnight 50 ml LB preculture was grown at 37°C, 160 rpm after single colony inoculation. 500 ml main culture (in 2 liters flask) was prepared with inoculation of 20 ml overnight grown preculture. Cells were grown at 37°C, 160 rpm till an OD<sub>600nm</sub> 0.9-1.0 was reached. Electro competent cells were kept on ice. The culture was transferred to a sterile falcon tubes and centrifuged at 3,500rpm, 15min at 4°C. The cell pellet was washed thrice in the ice-cold, sterile, double-distilled water and centrifuged at 3,500rpm, 15min at 4°C. The final washed pellet (~4ml) was resuspended in 5 ml sterile, ice-cold 10% glycerol (made in sterile water). Aliquot's of (50µl) cell suspension was made in prechilled 1.5 ml eppendorff tube, and frozen in liquid nitrogen. Electro competent cells were stored at -80°C for long term storage. Using this method, we routinely got at least  $6 - 8 \times (10^8)$  transformants/ µg DNA.

### **2.18.2. Transformation of electrocompetent bacteria *E.coli* DH10B**

The LB medium was kept at room temperature for 30 mins. The electroporation cuvette was kept in the ice for 10 mins. The electrocompetent bacteria were thawed on the ice for 1 mins. 2 µl of ligated DNA or plasmid DNA was added to the competence bacteria and this sample added to the pre chilled cuvette. Electric shock was given at 1200 mV current for 5 msec. Immediately after that, 1 ml of antibiotic free LB medium was added and the sample was transferred to the test tube and incubated at 37°C for 1 hr. After incubation, the sample was spreaded on suitable antibiotic selection plate and incubated for over night at 37°C. A single colony was innoculated in LB mediumcontaining specific antibiotic (ampicillin/kanamycine) and this culture was used for plasmid preparation.

## **2.19. ISOLATION OF PLASMID DNA**

### **2.19.1. Mini preparation**

Plasmid DNA was isolated from bacterial cultures using alkaline lysis method. Single bacterial colony was allowed to grow overnight in 5 ml of LB medium with appropriate amount of specific antibiotic at 37°C. 1 ml of culture was stored at 4°C for maxi preparation. 4 ml cultures were centrifuged in a 15 ml falcon tube at 4,000 rpm for

10 mins at 4°C. The pellet was resuspended with 250 µl of buffer 1. This mixture was transferred to 1.5 ml of microfuge tube. 250 µl of buffer 2 was added to that and mixed. After incubating at room temp for 5 mins, 350 µl of buffer 3 was added and incubated for 10 mins at room temperature. This sample was centrifuged at 13,000 rpm for 15 mins at 4°C. 600 µl supernatant was removed and mixed with 800 µl of isopropanol. This sample was centrifuged at 13,000 rpm for 20 mins. The supernatant was removed and the pellet was washed with 1 ml of 70% ethanol, air dried and resuspended in 40 µl of 1mM Tris HCl.

### **2.19.2. Maxi preparation**

Bacterial culture (usually 100ml) were harvested by centrifugation at 4000 rpm for 20 mins at 4° C. The pellet was resuspended in 5 ml of buffer 1 by vortexing. Then, 5 ml of buffer 2 was added to that and incubated for 10 mins at room temp. There after, 8 ml of buffer 3 was added and mixed thoroughly. This sample was centrifuged at 8500 rpm for 20 mins until no pellet appears. The supernatant was transferred to 50 ml Beckman centrifuge tube and 15 ml of isopropanol was added to that. After centrifugation at 13,000 rpm for 1 hr, supernatant was removed and the pellet was washed with 15 ml of 70% ethanol; air dried and resuspended in 1 ml of 1 mM Tris HCl pH (8.5).

### **2.19.3. Purification of plasmid DNA for sequencing**

100 µl of plasmid DNA was mixed with 500 µl of Qiagen binding buffer and added to the column after centrifuge at 13000 rpm for 1 min. 500 µl of PE wash buffer was added and centrifuged at 13000 rpm for 1 min. the supernatant removed and the above step repeated again. Finally, the column was centrifuged without any previous addition of buffer to remove the traces of alcohol. 50 µl of prewarmed 1mM Tris HCl was added to the column kept for incubation at room temp for 5 mins and centrifuged. The supernatant collected contain plasmid DNA. The OD value of DNA was measured by spectrophotometer. Roughly 2µg of DNA was sent for sequencing to MWG sequencing service centre.

### **2.20. Yeast Two Hybrid methods**

For Yeast-Two-Hybrid (YTH) analyses, the Gal4-based Matchmaker Yeast-Two-hybrid System (Clontech) was used according to the manufacturer's

instructions. For the YTH screening we used a bovine retinal YTH cDNA library from the retina (Tai et al., 1999). The cDNA of the resp. bait proteins were cloned in frame with the Gal4-DNA-binding domain of pGBKT7. The cDNA of the indicated prey proteins were cloned in frame with the Gal4-activation domain of pACT2 or pGADT7. The bait and prey plasmids confer tryptophan and leucine prototrophy to the respective. auxotrophic yeast strains.

## **2.20.1. Yeast cell transformation**

### **2.20.1.1. Preparation of electro competent yeast**

Preparation of electrocompetent yeasts and electroporation of yeasts were done as described by Helmuth et al., 2001. For identifying transformants, yeasts were plated on the respective selective plates to identify the resulting convertents to the respective prototrophy (drop out media Clontech/QBiogene). The yeast strain AH109 and Y187 were streaked from the glycerol stock on YPD plate and incubated at 30°C till the colony appeared. Precultures were made by inoculating the single colony in 10 ml of YPD medium by incubation overnight at 30°C. From this, all steps were carried out in ice. The cells were harvested by centrifugation at 2,000 rpm for 10 mins at 4°C. The cell pellet was washed twice with sterile cold distilled water. The cells were collected from washing each time by centrifugation at 2,000 rpm for 10 mins at 4°C. Then the cells were treated with 1M sorbitol followed by centrifugation at 2,000 rpm for 10 mins at 4°C. Then, the cells were incubated with 20 ml of incubation mixture containing 100 mM LiAc, 10mM  $\beta$  - mercaptoethanol and 1X TE buffer at 30°C for 30 mins at 250 rpm. The cells were collected by centrifugation at 2,000 rpm for 5 mins at 4°C. 1M sorbitol washing step was repeated once. The pellet was bathed in 100-200 ul of 1M sorbitol and it was used for electroporation.

### **2.20.1.2. Electroporation**

Electrocompetent (120 $\mu$ l) yeast cells were mixed with 1 ul of plasmid DNA and electroporated at 1,800 V for 5 msec. 1 ml of YPD medium was added to the mixture and incubated at 30°C for 1 hr at 600 rpm. After incubation, 100 ul of sample was spreaded on selection plates (AH109 -W plate; Y187 -L plate) and incubated at 30° C for 2-3 days.

## 2.20.2. Yeast mating

Yeast strains Y187 and AH109 were used that contain distinct auxotrophic marker genes: AH109 [MAT<sub>a</sub>, trp1-901, leu2-3, 112, ura3-52, his3-200, Gal4 $\Delta$ , gal80 $\Delta$ , LYS2::GAL1<sub>UAS</sub>-GAL1<sub>TATA</sub>-HIS3, GAL2<sub>UAS</sub>-GAL2<sub>TATA</sub>-ADE2, URA3::MEL1<sub>UAS</sub>-MEL1<sub>TATA</sub>-lacZ] (James et al., 1996); Y187 [MAT $\alpha$ , ura3-52, his3-200, ade2-101, trp1-901, leu2-3, 112, gal4 $\Delta$ , met, gal80 $\Delta$ , URA3::GAL1<sub>UAS</sub>-GAL1<sub>TATA</sub>-lacZ] (Harper et al., 1993). The bait (pGBKT7) and prey (pACT2/pGADT7) plasmids confer tryptophan and leucine prototrophy to the respective auxotrophic yeast strains. Bait plasmids were always electroporated into AH109 yeast, whereas all prey plasmids were transformed into Y187. For interaction analyses, AH109 yeasts containing the resp. bait plasmid were mated with Y187 yeasts containing the resp. prey plasmid. For the mating, pSE1111 and pSE1112 (Bai et al., 1996) as well as the empty bait and prey vectors were used as negative controls. Single colony from -L and -W plate (respective prey and bait construct) were added to the 1 ml of YPD medium and mixed. This sample was incubated at 30°C for 6 hours. After incubation, the samples were pelleted down by centrifugation at 3,000 rpm for 5 mins at 4°C. The supernatant was discarded and keep the cell pellet in 100  $\mu$ l of remaining supernatants. 50  $\mu$ l of cells were spreaded on selection plate -LW; and another 50  $\mu$ l of cells were spreaded on selection plate -ALWH +100  $\mu$ l of 10mM ATZ. The plates were incubated at 30°C until colony appears.

## 2.20.3. $\beta$ -GALACTOSIDASE ASSAY

Expression of  $\beta$ -galactosidase ( $\beta$ -gal) marker gene activity was qualitatively analyzed by filter assays (Stahl, et al., 1996).

### 2.20.3.1. Colony lift filter assay

To rule out the false positive that grown on dropout medium (-ALWH), this test was performed to determine which of the positive colonies are also LAC Z positive, by screening for blue colour colonies in  $\beta$ -galactosidase assay. The whatman filter paper (#1) was laid onto the yeast colonies. The filter paper was removed using forceps and immersed in liquid nitrogen by the facing colony side up. The Petridish was prepared with 20 ml Z buffer containing 340  $\mu$ l of 50 mg/ml X-gal. A replica of the yeast colonies were made with whatman filter. The filter paper with

the cracked yeasts placed on the Z buffer, by colony faced up with out air bubbles. The petridish was covered with a led and placed at room temperature.

### **2.21. Site directed mutagenesis**

Site-directed mutagenesis involves the introduction of mutations at the DNA level to alter the primary amino acid sequence of proteins. COMBO PCR methods for site-directed mutagenesis utilize four oligonucleotides primers in two rounds of PCR. In first round of PCR external forward and mutant reverse primers in one reaction (N-terminal PCR product); external reverse and mutant forward in another reaction (C-terminal PCR product). Pfu polymerase is used in this first round to prevent addition of 'A' which is done by Taq polymerase and which would result into a frame shift mutation. In second round of PCR, there two PCR products are annealed afterdenaturation and amplified using external forward and external reverse primers. Taq polymerase was used in this second round PCR.

#### **PCR Master Mix-I**

10X Pfu buffer	-5 $\mu$ l
10mM dNTPs	-1 $\mu$ l
100 $\mu$ M Forward Primer	-0.5 $\mu$ l
100 $\mu$ M Reverse Primer	-0.5 $\mu$ l
(Mutagenic)	
Template	-0.5 $\mu$ l
Pfu Polymerase	-0.5 $\mu$ l
Sterile dd H <sub>2</sub> O	-42 $\mu$ l

#### **PCR Master Mix-II**

10X Pfu buffer	- 5 $\mu$ l
10mM dNTPs	- 1 $\mu$ l
100 $\mu$ M Forward Primer	
(Mutagenic)	- 0.5 $\mu$ l
100 $\mu$ M Reverse Primer	- 0.5 $\mu$ l
Template	- 0.5 $\mu$ l
Pfu Polymerase	- 0.5 $\mu$ l
Sterile ddH <sub>2</sub> O	- 42 $\mu$ l

### PCR cycling condition

95°C -2 mins

8 cycles

95°C -30 secs; 55°C -30 secs ; 72°C -1 min

30 cycles

95°C -30 secs ; 65°C -30 secs ; 72°C -1 min

1 cycle

72° C -7 mins

### **2<sup>nd</sup> round-COMBO PCR**

#### PCR Master Mix

10X PCR buffer -5µl

10mM dNTPs -1µl

25mM MgCl<sub>2</sub> -1µl

100µM Forward Primer (353)-1µl

100µM Reverse Primer (354) -1µl

Template (PCR-I) -4µl

Template (PCR-II) -4µl

Taq Polymerase -1µl

Sterile dd H<sub>2</sub>O -35µl

#### PCR CYCLING CONDITION (PEQLAB PCR MACHINE)

95°C -5 mins

1 cycle

70°C -5 mins ; 65° C-5 mins ; 60°C -2 mins ; 72°C-3 mins

30 cycles

95°C-3 mins ;95°C -30 secs ; 65°C-30 secs ; 72°C-1:30 mins

1 cycle

72°C -10 mins

## **2.22.PREPARATION OF RECOMBINANT PROTEIN**

### **2.22.1. Protein expression**

The plasmid constructs, pGEX-KG, pGCAP2GEX-KG were electroporated into the electro-competent bacteria BL21 or DH10B and pMBP-C2, pRE (B) MBP-C2 to BL21 at 1,200 volt for 5 ms. 1 ml of LB medium was added to these bacteria and incubated for 1 hr at 37°C, 220 rpm. The bacterial cultures were spreaded on LB-

Amp plates and incubated at 37°C overnight. The precultures were prepared by inoculating the overnight grown isolated colonies in 5 ml of LB medium with 10 ul of ampicillin and incubated for over night at 37°C at 220 rpm. The 5 ml of precultures were transferred to 500 ml of LB medium with 1 ml of ampicillin and incubation was continued until an OD 600 of 0.8-0.9 at 37°C at 220 rpm. After reaching the appropriate OD, the cultures were incubated at room temperature for 30 mins. 600 ul of 100 mM IPTG was added to the growing culture for the induction of protein expression and incubation was continued for 5 hours at room temperature. From this step all experiments were done at 4°C. The cells were harvested by centrifugation at 3,500 rpm for 20 mins. The pellet were washed thrice by resuspension with 50 ml of ice cold PBS and centrifuged at 3,500 rpm for 15 mins. Then, the pellets were incubated with 500µl of 10 mg/ml freshly prepared lysozyme in a total volume of 20 ml of PBS for 1 hr at 4°C. The cell membrane was disrupted by sonication. The supernatants were collected by centrifugation at 13,000 rpm for 1 hr. This procedure was repeated until no pellet appears.

#### **2.22.2. Purification & elution of fusion proteins**

1 ml of pre-swollen glutathione agarose beads or amylose beads (depending on the applied tag) were washed thrice with ice cold PBS and added to the supernatant containing the GST, GCAP2-GST protein and MBP, RE (B) - MBP respectively. These samples were incubated for over night at 4°C in cold room for binding of GST and GST fusion protein to glutathione agarose beads; MBP and MBP fusion protein to amylose beads. Then, the samples were centrifuged at 1,500 rpm at 4°C for 2mins and the supernatant was removed. The pellets were washed thrice with 50 ml of ice cold PBS for three times by shaking for 30 mins at 4°C. After last washing the beads were saved as bathed in 1000 µl of PBS. 20 µl of beads were loaded on to the 10 % SDS-PAGE for checking the expression. The MBP and MBP fusion protein was eluted using elution buffer containing 10mM TRIS-HCl pH (8.5), 10% maltose in PBS in different fractions and checked it on 10% SDS-PAGE. The GST and GST fusion proteins were eluted in buffer containing 10mM reduced glutathione, 50mM TRIS-HCl pH (8.5).

### **2.22.3. Measurement of protein concentration**

The Bradford assay was used to estimate the protein concentration (Bradford,1975). The absorbance for the protein-specific dye, Coomassie brilliant blue G-250, shifts from 465 nm to 595 nm when binding to protein occurs. The measured absorbance at 595 nm was blotted against a reference curve obtained with known concentrations of BSA.

### **2.23. SDS-PAGE**

SDS PAGE was done by following Manniatis et al, 2005. One dimensional gel electrophoresis under denaturing conditions in presence of 0.1 % SDS separates proteins according to their molecular size. The polyacrylamide gel is casted as a separating gel topped by a stacking gel. Sample proteins were solubilized by boiling in 6X SDS loading buffer. Coomassie Brilliant Blue R- 250 binds non-specifically to almost all proteins, which allows detection of protein bands in polyacrylamide gels. Gels were stained with Coomassie staining solution with gentle shaking for 30 min at room temperature. The background was subsequently reduced by soaking the gel in acrylamide gel destaining solution. After that, gels were documented using either HP scanner or BIO RAD Gel Doc apparatus.

### **2.24. Western blotting**

Proteins were separated by SDS-PAGE and transferred from the polyacrylamide gel to a Nitrocellulose /Nylon membrane with a constant voltage (3 hrs, 50 volt at 4°C). After electroblotting, the membrane was stained with a Ponceau S for 2 mins. The Ponceau S stained membrane was documented using scanner. Then, the membrane was destained using PBS and blocked with 5% skim milk powder for 1 hour. For immunodetection of proteins, the primary antibodies were diluted in 5% skim milk powder and the membrane was incubated for over night in cold room with constant mild shaking. Then the membrane was washed three times with PBS. After that, the secondary antibody was diluted in 5% MMP and the membrane was incubated at room temp for 1 hour. Again the membrane was washed with PBS 3 times. Then, the membrane was incubated with ECL1 and ECL2 mixture (1:1 ratio; chemiluminescence's detection solution) and the signals were documented with BIO RAD Gel Doc apparatus. Also the band intensity was quantified using BIO RAD Gel Doc apparatus and the Gel Doc software.

## 2.25. GST pull down assay

GST and GST-GCAP2 bound to glutathione agarose beads were used as an immobilized partner (bait). The eluted MBP and RE (B)-MBP fusion protein were used as a prey for this assay. The eluted RE(B)-MBP fusion protein and MBP protein (control) were incubated with eluted GCAP2-GST fusion protein and GST protein (control) in equimolar concentration (0.8 $\mu$ M) in a total volume of 500  $\mu$ l incubation buffer (100mM Tris-HCl (pH 8.0) ,150mM NaCl,1mM EDTA and 0.25% TritonX-100). These samples were incubated for 4 to 6 hrs at 4°C. After incubation, the samples were centrifuged to remove the supernatant. The pellets were washed 5 times with incubation buffer every washing step was followed by centrifugation at 13,000 rpm for 1 min at 4°C. The pellet was boiled in SDS-PAGE loading buffer at 96°C for 5 mins. The eluted proteins were subjected to 10% SDS-PAGE followed by coomassie staining.

### Experiment set up

<b>Protein</b>	<b>nature</b>	<b>Concentration (mg/ml)</b>	<b>Amount of protein used for each experiment (<math>\mu</math>g)</b>
GST	Immobilized	2.1	10
GCAP2-GST	Immobilized	2.0	20
MBP	Eluted	1.4	20
RE(B)-MBP	Eluted	2.5	40

	Lane	Protein	Vol. (µl)	(%) in total	protein	Vol. (µl)	(%) in total
Input	1	GST	0.24	15			
	2	MBP	0.7	15			
	3	GCAP2-GST	0.5	15			
	4	RE(B)-MBP	0.8	15			
Pellet	1	GST	2.4	100	MBP	7.1	100
	2	GCAP2-GST	5	100	RE(B)-MBP	8	100
	3	GST	2.4	100	MBP	7.1	100
	4	GCAP2-GST	5	100	RE(B)-MBP	8	100
	5				Unbound fraction RE(B)MBP	40	8

Input-protein used in the experiment

Pellet – the portion which is settled after incubation followed by washing and centrifugation.

## 2.26. BOVINE RETINA CO-IMMUNOPRECIPITATION

All steps were performed at 4°C if not denoted otherwise. For each immunoprecipitation, a bovine retina was incubated with 2ml of lysis buffer (100mM Tris HCl, pH 7.4, 150mM NaCl, 1mM EDTA) containing 1% TritonX-100 for 30 min at 4°C. Then the sample was centrifuged at 13,000 rpm for 15 mins at 4°C. Subsequently, the samples were transferred to 2ml syringes and forcefully ejected through 20 gauge needles to mechanically disrupt the retinal tissue. Mechanical crushing through 23gauge needles was repeated 40-50times. The mechanical disruption is essential to fractionate synaptic ribbons and to make them accessible for immunoprecipitation. Without mechanical treatment no RIBEYE Immunoreactivity was observed in the respective tissue lysate. After mechanical disruption, lysis was allowed to proceed for further 30min on ice. Afterwards, samples were centrifuged twice at 13,000 rpm for 30 min. The supernatant was incubated with 10 µl of GCAP2

pre-immune serum for 1 hour at 4°C and 20 µl of washed protein A-sepharose beads. Afterwards, the sample was centrifuged at 13,000 rpm for 15 min and the pre-cleared lysate was divided into two aliquot and incubated either with 10µl of GCAP2 immune serum or with GCAP2 pre-immune serum (IgG control) together with 20µl of washed protein A sepharose beads (overnight). After overnight incubation, samples were centrifuged at 3,000rpm (2min) to pellet the protein A-sepharose beads. The pellet was washed three times with 1 ml of lysis buffer. The final pellet was boiled with SDS loading buffer and subjected to SDS-PAGE followed by western blotting.

## **2.27. PURIFICATION SYNAPTIC RIBBON (Schmitz *et al.*, 1996)**

### **2.27.1. Purification of photoreceptor synaptic complexes (OPL-fraction)**

As a first step in the purification of photoreceptor synapses, a crude synaptic membrane fraction was prepared as described previously (Schmitz *et al.*, 1993). Briefly, retinae freshly isolated from bovine eyes (obtained from a local slaughterhouse within 30 min post-mortem) and detached from pigment epithelium were disrupted by shear forces exerted by an ultraturrax for 3 min on ice (Type TP 18/10; Janke and Kunkel, Staufen, Germany) in hypotonic homogenization buffer containing 15 mM Na<sub>2</sub>HPO<sub>4</sub>, pH 7.4, 1 mM EGTA, 1 mM MgCl<sub>2</sub>, and 1 mM phenylmethylsulfonyl fluoride for 3 min at 4°C. Thirty-five ml of homogenization buffer were used for eight isolated retinae. For preparation of crude synaptic membranes, 20 ml of homogenate was over layered on 10 ml of a sucrose cushion containing 50% sucrose (w/v) in homogenization buffer and centrifuged for 50 min at 15,000 rpm ( $\sim 27,200 \times g_{\max}$ ) at 4°C in a JA20 rotor (Beckman, Palo Alto, CA). At the interface between the sucrose cushion and the supernatant, a broad opaque band of membranes was visible and used for the subsequent purification of photoreceptor synapses. This band was removed carefully with a Pasteur pipette and diluted with approximately twofold its volume with homogenization buffer. This diluted suspension was spun in a JA20 rotor at 20,000 rpm ( $\sim 48,400 \times g_{\max}$ ) for 10 min (4°C). The supernatant was discarded, and the pellet was resuspended with approximately the same volume of homogenization buffer. For convenience, this resulting membrane suspension containing crude synaptic membranes (CSMs) was denoted CSM-fraction. The CSM-fraction was over layered on a linear sucrose

gradient ranging from 35 to 50% sucrose (w/v) in homogenization buffer. Membranes were spun at 13,000 rpm ( $\sim 30,000 \times g_{\max}$ ) for 1.5 hr at 4°C in an SW40 rotor. After this spin, two bands and a large pellet were visible. A membrane fraction that was recovered as a broad band at a sucrose density of  $\sim 40\%$  (w/v) in homogenization buffer (sucrose density calculated by its distance between the top and bottom of the gradient) was denoted OPL-fraction and characterized as described below. Membrane fractions were analyzed by Immunoblotting and immunofluorescence microscopy with the ribbon antiserum. To analyze the retinal fractions by immunofluorescence, microscopy samples were diluted with the twofold volume of homogenization buffer, sedimented in an Eppendorf centrifuge (model 5415C, Eppendorf, Hamburg, Germany) at 14,000 rpm ( $\sim 15,900 \times g_{\max}$ ) at 4°C for 10 min, and flash-frozen in liquid nitrogen. From these frozen samples, 10- $\mu\text{m}$ -thick cryostat sections were cut and immunolabeled with the ribbon antiserum as described above.

### **2.27.2. Purification of synaptic ribbons from the OPL fraction**

OPL membranes were diluted with the twofold volume of homogenization buffer and spun in a JA20 rotor at 11,000 rpm ( $\sim 14,600 \times g_{\max}$ ) for 10 min at 4°C. The resulting sediment was resuspended in homogenization buffer containing 1% Triton X-100 (w/v) to a protein concentration of  $\sim 1$  mg/ml. The pellet was homogenized three times with a tight-fitting Teflon pestle and kept on ice for  $\sim 30$  min. After this incubation period, the Triton-insoluble fraction of photoreceptor synapses was sedimented in a JA20 rotor at 11,000 rpm ( $\sim 14,600 \times g_{\max}$ ) for 10 min at 4°C. The sediment was resuspended with approximately the same volume of homogenization buffer containing 20% sucrose. This suspension was overlaid on a sucrose step gradient containing 2 ml of each of the following sucrose concentrations (in homogenization buffer): 30, 40, 50, and 70%. Then the sample was centrifuged in an SW40 rotor at 11,000 rpm ( $\sim 20,000 \times g_{\max}$ ) for 75 min at 4°C. The opaque protein bands at the respective interfaces of the sucrose step gradient were tested for the presence of synaptic ribbons by immunofluorescence and electron microscopy. The retinal subfraction between the 50 and 70% sucrose step contained the highest density and purity of synaptic ribbons and was denoted SR-fraction.

### **2.28. GST pull down assay in the presence of NAD<sup>+</sup>/NADH**

GCAP2-GST or GST alone bound to glutathione agarose beads as an immobilized bait protein and the eluted RE (B)-MBP or MBP alone as a prey protein were used for this assay. The eluted RE(B)MBP were incubated with GCAP2-GST in equimolar concentration (0.8 $\mu$ M) in a total volume of 500  $\mu$ l incubation buffer(100mM Tris-HCl(pH 8.0), 150mM NaCl,1mM EDTA and 0.25% Triton X-100). The NADH or NAD<sup>+</sup> was added as an increasing concentration ranging from 1nM-20 $\mu$ M in the incubation mixture of GCAP2-GST and RE(B)-MBP. These samples were incubated for 5 to 6 hrs at 4° C. Then, the samples were centrifuged and the pellets were washed 3 times with incubation buffer. Every washing step was followed by centrifugation at 3,000 rpm for 2 mins at 4° C. The pellet was boiled in SDS-PAGE loading buffer at 96° C for 5 mins. The eluted proteins were subjected to 10% SDS-PAGE .

### **2.29. Preabsorption experiments**

Preabsorption for western blotting: 50 $\mu$ l of GCAP2 immune serum (6<sup>th</sup> immune serum) was added to GST-GCAP2 (20 $\mu$ g) and GST (20 $\mu$ g) fusion protein bound to beads in a final volume of approx. 75  $\mu$ l and incubated overnight at 4°C in an overhead rotator. After incubation, samples were centrifuged at 13,000rpm for 3 mins at 4°C and the respective supernatants were taken for the subsequent experiments. For western blot analyses of bovine crude retinal extract the two preabsorbed antisera described above were used at a dilution of 1:1,000 in blocking buffer (5% skim milk powder in PBS).

### **2.30. Preabsorption for immunofluorescence**

Pre-absorption with fusion protein for immunofluorescence microscopy was done as described above for western blotting. The preabsorbed antisera (preabsorbed either with GST or GCAP2-GST) were subsequently tested at identical dilutions for immunolabeling on cryostat sections of the bovine retina.

### **2.31. Immunolabeling analyses**

Immunolabeling analyses were performed as previously described (Schmitz et al., 2000, 2006; Alpadi et al., 2008) using a Zeiss inverted Axiovert200M microscope (Carl Zeiss) equipped for conventional epifluorescence microscopy. In brief, 10µm thick cryostat sections were heat-fixed for 10 mins at 50°C and subsequently treated with 0.5% BSA for 1hr (RT) before the primary antibodies were applied at the indicated dilutions (see also section 2.7). Primary antibodies were usually applied overnight at 4°C if not indicated otherwise. After removing unbound antibody by several washes with PBS, secondary antibodies were applied at the dilutions in PBS (1hr, RT). After removing unbound antibody with PBS sections were mounted in NPG-antifade (Magupalli et al., 2008). Incubations only with secondary antibody (without primary antibody) and irrelevant primary antibodies served as negative controls.

### **2.32. Double-labeling of cryostat sections of the bovine retina with GCAP2 antibodies and Peanut agglutinin (PNA)**

Cryosection of bovine retina were heat fixed for 10 min @ 50° C and incubated with blocking buffer containing (0.5 % BSA, 0.02 % Triton X -100 in PBS) at RT for 45 mins. Section were then incubated with primary polyclonal GCAP2 antibody at a 1:500 dilution in blocking buffer overnight, 4°C. After brief washing with blocking buffer, sections were incubated with secondary antibody GAR-Cy3 (1hr, RT). Section were next incubated with Peanut agglutinin (PNA)–Alexa 488 (1:250 dilution) in blocking buffer for 3hrs at RT. After washing once with PBS, sections were mounted in NPG-antifade for microscopic analysis.

### **2.33. Generation of recombinant Semliki-Forest Virus**

#### **2.33.1. Cell culture**

BHK-21 cells were cultured in OPTIMEM/GlutaMax™ medium (Gibco) supplemented with 10 % (v/v) tryptose phosphate broth, 20 mM HEPES, 2.5 % FCS at 37 °C, 5 % CO<sub>2</sub>, and used between passage numbers 5 to 25.

### 2.33.2. Generation of recombinant SFV particles

The Semliki forest virus expression vector GCAP2-EGFPpSFV was constructed in three steps. First, PCR was used to generate a *Bgl*III-*Bam*HI flanked EGFP fragment using the following forward and reverse primers: forward (5'-TTTAGATCTGCCACCATGGTGAGCAAGGGCGA) and reverse (5'-TTTGATCCCTTGACAGCTCGTCCAT) for ligation into the *Bam*HI site of the pSFV1 expression vector. Next, a *Bam*HI-*Bss*HII flanking GCAP insert was amplified by PCR (5'-TTTTGGATCCATGGGGCAGCAGTTCAGC, forward primer), (5'-TTTTGCGCGCTCAGAACATGGCACTTTTCC, reverse primer) and GCAP2(aal-204)pGEX as a template. The PCR product was cloned into the *Bam*HI-*Bss*HII site of EGFPpSFV (Ashery et al., 1999). The IRES site of pSFV was deleted by digestion with *Bss*HII-*Cla*I, fill-in with Klenow and religation of the vector. EGFPpSFV was used as control plasmid/control virus (Ashery et al., 1999). mRNA was generated from pSFV1 expression vector (GCAP2-EGFPpSFV; EGFPpSFV) and pSFV2 helper vector by linearizing both vectors with *Spe*I and *in-vitro* transcription using SP6 RNA polymerase according to the manufacturer's instructions (mMessage mMachine SP6- Kit, Ambion). 10µg of purified mRNA was electroporated into  $1 \times 10^7$  BHK-21 cells in OPTIMEM/GlutaMax™ medium without supplements at 360V, 75 µF and pulsed twice using a Bio-Rad GenePulser II apparatus. Cells were resuspended in 10 ml of complete OPTIMEM/GlutaMax™ growth medium (see under A) and plated for 24hrs at 31°C, 5% CO<sub>2</sub>. Medium was recovered from the flasks and centrifuged at 400xg for 5 mins. The supernatants were aliquoted and stored at -80°C. Virus titer of the virus suspensions was determined exactly as previously described (Ashery et al., 1999).

### 2.33.3. Infection of mouse organotypic retinal cultures

The virus-containing stock was supplemented with an equal volume of OPTIMEM/GlutaMax™ containing 0.2% BSA. Virus was activated by the addition of chymotrypsin (0.2 mg/ml, Sigma-Aldrich) and subsequent incubation for 40 mins at room temperature. Proteolytic activation of the virus was stopped by the addition of aprotinin (0.6 mg/ml, Sigma-Aldrich). Organotypic retina cultures were incubated with the respective virus ( $4-5 \times 10^7$  infectious units/ml) for 16-24hrs at 31°C, 5% CO<sub>2</sub>, before being replaced by normal growth medium.

### **2.34. Organotypic culture of retinal explants**

Preparation of organotypic cultures was performed largely as previously described (Fischer et al., 2000; Pérez-León et al., 2003; Zhang et al, 2008), with some modifications. Briefly, freshly isolated eyes enucleated from adult mice housed under ambient light conditions were immediately immersed into ice-cold RPMI 1640 (supplemented with 10 % fetal calf serum, 10 mM HEPES, 2 mM L-glutamine, 1 mM sodium pyruvate, and 50  $\mu$ M  $\beta$ -mercaptoethanol, 100U/ml penicillin and 100 $\mu$ g/ml streptomycin). The anterior portion of the eye was removed by incision along the ora serrata. After removal of lens and vitreous body, the optic nerve was cut and the retina subsequently gently removed from the posterior eyecup. The retina was mounted photoreceptor side down on PET (polyethylene terephthalate) cell culture inserts (8,0  $\mu$ m pore size, Falcon) placed in six-well plates containing 1ml of RPMI 1640 with the above described supplements. Explants were incubated for 1h at 31°C/5% CO<sub>2</sub> and then infected with recombinant Semliki Forest virus. For infection with recombinant Semliki Forest virus, RPMI1640 medium was replaced by 1ml of the activated virus solution (see above, virus titer typically between 4-5  $\times 10^7$  infectious units per ml) and incubated overnight at 31°C /5% CO<sub>2</sub>. After 16-24hrs of infection, the virus-containing medium was removed from the cell culture dishes by three washes with RPMI (with supplements). The explants were allowed to recover for several hours before being processed for whole mount immunostaining.

### **2.35. Whole mount immunostaining of organotypic retinal explants**

One day after infection retinal explants were fixed in 4% PFA for 20 min at 4°C. Explants were permeabilized for 30 min at RT in incubation buffer (PBS with 0.3% Tx-100 and 0.5% BSA) and subsequently incubated with primary antibody (U2656, 1/500 diluted in incubation buffer) overnight at 4°C. Unbound antibody was removed by intensive washing with washing buffer (PBS, 0.5% Tween-20, 0.5% BSA). Explants were then incubated with the indicated fluorophore-conjugated secondary antibody (1/1000 in incubation buffer; see also section 2.7) overnight at 4°C. Unbound antibody was again removed by intensive washing with washing buffer. Explants were then fixed with 4% PFA (15 mins, 4°C), cut with a cryostat (10 $\mu$ m-thick sections) and thawed on uncoated SUPERFROST coverslides. Sections were analyzed with a Zeiss Axiovert200M microscope equipped with an apotome and the respective filter sets (EX BP 450-490nm/BS FT510/EM BP 515-565; EX BP

546/12/BS FT 580/EM LP 590). For counting terminals were observed in the apotome mode.

### **2.36. 3D-reconstruction of immunolabeled structures in retinal explants**

For 3D-reconstructions retina sections were observed with the Zeiss Axiovert200 microscope. Z-stacks were taken using the apotome and 3D-reconstruction was performed using the Inside4D software module from Zeiss.

### **2.37. *In-situ* Proximity Ligation Assays (*In-situ* PLA)**

Proximity ligation assays are a highly sensitive and specific way to detect protein-protein interaction *in-situ* e.g. in tissue sections (Gustafsdottir et al., 2005; Söderberg et al., 2006, 2008). Proximity ligation reactions critically depends on the distance of the two interaction partners. Positive PLA interaction signals indicate that the interacting proteins are localized in less than 40 nm distance from each other (Söderberg et al., 2006). PLA assay components (Gustafsdottir et al., 2005) were purchased from Eurogentec and performed according to the manufacturer's instructions. The following components were purchased from Eurogentec: anti-rabbit immunoglobulins coupled to the "PLUS" oligonucleotide (PLA PLUS probe), anti-mouse immunoglobulins PLA "MINUS" probe and the fluorescence detection kit 563 containing the linker oligonucleotide, enzymes for rolling circle amplification and fluorescent probe for product detection. In brief, 10µm thick sections of flash-frozen mouse eyes (prepared as described above) were heat-fixed for 10 mins at 50°C and subsequently treated with the Duolink blocking solution supplied by the manufacturer (Olink Biosciences, Eurogentec, Belgium) for 30 mins at 37°C. Next, sections were incubated with primary antibody dilutions (in Duolink antibody dilution solution; Olink Bioscience; Eurogentec, Belgium). The following antibodies were used at the indicated dilutions: polyclonal rabbit GCAP2 antibody (1:500); monoclonal anti-RIBEYE(B)/CtBP2 (BD) (1:500); polyclonal rabbit RIBEYE antibody (U2656, 1:500); mouse monoclonal antibody against opsin (Rho1D4, 1:500); polyclonal antibody against mGluR6 (Neuromics/Acris antibodies, RA13105) (1:500). Duolink *in-situ* PLA were performed as described by the manufacturer: After incubation with the primary antibodies, combinations of the PLA probes (anti-rabbit PLUS probe, anti-mouse MINUS probe: both diluted 1:8 in Duolink antibody dilution buffer) were added to the sections for 2hrs at 37°C in a wet chamber. After washing

the sections with TBS (2x5mins) hybridization with the linker oligonucleotide was performed for 15 mins at 37°C. Tissue was washed for 1min with TBS before ligation was performed for 15 mins at 37°C in a humid chamber. After washes with TBS for 5 mins, rolling circle amplification was done for 90 mins at 37°C precisely following the manufacturer's protocol. The product of the rolling circle amplification was detected with the Duolink detection kit 563 (Olink Bioscience, purchased via Eurogentech, Belgium) using Duolink fluorophore 563-labeled oligonucleotide diluted 1:5 with H<sub>2</sub>O. The detection reaction was performed for 60 mins at 37°C. As negative controls, PLA assays were done without primary antibodies or with only one primary antibody. Sections were subsequently washed with 2x SSC (2mins), 1xSSC (2mins), 0.2xSSC (2mins) and 0.02x SSC (1min). Afterwards, sections were mounted with Duolink mounting medium, sealed with a coverslip and analyzed by epifluorescence microscopy as described above. As further control to test for the spatial sensitivity/proximity requirements of the *in-situ* PLA reactions we also analyzed for PLA signals between a presynaptic marker (RIBEYE) and a postsynaptic marker at the tips of invaginating ON-bipolar cells (mGluR6). As positive controls we used a combination of the following two antibodies (rabbit polyclonal RIBEYE U2656/mouse anti-RIBEYE(B)/CtBP2) (Fig. 20L) and mouse monoclonal anti-opsin (Rho1D4)/rabbit polyclonal GCAP2) (Fig. 20K). The antibodies that were used in the Olink PLA assays are summarized as following with their indicated working dilutions: rabbit polyclonal GCAP2 antibody (1:500); Rabbit polyclonal antibody against RIBEYE U2656 (1:500); rabbit polyclonal antibody against mGluR6 (1:500); mouse monoclonal antibody against RIBEYE(B)/CtBP2, mouse monoclonal antibody against opsin (Rho1D4) (1:500). Antibody combinations were used as indicated in Fig. 20.

## **CHAPTER 3**

---

### **RESULTS**

### 3.1. Identification of GCAP2 as a RIBEYE interacting protein

In order to identify novel RIBEYE interacting proteins, RIBEYE (B)-domain (aa 564-988) was used as bait in YTH screen of a bovine retina cDNA library. The GCAP2 prey clone we obtained started at histidine H95 of bovine GCAP2 (GCAP2(95-204) and coded for the two carboxyterminal EF hands and the carboxyterminal region (CTR) of GCAP2. The interaction was confirmed by growth of mated yeast on -ALWH selective plates and the expression of  $\beta$ -galactosidase marker gene activity. The prey clone was not auto-activating as judged by the respective control matings (Fig. 9C) and thus pointed to an interaction between RIBEYE and GCAP2 in the YTH system. In order to further consolidate these finding we cloned full-length GCAP2 and the indicated GCAP2 constructs from bovine retinal cDNA into the respective yeast vectors and tested them for interaction with RIBEYE(B) in the YTH system (Fig.9C). The GCAP2 constructs were designed based on the known domain structure of GCAP2 (Fig. 9D). All of the tested GCAP2 constructs-except for full-length GCAP2 with an intact aminoterminal myristoylation signal- interacted with RIBEYE(B) (Fig.9). Full-length GCAP2 with intact aminoterminal myristoylation signal encoded by the first two amino acids (MG) did not interact with RIBEYE (Fig. 9C, D). If the aminoterminal myristoylation signal in full-length GCAP2 was deleted by deleting the two aminoterminal amino acids GCAP2 interacted with RIBEYE(B) in the YTH system (Fig. 9D). Thus, the myristoylation of GCAP2 at glycin G2 and the resulting membrane association prevent GCAP2 from entering the nucleus were the interaction needs to take place in the Gal4-based YTH system. This finding confirmed the interaction between RIBEYE(B) and GCAP2. This was further addressed by deletion mapping using RIBEYE(B) and GCAP2 deletion constructs. The mapping analyses revealed that RIBEYE interacted with GCAP2 even when all EF-hands of GCAP2 were deleted by aminoterminal truncations (Fig. 9). The carboxyterminal region of GCAP2 that starts after the fourth EF hand (abbreviated as CTR in the following text) retained the capability to interact with RIBEYE(B) in the YTH system. Therefore, we conclude that the CTR of GCAP2 mediates the interaction with RIBEYE.

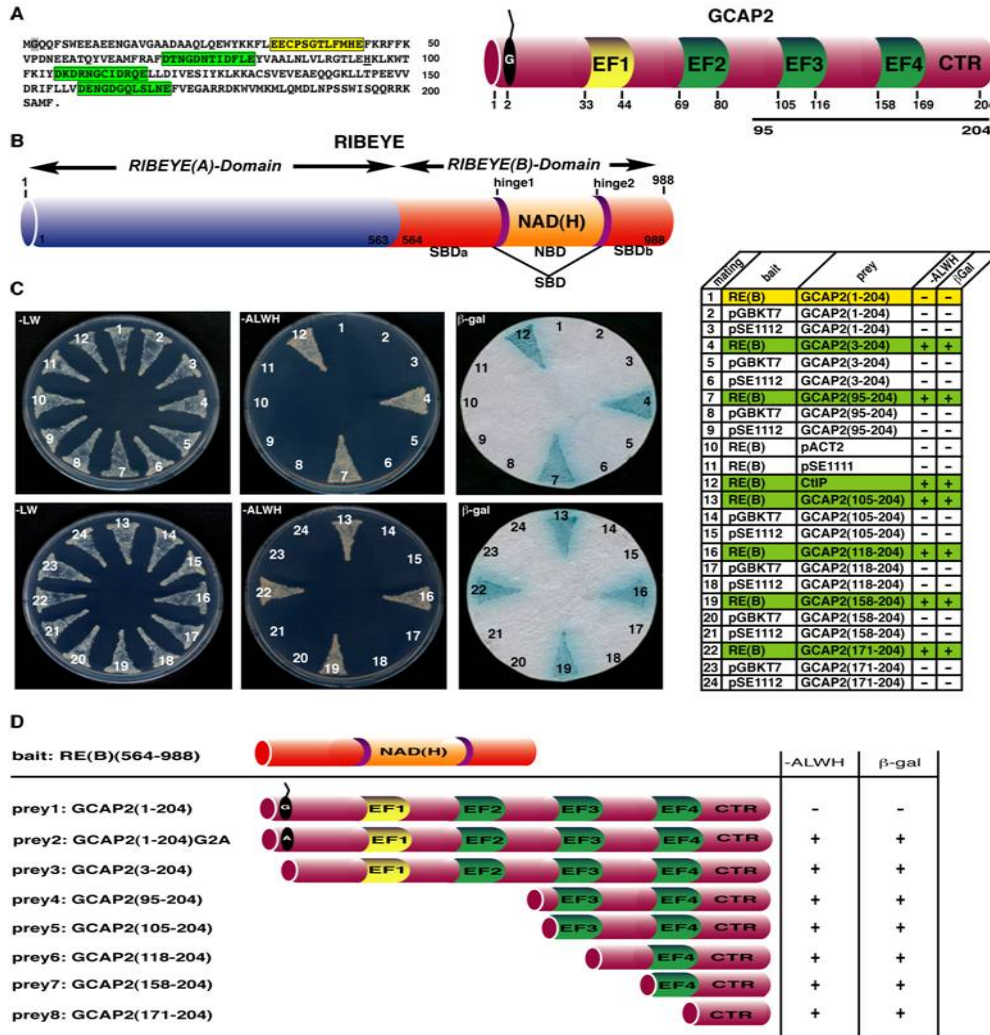


**Figure 9. RIBEYE interacts with GCAP2 in the YTH system.**

A) Sequence of bovine GCAP2 given in the single letter amino acid code. The 4 EF hands of GCAP2 are indicated in color. EF hand 1 (colored in yellow) is non-functional and does not bind  $\text{Ca}^{2+}$ ; EF hands 2-4 (colored in green) are functional and do bind  $\text{Ca}^{2+}$ . The bold bar that underlines the schematic drawing of GCAP2 denotes the extension of the obtained GCAP2 prey clone (see also Fig. 1D, prey 4). B) Domain structure of RIBEYE. RIBEYE consists of an aminoterminal A-domain and a carboxyterminal B-domain. The B-domain can be further subdivided into a contiguous central NAD(H)-binding sub-domain (NBD) and a discontinuous substrate-binding sub-domain (SBD). The SBD consists of two sequence stretches, SBDa and SBDb, that are linked to the NBD via two flexible hinge regions, hinge 1 and hinge 2 (see also Fig. 4A,B). C) GCAP2 interacts with RIBEYE(B) in the YTH system. Summary plates of YTH analyses obtained with the indicated bait and prey plasmids. For convenience, experimental bait-prey pairs are underlayered in color (green in case of interacting bait-prey pairs; yellow in case of non-interacting bait-prey pairs); control matings are non-colored. RIBEYE(B) interacts with GCAP2 as judged by growth on selective plates (-ALWH) and expression of  $\beta$ -galactosidase expression (yeast matings #4,7,13,16,19,22; Fig. 1C). The respective control matings (auto-activation controls; yeast matings # 2-3, 5-6, 8-11, 14-15, 17-18, 20-21, 23-24) did not show growth on -ALWH plate and no expression of  $\beta$ -galactosidase activity. Growth on -LW plates (Fig. 1C) demonstrates the presence of the bait and prey plasmids in the mated yeasts. Full-length GCAP2 containing an intact myristoylation site did not interact with RIBEYE(B) (mating #1, Fig.1C) because the myristoylation prevents the entry of the prey protein into the nucleus (see text). If the myristoylation signal is deleted by a point mutation (G2A) full-length GCAP2 also interacts with RIBEYE(B) (Suppl. Fig. 1). Similarly, deleting the myristoylation signal by truncation of the first two amino acids also results in interaction between RIBEYE(B) and GCAP2 (mating #4; Fig. 1C). Mating #12 is an unrelated positive control mating (Alpadi et al., 2008). D) Schematic summary of the mapping analyses obtained with the YTH system. RIBEYE(B) interacts with all tested GCAP2 constructs except for full-length GCAP2 that contains an intact myristoylation signal (prey 1). If the myristoylation signal is deleted by a point mutation (G2A) (prey 2, Fig. 1D) full-length GCAP2 also interacts with RIBEYE(B).

### 3.2. RIBEYE interacts myristoylation deficient full-length GCAP2

All of the tested GCAP2 constructs -except for full-length GCAP2 with an intact aminoterminal myristoylation signal- interacted with RIBEYE(B) (Fig. 9C,D) in the YTH system. If the aminoterminal myristoylation signal in full-length GCAP2 (encoded by the first aminoterminal amino acids: MG) was deleted by point-mutating glycine 2(G2) into alanine (G2A), GCAP2 interacted with RIBEYE(B) in the YTH system (Fig.10). Thus, the myristoylation of GCAP2 at glycine G2 and the resulting membrane association prevent GCAP2 from entering the nucleus where the interaction needs to take place in the Gal4-based YTH system.

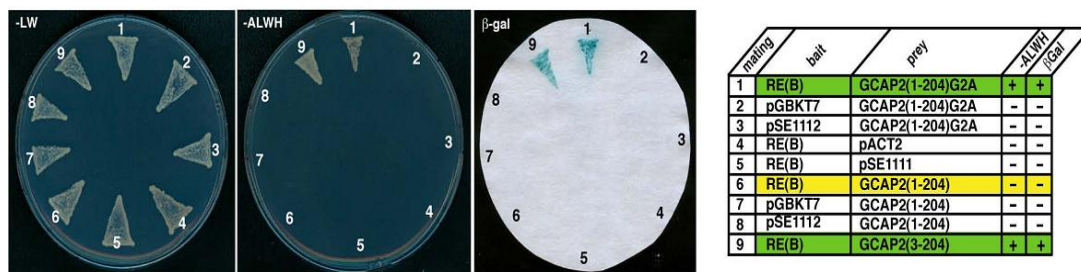


**Figure 10. RIBEYE interacts with myristoylation-deficient full-length GCAP2.**

Summary plates of YTH analyses obtained with the indicated bait and prey plasmids. For convenience, experimental bait-prey pairs are underlayered in color (green in case of interacting bait-prey pairs; yellow in case of non-interacting bait-prey pairs); control matings are non-colored. RIBEYE(B) interacts with myristoylation-deficient full-length GCAP2 (GCAP2(1-204)G2A) as judged by growth on selective plates (-ALWH) and expression of  $\beta$ -galactosidase activity (yeast mating #1). The respective control matings (auto-activation controls; yeast matings #2 - 5, #7 - 8) did not show growth on -ALWH selective plates and expression of  $\beta$ -galactosidase activity. RIBEYE(B) does not interact with full-length GCAP2 with an intact myristoylation signal (mating #6). Mating #9 is a positive control.

### 3.3. Mutation of the CTR of GCAP2 abolish interaction with RIBEYE(B)

The carboxyterminal region of GCAP2 that starts after the fourth EF-hand retained the capability to interact with RIBEYE(B) in the YTH system. Therefore, we conclude that the CTR of GCAP2 mediates the interaction with RIBEYE. This assumption is further supported by our finding that point mutants of the CTR GCAP2(171-204)E172D of GCAP2 no longer interacted with RIBEYE(B).

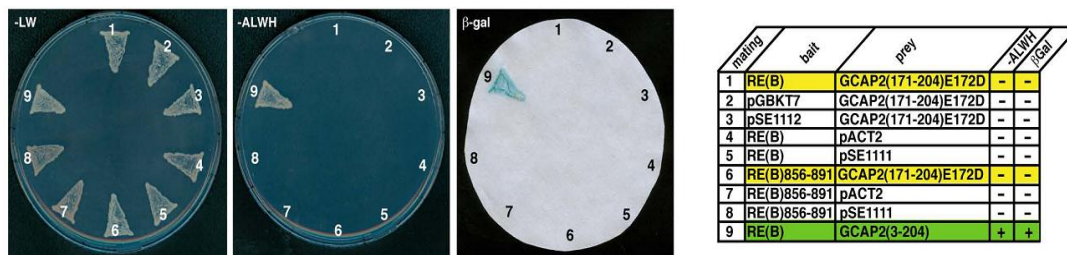
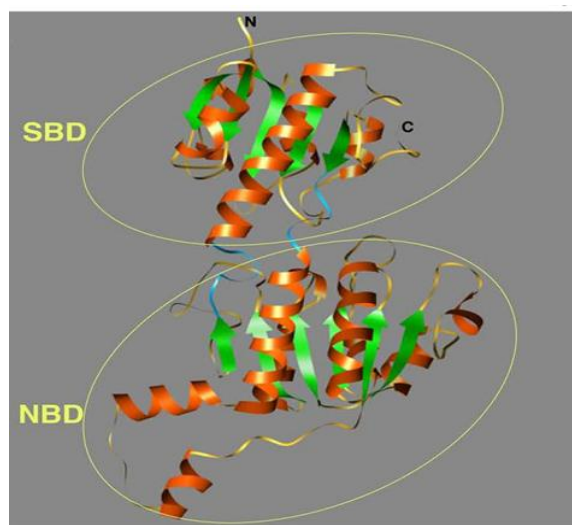


**Figure 11. Mutations of the carboxyterminal region (CTR) of GCAP2 abolish interaction with RIBEYE.** Summary plates of YTH analyses obtained with the indicated bait and prey plasmids. For convenience, experimental bait-prey pairs are underlayered in color (green in case of interacting bait-prey pairs; yellow in case of non-interacting bait-prey pairs); control matings are non-colored. RIBEYE(B) does not interact with a point-mutated CTR of GCAP2, GCAP2(171-204)E172D (matings #1, #6), although it interacts with the wildtype CTR, GCAP2(171-204) (Fig. 1). The respective control matings (auto-activation controls; yeast matings # 2-5, # 7-8) did not show growth on -ALWH selective plates and expression of  $\beta$ -galactosidase activity. Mating #9 is a positive control. RE(B)856-891 encodes for the hinge 2 region of RIBEYE(B) which was shown to be responsible for interaction with GCAP2 (Fig. 3).

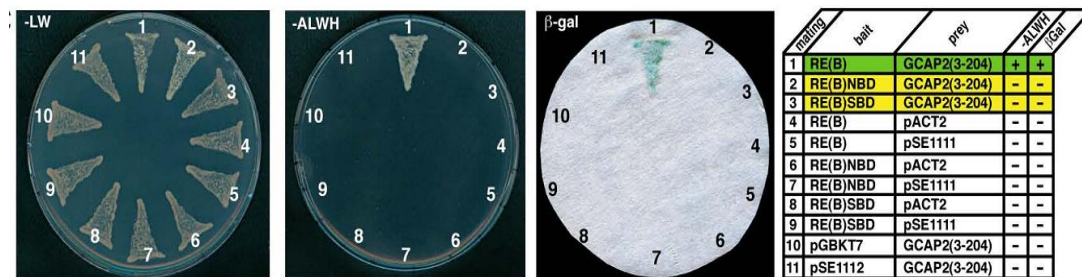
### 3.4. GCAP2 does not interact with SBD and NBD of RIBEYE(B)

The B-domain of RIBEYE consists of a NAD(H)-binding sub-domain (NBD) and a substrate-binding sub-domain (SBD). In order to map which parts of RIBEYE(B) are important for interaction with GCAP2 we tested whether the SBD and NBD of RIBEYE alone can interact with GCAP2. Surprisingly, both the SBD and NBD alone did not interact with GCAP2 in the YTH system (Fig. 12B).

A



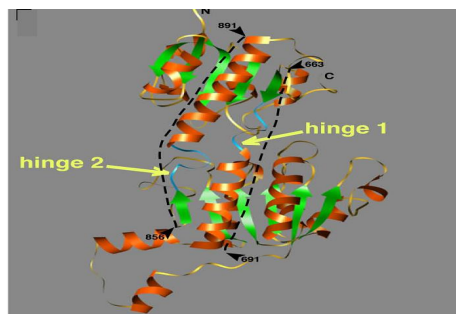
**Figure 12A)** Structure model of the B-domain of RIBEYE based on the crystal structure of tCtBP1 (Kumar et al., 2002; Nardini et al., 2003; see also Magupalli et al., 2008; Alpadi et al., 2008). The B-domain of RIBEYE consists of a NAD(H)-binding sub-domain (NBD) and a substrate-binding sub-domain (SBD)

**B****Figure 12B. GCAP2 not interact with the NBD and SBD of RIBEYE(B).**

Summary plates of YTH analyses obtained with the indicated bait and prey plasmids. For convenience, experimental bait-prey pairs are underlayered in color (green in case of interacting bait-prey pairs; yellow in case of non-interacting bait-prey pairs); control matings are non-colored. GCAP2 interacts with intact RIBEYE(B) as judged by growth on selective plates (-ALWH) and expression of  $\beta$ -galactosidase expression (yeast mating #1; positive control). In contrast, GCAP2 does not interact either with the NBD (mating #2) or the SBD (mating #3) of RIBEYE alone. The respective control matings (auto-activation controls; yeast matings # 4 - 11) did not show growth on -ALWH plates and expression of  $\beta$ -galactosidase activity. Growth on -LW plates (Fig. 2C) demonstrates the presence of the bait and prey plasmids in the mated yeasts.

### 3.5. GCAP2 interacts with flexible region of hinge2 region of RIBEYE(B)

Since the NBD- and SBD- constructs used above did not contain the connecting hinge regions, hinge 1 and hinge 2, we tested next whether the hinge regions of RIBEYE might mediate interaction with GCAP2. Indeed, the hinge 2 region of RIBEYE interacted with GCAP2 whereas the hinge 1 region did not in the YTH system (Fig. 13B) Therefore, the flexible hinge 2 region that connects the NBD with the SBD is the essential binding site for GCAP2 (Fig. 13A).

**A****Figure 13A. Structure model of the B-domain of RIBEYE.**

Based on the crystal structure of tCtBP1 (Kumar et al., 2002; Nardini et al., 2003; see also Magupalli et al., 2008; Alpadi et al., 2008). The B-domain of RIBEYE consists of a NAD(H)-binding subdomain (NBD) and a substrate-binding subdomain (SBD) which are connected by two flexible hinge regions, hinge 1 and hinge 2 (colored in blue). The dotted lines indicate the extensions of the hinge 1 and hinge 2 constructs tested in Fig. 5B with the YTH system

## B

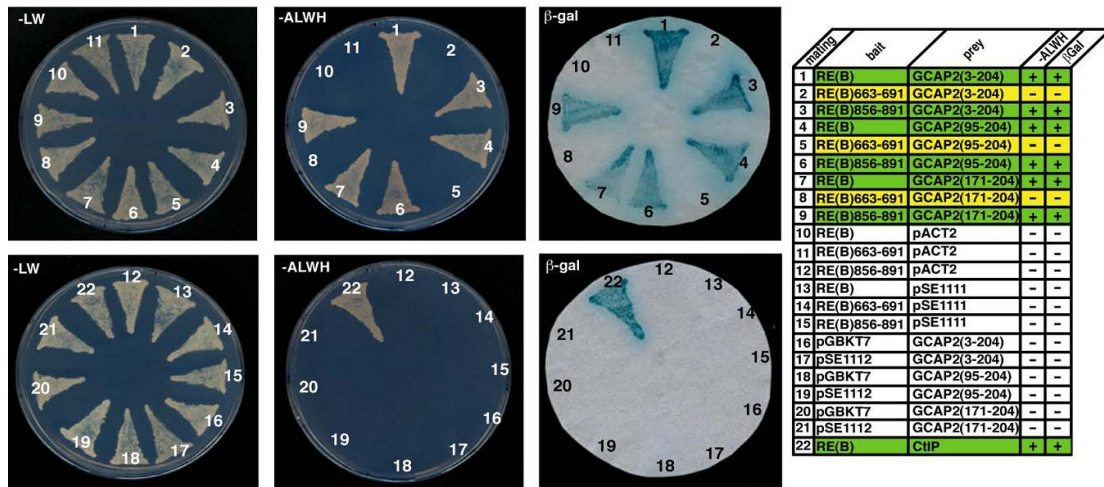


**Figure 13B. GCAP2 interacts with the hinge 2 region of RIBEYE(B).**

Summary plates of YTH analyses obtained with the indicated bait and prey plasmids. For convenience, experimental bait-prey pairs are underlayered in color (green in case of interacting bait-prey pairs; yellow in case of non-interacting bait-prey pairs); control matings are non-colored. GCAP2 interacts with the hinge 2 region of RIBEYE(B)856-891 (yeast matings #3, #6, #9) but not with the hinge1 region of RIBEYE(B)663-691 (yeast matings #2, #5, #8) as judged by growth on selective plates (-ALWH) and expression of  $\beta$ -galactosidase activity. The respective control matings (auto-activation controls; yeast matings #10-21) did not show growth on -ALWH plate and expression of  $\beta$ -galactosidase activity. Growth on -LW plates (Fig. 2B) demonstrates the presence of the bait and prey plasmids in the mated yeasts. Mating #1 represents a positive control mating (RE(B)/GCAP2; see also Fig. 1). Mating #22 represents an unrelated positive control mating (Alpadi et al., 2008). Abbreviations: NBD, NAD(H)-binding sub-domain of RIBEYE(B); SBD, substrate-binding sub-domain of RIBEYE(B).

### 3.6. Point mutants of the hinge2 region of RIBEYE(B) disrupt interaction with GCAP2

The hinge 2 region (aa856-aa891) of RIBEYE(B) interacted with GCAP2 whereas the hinge 1 region (aa663-691) did not (Fig. 13B). Therefore, the flexible hinge 2 region that connects the NBD with the SBD is the essential binding site for GCAP2 (Fig. 13A). This assumption is further supported by the analysis of point mutants of the hinge 2 region, i.e. RIBEYE(B)W867E and RIBEYE(B)T856S (Fig. 14A). These point mutants of the hinge 2 region of RIBEYE(B) no longer interacted with GCAP2 in the YTH system (Fig. 14B).

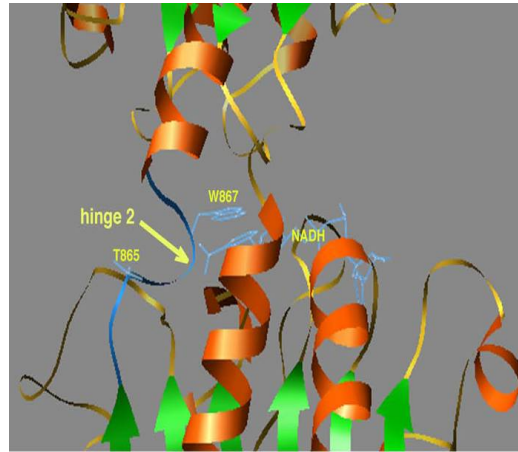


**Figure 14A. Structure model of RIBEYE(B)-domain in which the interface region between NBD and SBD is magnified.** W867 and T865 indicate amino acid residues within the hinge 2 region that disrupt interaction with GCAP2 when mutated. The hinge 2 region with W867, T865 and bound NAD(H) are colored in blue. W867 is located close to the nicotinamide moiety of NAD(H).

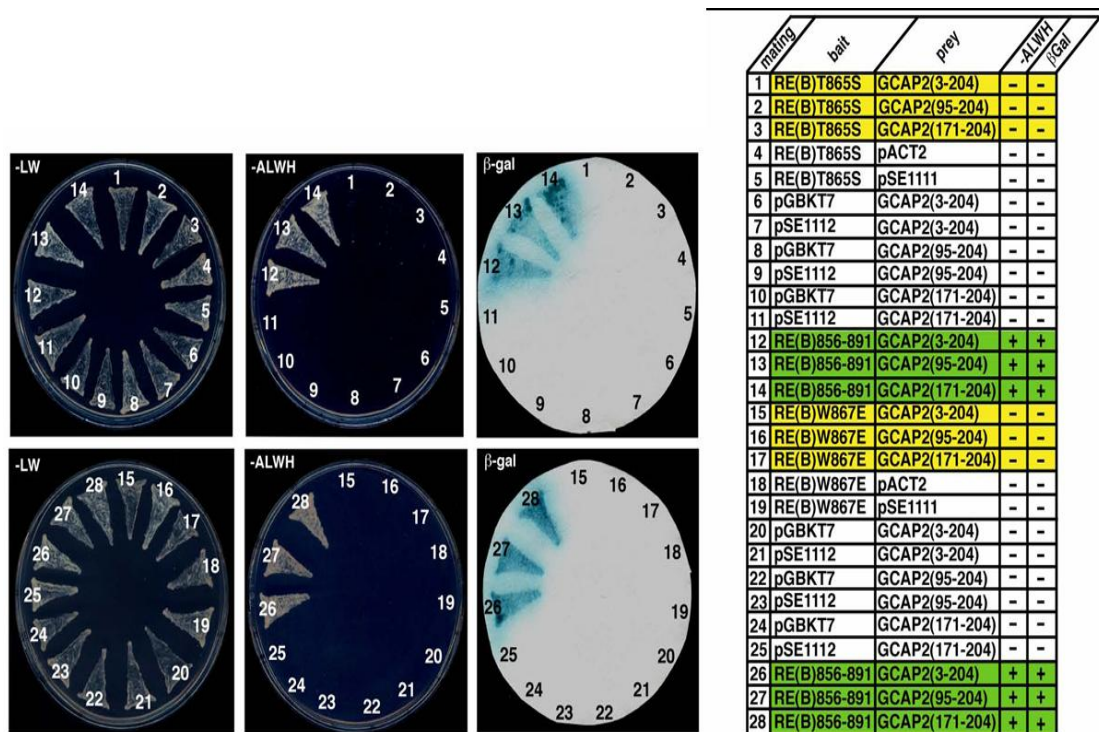


**Figure 14B. point mutants of the hinge 2 region of RIBEYE(B) disrupt interaction with GCAP2.** Summary plates of YTH analyses obtained with the indicated bait and prey plasmids. For convenience, experimental bait-prey pairs are underlayered in color (green in case of interacting bait-prey pairs; yellow in case of non-interacting bait-prey pairs); control matings are non-colored. Point mutants of the RIBEYE(B) hinge 2 region RE(B)T865S and RE(B)W867E do not interact with GCAP2 (matings #1-3, #15-17). The respective control matings (auto-activation controls; yeast matings #4-11, #18-25) did not show growth on -ALWH selective plates and expression of β-galactosidase activity. Matings #12-14, 26-28 are positive control matings.

### 3.7. The A-domain of RIBEYE does not prevent GCAP2/RIBEYE(B) interaction

RIBEYE expresses endogenously as full length (A+B domain) in the retina. Therefore, we tested whether the full length RIBEYE (contains both A domain and B domain) also interacted with GCAP2. RE(AB) also shows interaction with GCAP2 indicating that the A-domain of RIBEYE is not inhibiting the interaction of RIBEYE (B)-domain with GCAP2 (Fig.15). In YTH assay, the confirmation of bait and prey plasmids in the yeast was confirmed by growth on -LW plates. The interactions were judged by the growth on -ALWH selection plates, selective for protein interaction (Fig.15) by qualitative assessment of  $\beta$ -galactosidase marker gene expression.

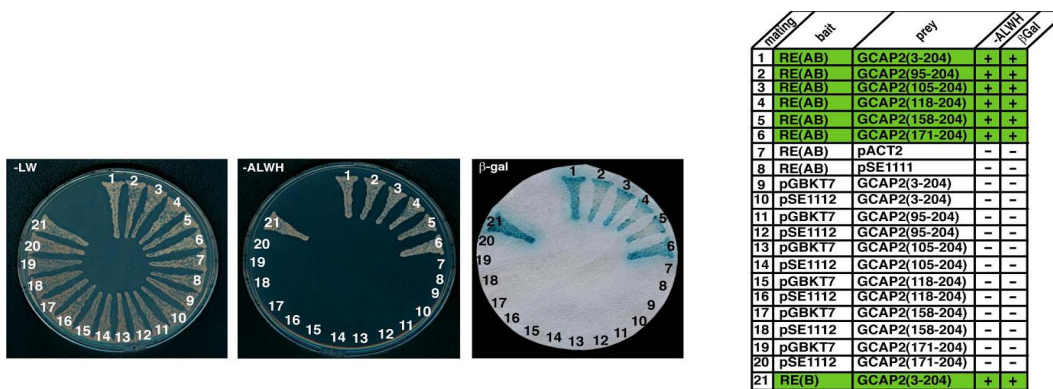
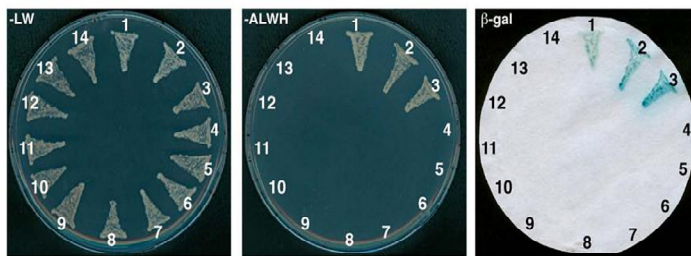


**Figure 15. The A-domain of RIBEYE does not prevent GCAP2/RIBEYE(B) interaction.**

Also full-length RIBEYE (RE(AB)) and not only RIBEYE(B) interacts with GCAP2 indicating that the A-domain of RIBEYE does not prevent RIBEYE(B)/GCAP2 interaction. For convenience, experimental bait-prey pairs are underlayered in color (green in case of interacting bait-prey pairs; yellow in case of non-interacting bait-prey pairs); control matings are non-colored. RIBEYE(AB) interacts with GCAP2 (matings #1-6). The respective control matings (auto-activation controls; yeast matings #7-20) did not show growth on -ALWH selective plates and expression of  $\beta$ -galactosidase activity. Mating #21 is an interaction positive control mating.

### 3.8. GCAP2 binds to monomeric RIBEYE(B) and GCAP2 binding is independent upon RIBEYE(B) homodimerization

RIBEYE(B) is known to homo-dimerize (Magupalli et al., 2008). Analyses of a RIBEYE(B)-dimerization deficient mutant RIBEYE(B) $\Delta$ HDL (Magupalli et al., 2008), revealed that RIBEYE(B)-GCAP2 interaction does not require RIBEYE(B) homo-dimerization. RIBEYE(B) $\Delta$ HDL interacted with GCAP2 in the YTH system ( Fig. 16). Therefore, GCAP2 can interact with monomeric RIBEYE(B).



matings	bait	prey	-ALWH	βgal
1	RE(B)	GCAP2(3-204)	+	+
2	RE(B)ΔHDL	GCAP2(3-204)	+	+
3	RE(B)ΔHDL	Munc119	+	+
4	RE(B)ΔHDL	RE(B)	-	-
5	RE(B)	pACT2	-	-
6	RE(B)	pSE1111	-	-
7	RE(B)ΔHDL	pACT2	-	-
8	RE(B)ΔHDL	pSE1111	-	-
9	pGBKT7	GCAP2(3-204)	-	-
10	pSE1112	GCAP2(3-204)	-	-
11	pGBKT7	Munc119	-	-
12	pSE1112	Munc119	-	-
13	pGBKT7	RE(B)	-	-
14	pSE1112	RE(B)	-	-

**Figure 16. GCAP2 binds to monomeric RIBEYE(B).**

For convenience, experimental bait-prey pairs are underlayered in color (green in case of interacting bait-prey pairs; yellow in case of non-interacting bait-prey pairs); control matings are non-colored. RIBEYE(B)ΔHDL interacts with GCAP2 (mating #2) although it does not interact with RIBEYE(B) (mating #4). The respective control matings (auto-activation controls; yeast matings #5-14) did not show growth on -ALWH selective plates and expression of β-galactosidase activity. Mating #1 is the interaction positive control mating. Mating #3 represents an unrelated positive control mating demonstrating proper folding of the dimerization-deficient RIBEYE(B) mutant (Alpadi et al., 2008).

### 3.9. GCAP2 interacts with RIBEYE(B) in fusion protein pull-down assays

The YTH analyses demonstrated RIBEYE/GCAP2 interaction in the YTH system. In order to verify this interaction also by further independent approaches we first performed fusion protein pull-down analyses (Fig. 17). GST-tagged GCAP2 was used as an immobilized bait protein. GST alone served as control protein. RIBEYE(B)-MBP or MBP alone (control protein) were used as soluble prey proteins. GST-GCAP2 (but not GST alone) pulled down RIBEYE(B)-MBP (but not MBP alone) demonstrating a specific interaction between RIBEYE(B) and GCAP2 (Fig. 17). The binding between RIBEYE(B)-MBP and GST-GCAP2 as shown by both coomassie staining of SDS PAGE as well as by western blot analysis with respective antibodies (Fig. 17A,B). In western blotting, the membrane was first incubated with anti-MBP to show the binding of RIBEYE(B) to GST-GCAP2 (Fig. 17Ba) and then the same blot was incubated with anti-GST (after stripping) to demonstrate the equal loading of bait proteins (Fig. 17Bb). Based on semiquantitative evaluation GCAP2-GST pulled-down at least ~15% of total RIBEYE(B)-MBP in these experiments. Using quantification of the bound proteins, we estimate a  $K_D$  of 2,72 ( $\pm 0.19$ )  $\times 10^{-6}$  mol/L for GCAP2/RIBEYE interaction.

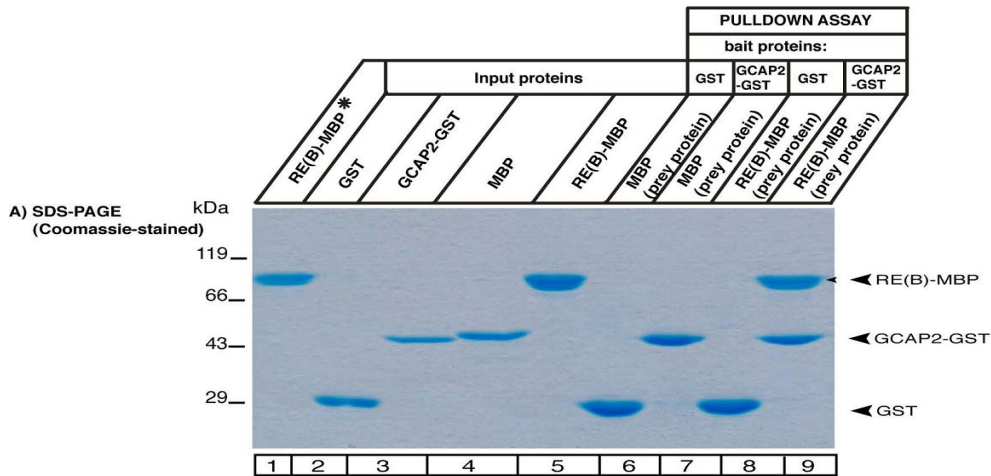


**Figure 17A. RIBEYE(B) interacts with GCAP2 in protein pull-down analyses.**

GCAP2-GST and GST alone (control protein) were used as immobilized bait proteins and RIBEYE(B)-MBP and MBP alone (control protein) as soluble prey proteins. After incubation and subsequent washing of the immobilized prey proteins, binding of the soluble prey proteins to the immobilized prey proteins was tested by SDS-PAGE (10% polyacrylamide gels) in (A). RIBEYE(B)-MBP binds to GCAP2-GST (lane 9, arrowhead) but not to GST alone (lane 8). MBP alone does not bind to either GCAP2-GST (lane 7) or GST alone (lane 6). 10% of the total proteins were loaded in the input lanes (lanes 2-5); 100% of the immobilized protein pellets were loaded (lanes 6-9). 8% of the unbound fraction (marked by asterisk) was loaded in lane 1.

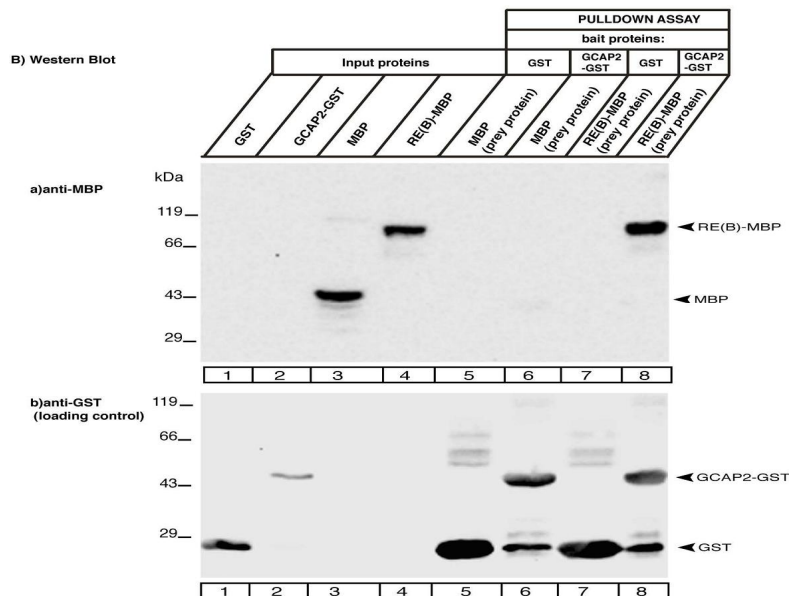


**Figure 17B. RIBEYE(B) interacts with GCAP2 in protein pull-down analyses (Western blot).**

**Figure 17Ba.** RIBEYE(B)-MBP binds to GCAP2-GST (arrowhead in lane 8) but not to GST alone (lane 7). It shows specific interaction of GCAP2/RIBEYE(B). Lane 3 and lane 4 are input fractions. **Figure 17Bb** shows the same blot as in Fig. 3Ba but after stripping and reprobings of the nitrocellulose with anti-GST antibodies to show equal loading of bait proteins. In (Fig. 3Ba,b) 10% of the input (lanes 1-4) was loaded. Always 100% of the immobilized protein pellets were loaded (lanes 5-8).

### 3.10. Characterisation of GCAP2 antibody

A polyclonal antibody against full-length bovine GCAP2-fusion protein was generated in rabbits by using purified, bacterially expressed GST-tagged full-length bovine GCAP2(1-204) as antigen(fig. 18).

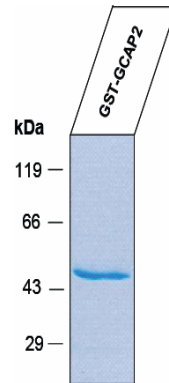


**Figure 18. Expression of GST-GCAP2 fusion protein.**

Coomassie Blue-stained SDS-PAGE shows the expression of GST-GCAP2 (49kDa) fusion protein which is expressed in BL21 electrocompetent bacterial cell

The 6<sup>th</sup> immune bleed (obtained 90 days after initial immunization) was used in the present experiments. The polyclonal GCAP2 antibody raised against full-length GCAP2 cross-reacts with GCAP1 (Fig. 19). A mouse monoclonal antibody against human GCAP2 that reacts with bovine GCAP2 but not with bovine GCAP1 (Fig. 22) was purchased from Santa Cruz (clone A1, sc-59543).

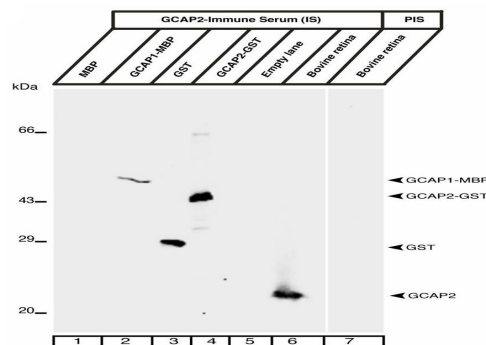


**Figure 19. Polyclonal GCAP2 antiserum cross-reacts with GCAP1.**

The polyclonal GCAP2 antiserum (generated against full-length bovine GCAP2 tagged with GST) detects GCAP2-GST (lane 4) as well as GCAP2 in bovine retinal extracts (lane 6). It also cross-reacts with GCAP1 (tested with purified GCAP1-MBP fusion protein lane 2). This cross-reactivity of the polyclonal GCAP2 immune serum with GCAP1 is not surprising because GCAP1 and GCAP2 are highly homologous (for review, see Palczewski et al., 2004). The GCAP2 pre-immune serum does not detect any protein band in the bovine retina (lane 7) and does not react with purified GCAP2-GST fusion protein (not shown).

### 3.11. Detection of GCAP2 in the bovine retina can be blocked by GCAP2-GST pre-absorption but not by GST pre-absorption.

The GCAP2 immunosignals were specific because the signal could be completely blocked by preabsorbing the polyclonal antiserum with GCAP2-GST fusion protein but not GST protein alone (Fig. 20).

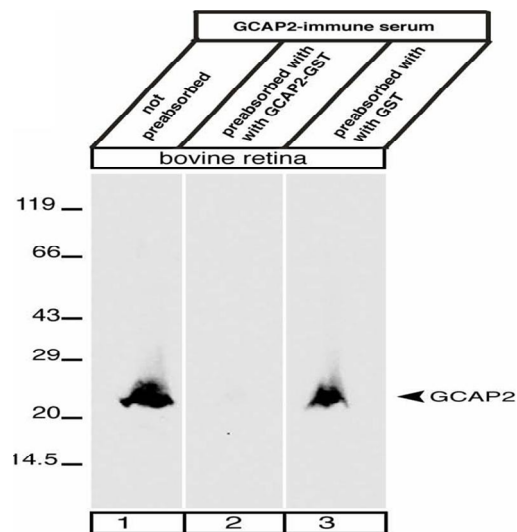


**Figure 20. Detection of GCAP2 in bovine retina can be blocked by GCAP2-GST but not by GST pre-absorption.** The polyclonal GCAP2 antibody specifically detected GCAP2 in a crude retinal extract as a single band of the expected molecular weight of approx. 24kDa. This band is specific because it is completely blocked if our GCAP2 antiserum was pre-absorbed with its antigen (GCAP2-GST, lane 2) but not by GST alone (lane 3).

### 3.12. RIBEYE INTERACTS WITH GCAP2 BUT NOT WITH GCAP1

As described above (Fig.19), the polyclonal GCAP2 antibody raised against full-length GCAP2 cross-reacts with GCAP1. Therefore, we analyzed whether GCAP1 interacts with RIBEYE in the YTH system. We found that RIBEYE(B) only interacts with the carboxyterminal region (CTR) of GCAP2 but not with the CTR of GCAP1 (Fig. 21B) indicating that RIBEYE specifically interacts with GCAP2 but not with GCAP1.

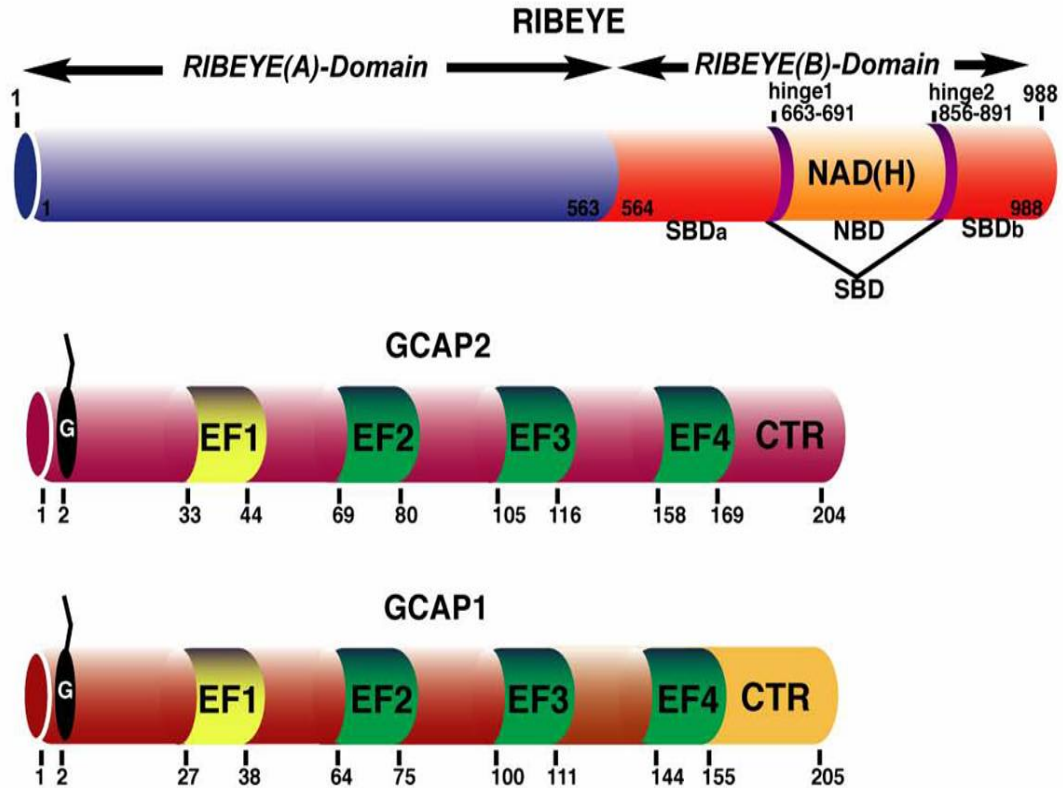


**Figure 21A.** Schematic depiction of the domain structure of RIBEYE, GCAP2 and GCAP1. GCAP1 and GCAP2 contain four EF-hands from which the first EF-hand (EF1, colored in yellow) is non-functional.

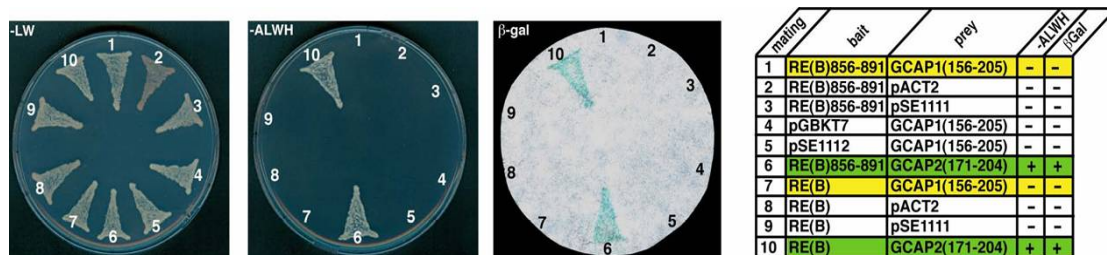


**Figure 21B. RIBEYE interacts with GCAP2 but not with GCAP1.**

YTH analyses showed that RIBEYE(B) interacts with the carboxyterminal region (CTR) of GCAP2 but not with the CTR of GCAP1. For convenience, experimental bait-prey pairs are underlayered in color (green in case of interacting bait-prey pairs; yellow in case of non-interacting bait-prey pairs); control matings are non-colored. The hinge 2 region of RIBEYE(B) interacts with the CTR of GCAP2 (mating #6) but not with the CTR of GCAP1 (matings #1, #7). The respective control matings (auto-activation controls; yeast matings #2-5, #8-9) did not show growth on -ALWH selective plates and expression of β-galactosidase activity. Mating #10 is an interaction positive control. RE(B)856-891 encodes for the hinge 2 region of RIBEYE(B) which was shown to be responsible for interaction with GCAP2 (Fig. 3C,D). Abbreviations: CTR, carboxyterminal region; EF1-EF4, EF-hand 1 - EF-hand 4.

### 3.13. Monoclonal GCAP2 antibody is specific for GCAP2

Since our polyclonal antibody against GCAP2 cross-reacts with GCAP1, we further tested whether commercially available monoclonal antibody against GCAP2 can cross-reactivity with GCAP1 but it reacts with bovine GCAP2 but not cross-react with bovine GCAP1(Fig. 22).

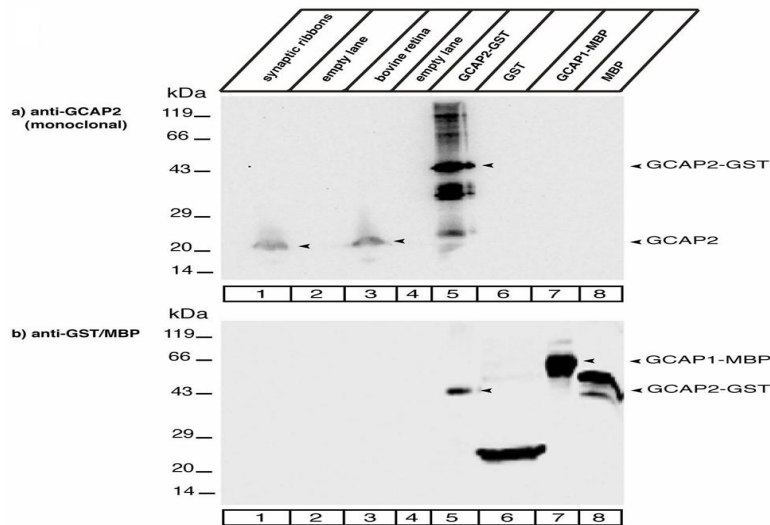


**Figure 22. The monoclonal GCAP2 antibody is specific for GCAP2 and does not react with GCAP1.** This monoclonal antibody detects GCAP2-GST (lane 5), but not GST alone (lane 6), GCAP1-MBP (lane 7) or MBP alone (lane 8). The monoclonal GCAP2 antibody specifically detects GCAP2 in purified synaptic ribbons (lane 1, Fig.14Ba) and in crude bovine retina extracts (lane 3, Fig.14Ba). the same blot as in Fig. 13Ba as shown after stripping and reprobing the blot with a mixture of anti-GST/anti-MBP antibodies to document the loading of fusion proteins.

### 3.14. RIBEYE and GCAP2 can be co-immunoprecipitated from the bovine retina

To analyse whether this interaction also occurs *in vivo*, we performed co-immunoprecipitation experiments using extracts from bovine retina. In fact, GCAP2 immune serum co-immunoprecipitated RIBEYE (Fig. 23A) whereas GCAP2 pre-immune serum did not demonstrating the specificity of the experiments. Identical results were obtained when RIBEYE antibodies were used for immunoprecipitation. RIBEYE immune serum but not RIBEYE pre-immune serum specifically co-immunoprecipitated GCAP2 (Fig. 23B).

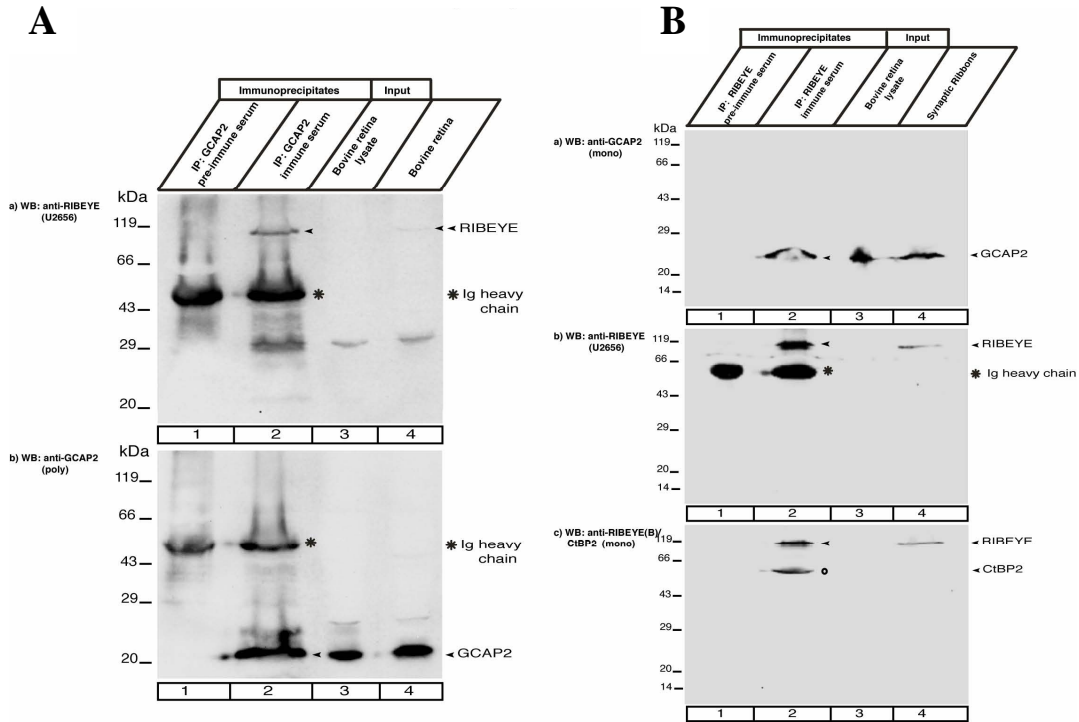


**Figure 23. Co-immunoprecipitation of RIBEYE and GCAP2 from the bovine retina.** In **A**) GCAP2 immune serum and GCAP2 pre-immune serum were tested for their capability to co-immunoprecipitate RIBEYE. RIBEYE is co-immunoprecipitated by GCAP2 immune serum (lane 2, Fig. 23Aa) but not by GCAP2 pre-immune serum (lane 1, Fig. 23Aa). Fig. 23Ab) shows the same blot as in Fig. 23Aa but reprobed with rabbit polyclonal anti-GCAP2 antibodies. This blot shows the presence of GCAP2 precipitated by the GCAP2 immune serum (lane 2) but not by the pre-immune serum (lane 1). Asterisks indicate the immunoglobulin heavy chains. In **B**) RIBEYE immune serum and RIBEYE pre-immune serum were tested for their capability to co-immunoprecipitate GCAP2. GCAP2 is co-immunoprecipitated by RIBEYE immune serum (lane 2, Fig. 23Ba) but not by RIBEYE pre-immune serum (lane 1, Fig. 23Ba). Fig. 23Bb) shows the same blot as in Fig. 15Ba but reprobed with polyclonal anti-RIBEYE (U2656). This blot shows the presence of RIBEYE that was immunoprecipitated by the immune serum but not by the pre-immune serum. Asterisks indicate the immunoglobulin heavy chains. Fig. 23Bc) shows the same blot as in Fig. 15Bb but reprobed with mouse monoclonal anti-CtBP2 antibodies which detects the B-domain of RIBEYE. This blot also shows the presence of RIBEYE precipitated by the immune serum (lane 2) but not by the pre-immune serum (lane 1). Asterisks indicate the immunoglobulin heavy chains. In addition to RIBEYE, a further protein at approx 50kDa is present in the experimental precipitate but not in the control immunoprecipitate. This band very likely is CtBP2 (circle in lane 2; Fig. 23Bc). CtBP2 is absent from purified synaptic ribbons which contain RIBEYE and CtBP1 but not CtBP2 (Schwarz et al., unpublished data). In the input lanes, 0.5% of total input was loaded in (A) and 1% of total input in (B). The immunoprecipitates are always 100%.

The co-immunoprecipitation experiments prove that the RIBEYE/GCAP2 interaction also occurs *in-situ* in the retina and emphasizes the physiological relevance of the RIBEYE/GCAP2 interaction. This assumption is further supported by our findings that GCAP2 is also a component of purified synaptic ribbons as shown both with a polyclonal as well as with the monoclonal GCAP2 antibody (Fig. 23A,B).

### 3.15. GCAP2 present in purified synaptic ribbons

RIBEYE is a major component of synaptic ribbons (Schmitz et al., 2000; Zenisek et al., 2004; Wan et al. 2005, Magupalli et al., 2008). Therefore it is important to know whether GCAP2 present in purified synaptic ribbons. We used both GCAP2 polyclonal (rabbit) and monoclonal (mouse) antibodies to answer this question. The polyclonal GCAP2 antiserum detects GCAP2 both in extracts of the bovine retina (lane 2) as well as in the purified synaptic ribbon fraction (lane 1) (100 $\mu$ g of protein loaded in each lane) (Fig. 24A). Similar to the findings obtained with the polyclonal GCAP2 antibody, the monoclonal GCAP2 antibody also detects GCAP2 in both retinal extracts (lane 1, 100 $\mu$ g of protein loaded) and purified synaptic ribbon fraction (lane 2, 30 $\mu$ g of protein loaded) (Fig. 24B).

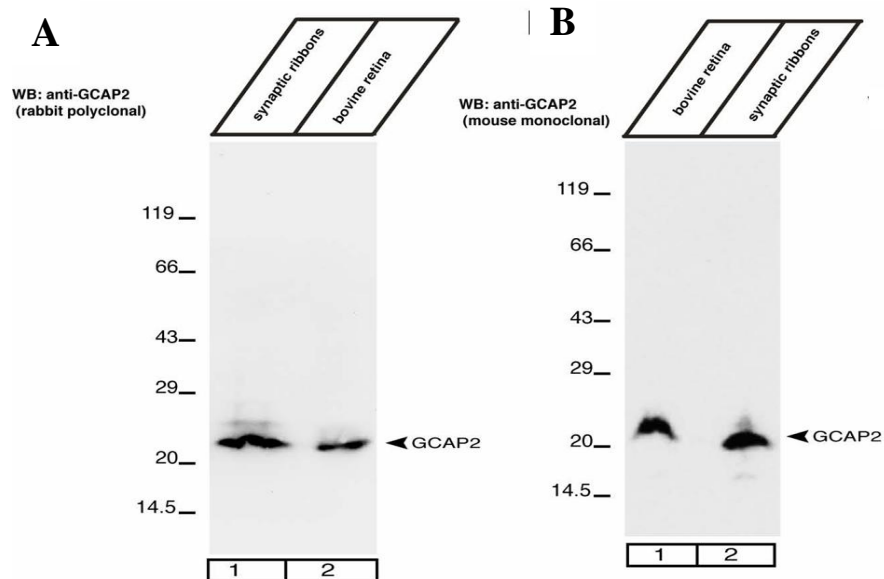


**Figure 24. GCAP2 is present on purified synaptic ribbons.**

(A) The polyclonal GCAP2 antiserum detects GCAP2 both in extracts of the bovine retina (lane 2) as well as in the purified synaptic ribbon fraction (lane 1) (100 $\mu$ g of loaded protein in each lane). (B) The monoclonal GCAP2 antibody detects GCAP2 both in retinal extracts (lane 1, 100 $\mu$ g of protein loaded) as well as in the purified synaptic ribbon fraction (lane 2, 30 $\mu$ g of protein loaded).

### 3.16. GCAP2 co-localizes with synaptic ribbons in photoreceptor ribbon synapses

We performed immunolabeling experiments with a polyclonal GCAP2 antibody raised against bacterially expressed and purified full-length bovine GCAP2 as well as with the commercial monoclonal mouse GCAP2 antibody (Fig. 25A-F).

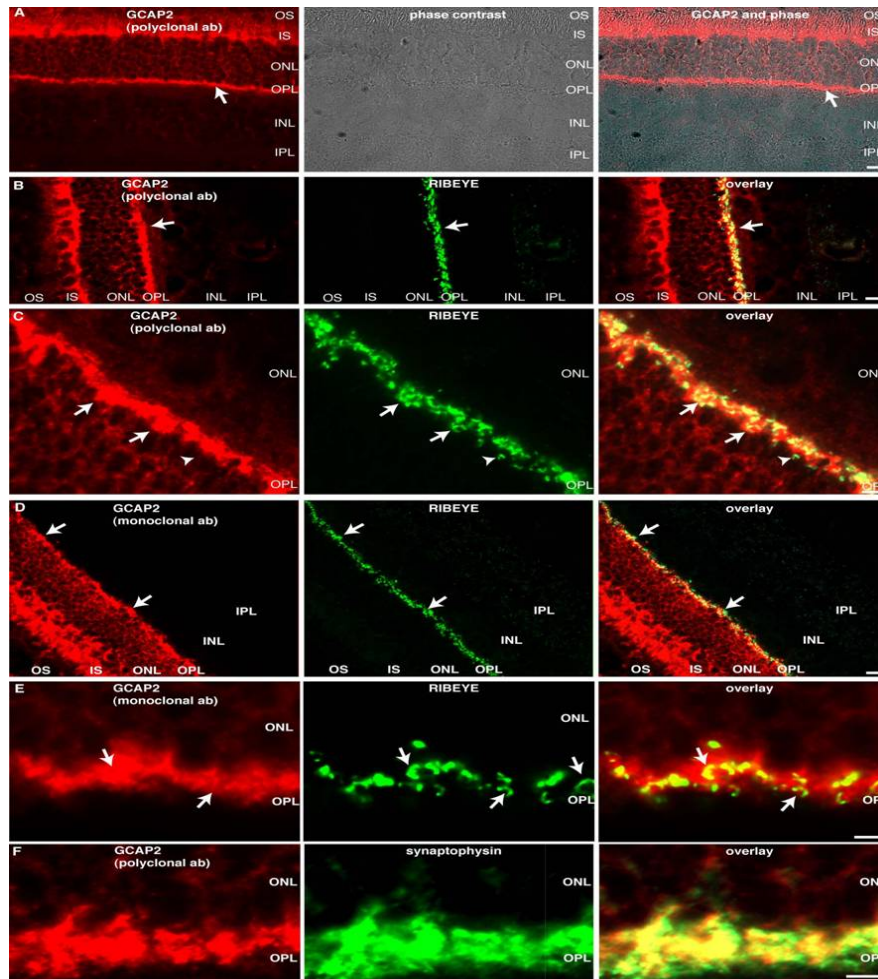


**Figure 25. GCAP2 co-localizes with synaptic ribbons in photoreceptor ribbon synapses.** Immunolabeling of the bovine retina with rabbit polyclonal antibodies against GCAP2 and mouse monoclonal antibodies against RIBEYE(B)/CtBP2 (A-C) or mouse monoclonal antibodies against GCAP2 (A1, Santa Cruz) and rabbit polyclonal antibodies against RIBEYE (U2656) (D,E). Both the polyclonal (A-C) as well as the monoclonal (D) GCAP2 antibody generated a strong immunolabel particularly in the inner segments (IS) of bovine photoreceptor cells. In addition, the OPL that contains photoreceptor ribbon synapses is strongly labeled by the polyclonal (A-C) and monoclonal GCAP2 antibodies (D-E). The OPL which is immunolabeled by the polyclonal (A,B) and monoclonal GCAP2 antibodies (D-E) is labeled by arrows in (A,B). The GCAP2 immunosignal co-localized with synaptic ribbons which were visualized by immunolabeling with RIBEYE antibodies (B-E, arrows). Strong immunosignals of GCAP2 were found at synaptic ribbons and in close vicinity to synaptic ribbons. Most, but not all ribbons, co-localize with GCAP2. The arrowhead in (C) denotes synaptic ribbons which were not associated with detectable amounts of GCAP2. (F) The GCAP2 immunosignal in the outer plexiform layer (OPL) largely co-localizes with the immunosignal of synaptophysin, a marker protein of synaptic vesicles highly enriched in the presynaptic terminals (arrow in F). Abbreviations: OS, outer segment; IS, inner segment; ONL, outer nuclear layer; OPL, outer plexiform layer; INL, inner nuclear layer; IPL, inner plexiform layer. Scale bar: 15µm (A,B,D); 10µm (C,E,F).

**In collaboration with Sivaraman Natarajan**

we observed a strong GCAP2 immunolabeling in the synaptic terminals of bovine photoreceptors in addition to a strong expression particularly in the inner segments (Fig. 25A-F). A strong immunolabeling of the rod presynaptic terminals was observed, the labeling of the larger cone terminals was less intense. Double immunolabeling demonstrated that RIBEYE and GCAP2 co-localized in the presynaptic terminals of photoreceptors (Fig. 25B-E). In Fig. 25F presynaptic terminals were labelled with antibody against Synaptophysin. GCAP2 was found at synaptic ribbon sites (immunolabeled by RIBEYE antibodies) and close to synaptic ribbons. Most but not all ribbons were labelled (Fig. 25). Furthermore, identical results, as described above for the polyclonal GCAP2 antibody, were obtained with a commercially available monoclonal antibody against GCAP2 (Fig. 25D-E).that does not cross-react with GCAP1 (Fig. 22).

### **3.17. GCAP2 is weakly expressed in cone photoreceptor ribbon synapses**

The bovine retina is a mixed retina that contains both rod and cone photoreceptors. As already shown in Fig. 25 GCAP2 is strongly expressed in rod photoreceptor synapses where it co-localizes with synaptic ribbons (immunolabeled with RIBEYE antibodies). Rod synapses only contain a single synaptic ribbon in their active zone (Schmitz et al., 1996, 2000). The cone synapses (arrows) only show a weak GCAP2 immunoreactivity. Cone synapses can be readily identified in these sections and discriminated from rod synapses based on their typical localization closer to the inner nuclear layer (INL), their large size and the presence of numerous synaptic ribbons (Schmitz et al., 1996; 2000). In (Fig. 26C,D) cone synapses were visualized with polyclonal antibodies against SV2A which is only expressed in cone synapses but not in rod synapses (Wang et al., 2003; Morgans et al., 2009); GCAP2 was immunodetected with monoclonal GCAP2 antibody in (Fig. 26C,D). In (Fig. 26E) cone synapses were identified with fluorescently labelled peanut agglutinin (PNA) (Wang et al., 2003; Morgans et al., 2009). In these incubations, the GCAP2 immunosignal neither co-localized with SV2A (Fig. 26C,D) nor with PNA (Fig. 26E) further demonstrating that GCAP2 is not or weakly expressed in cone photoreceptor synapses.

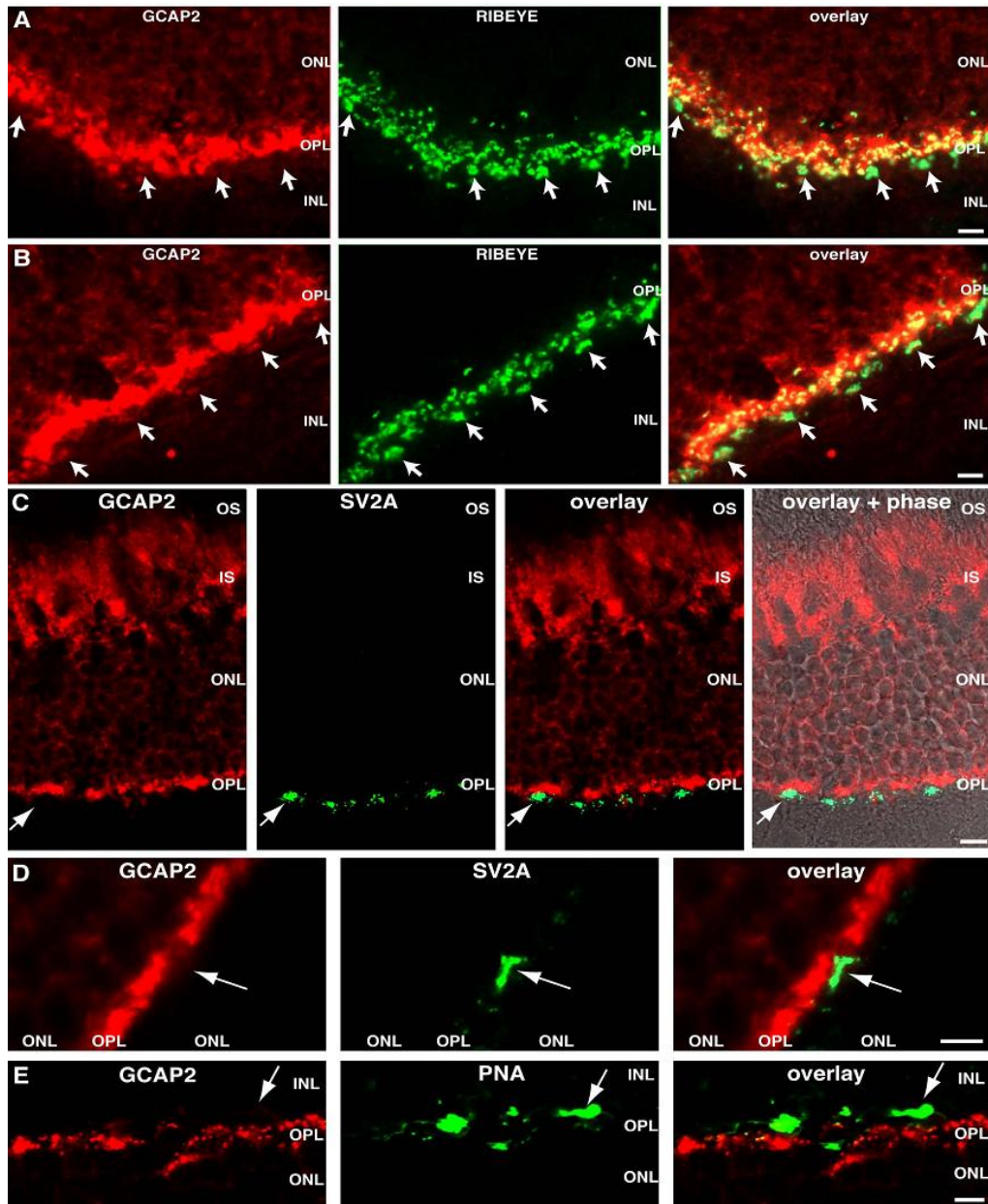


**Figure 26. GCAP2 is weakly expressed in cone photoreceptor ribbon synapses.**

Cryostat sections of the bovine retina immunolabeled with rabbit polyclonal antibodies against GCAP2 and monoclonal antibodies against RIBEYE(B)/CtBP2 (BD Transduction Laboratories) (A,B). In (C,D) cone synapses were visualized with polyclonal antibodies against SV2A which is only expressed in cone synapses but not in rod synapses (Wang et al., 2003; Morgans et al., 2009); GCAP2 was immunodetected with monoclonal GCAP2 antibody in (C,D). In (E) cone synapses were identified with fluorescently labelled peanut agglutinin (PNA) (Wang et al., 2003; Morgans et al., 2009). In these incubations, the GCAP2 immunosignal neither co-localized with SV2A (C,D) nor with PNA (E) further demonstrating that GCAP2 is not or weakly expressed in cone photoreceptor synapses. Abbreviations: ONL, outer nuclear layer; OPL, outer plexiform layer; INL, inner nuclear layer. Scale bars: 10µm.

**Contributed by Sivaraman Natarajan**

### 3.18. Labeling of presynaptic GCAP2 immunosignals can be blocked by pre-absorption with GCAP2-GST but not by GST .

GCAP2 was found at synaptic ribbon sites (immunolabeled by RIBEYE antibodies) and close to synaptic ribbons (Fig. 26). Most but not all ribbons were labeled (Fig. 26).

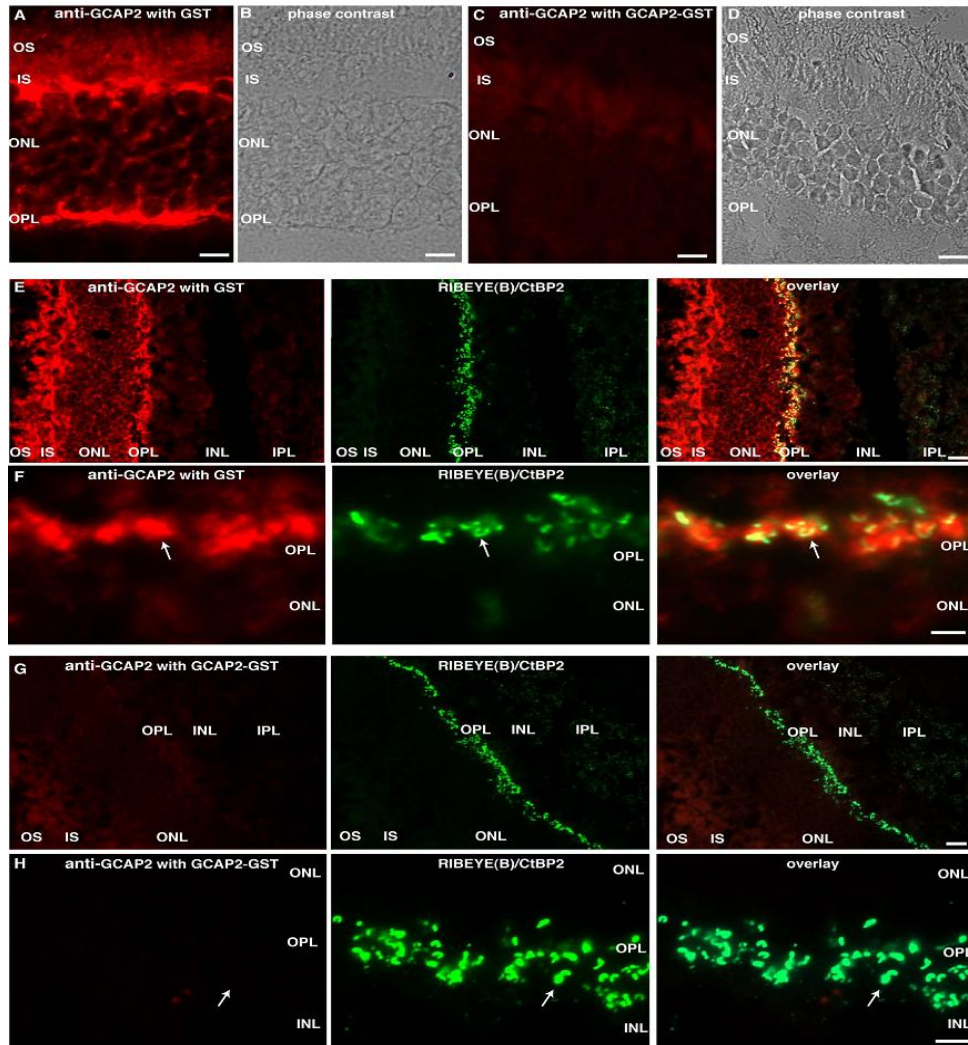


**Figure 27. Labeling of presynaptic GCAP2 immunosignals can be blocked by GCAP2-GST but not by GST pre-absorption.** Cryostat sections immunolabeled with polyclonal anti-GCAP2 antiserum pre-absorbed with GST (A,B,E,F) or GCAP2-GST (C,D,G,H). (A-D) The GCAP2 immunolabeling in the OPL, as well as in the IS and OS cannot be blocked by pre-absorption with GST (A) but by pre-absorption with GCAP2-GST (C). After pre-absorption of the GCAP2 polyclonal antiserum the GCAP2 immunosignal is gone (C) whereas after pre-absorption with GST the GCAP2 immunosignal remained unchanged (A). (B,D) represent the respective phase pictures for (A,C). (E,F) Pre-absorption of GCAP2 antiserum with GST does not influence the GCAP2- as well as the RIBEYE- immunosignal in ribbon synapses of the OPL and IPL. In contrast, pre-absorption of the GCAP2 antiserum with GCAP2-GST (G,H) abolishes GCAP2 immunosignals but not the RIBEYE immunosignals demonstrating the specificity of the GCAP2 pre-absorption. (E,G) are low magnification micrographs from the indicated immunolabelings (F,H) are high magnification micrographs from the indicated immunolabelings. Abbreviations: OS, outer segment; IS, inner segment; ONL, outer nuclear layer; OPL, outer plexiform layer; INL, inner nuclear layer; IPL, inner plexiform layer. Scale bars: 10  $\mu$ m (A-D, F,H); 30  $\mu$ m (E, G).

**Contributed by Sivaraman Natarajan**

The GCAP2 immunosignals were specific because the signal could be completely blocked by preabsorbing the polyclonal antiserum with GCAP2-GST fusion protein but not GST protein alone (Fig. 27) polyclonal anti-GCAP2 antiserum pre-absorbed with GST (**A,B,E,F**) or GCAP2-GST (**C,D,G,H**). The GCAP2 immunolabeling in the OPL, as well as in the IS and OS cannot be blocked by pre-absorption with GST (**A**) but by pre-absorption with GCAP2-GST (**C**). After pre-absorption of the GCAP2 polyclonal antiserum the GCAP2 immunosignal is gone (**C**) whereas after pre-absorption with GST the GCAP2 immunosignal remained unchanged (**A**). Pre-absorption of GCAP2 antiserum with GST (**E,F**) does not influence the GCAP2- as well as the RIBEYE- immunosignal in ribbon synapses of the OPL and IPL. In contrast, pre-absorption of the GCAP2 antiserum with GCAP2-GST (**G,H**) abolishes GCAP2 immunosignals but not the RIBEYE immunosignals demonstrating the specificity of the GCAP2 pre-absorption.

### **3.19. RIBEYE and GCAP2 are localized very close to each other in photoreceptor synapses as judged by *in-situ* Proximity Ligation Assays (PLA).**

The close association of RIBEYE and GCAP2 *in-situ* was further supported by *in-situ* Proximity Ligation Assays (PLA assays; Gustafsdottir et al., 2005) on flash-frozen mouse retinal sections (Fig. 28). PLA *in-situ* interaction assays critically depend on the close proximity of the interaction partners (Söderberg et al., 2006). In PLA assays, the secondary antibodies are labeled with specific oligonucleotides. Only if the two antigens detected by two different primary antibodies are in close proximity to each other (less than 40nm), a linker oligonucleotide can hybridize to the distinct PLUS/MINUS oligonucleotides conjugated to the secondary antibodies and provide the template for a rolling circle amplification (Söderberg et al., 2006, 2008). The product of the rolling circle amplification is then specifically detected by a fluorescent oligonucleotide probe (Fig. 28). In case of RIBEYE and GCAP2 a strong PLA interaction signal was observed in the OPL (Fig. 28A-E).

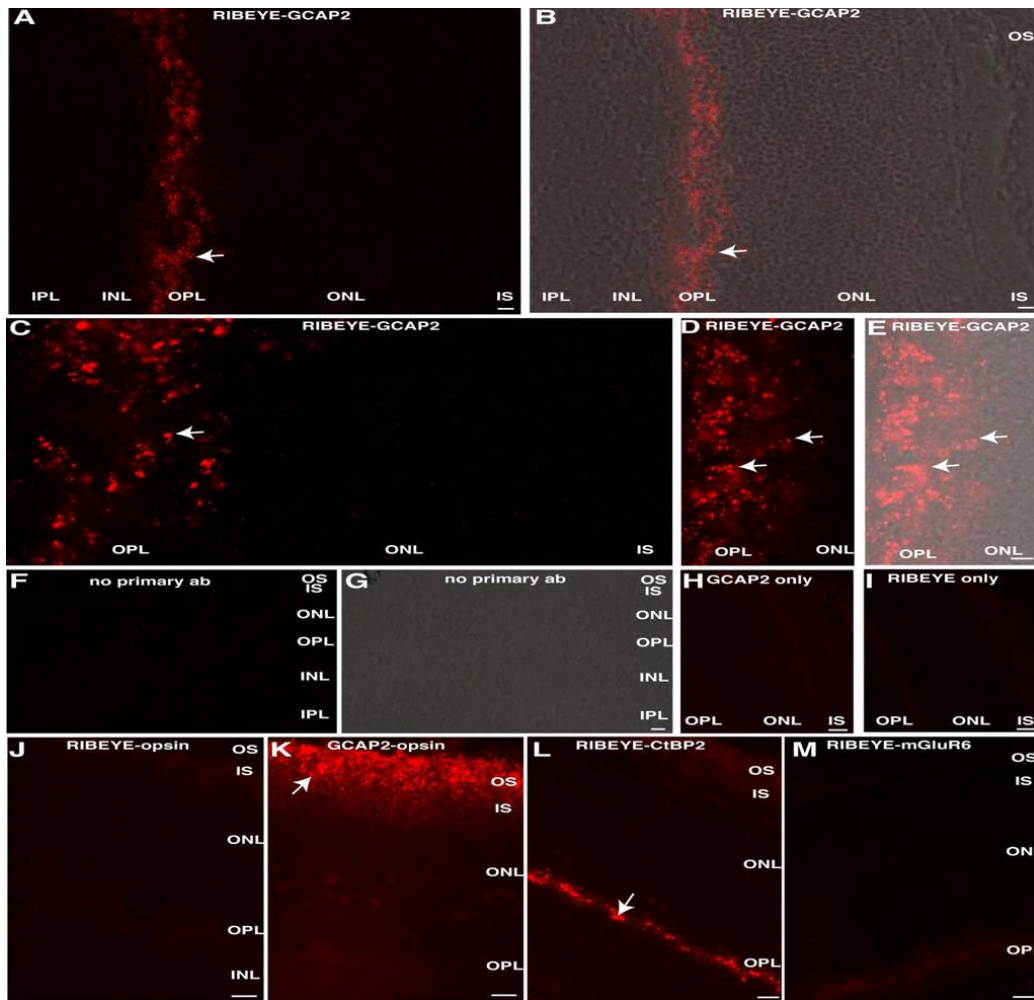


**Figure 28. Co-localization of RIBEYE and GCAP2 as analyzed by *In-situ* Proximity Ligation Assays (PLA).** Co-localization of RIBEYE and GCAP2 in retinal sections *in-situ* was analyzed using proximity ligation assays (Gustafsdottir et al., 2005; Söderberg et al., 2008). This assay critically depends upon the distance of the interaction partners and a positive PLA interaction signal is only generated if the interaction partners are located in a distance of less than 40nm (Söderberg et al., 2006). A strong PLA interaction signal in the OPL, as visualized by the red fluorescence signal, was observed between RIBEYE and GCAP2 (Fig. 28A-E). In Fig. 28A,B an overview of the PLA signals is given at a low magnification. Fig. 28C-E are high magnifications of the OPL. In Fig. 28B and in Fig. 28E the PLA signals of Fig. 28A and Fig. 28D is superimposed onto the respective phase images. Arrows point to PLA interaction signals in the OPL indicating close proximity of RIBEYE and GCAP2. No PLA interaction signal was present in the OPL if both primary antibodies were omitted (Fig. 28F,G) or if only one primary antibody was applied (Fig. 28H,I) demonstrating the specificity of the detection assay. In Fig. 28G the PLA signal of Fig. 19F is superimposed onto the respective phase image. As a further negative control RIBEYE and opsin were tested for interaction by PLA and did not produce any signal in the OPL (Fig. 28J) again demonstrating specificity of the PLA interaction assays. In contrast, a mixture of RIBEYE (U2656)/CtBP2 antibodies (positive control) gave a strong PLA interaction signal in the OPL (Fig. 28L). A mixture of GCAP2/opsin antibodies generated a strong PLA interaction signal in the outer/inner segments but not in the OPL (Fig. 28K). RIBEYE and mGluR6 which are located relatively closely together but beyond the critical distance of PLA assays of ~40nm (Söderberg et al., 2006) did not produce a PLA interaction signal in the OPL (Fig. 28M) demonstrating that PLA interaction signals clearly indicate very close proximity of the analyzed antigens. The arrows in K and L point to PLA interaction signals. Abbreviations: IS, inner segments; ON, outer nuclear layer; OPL, outer plexiform layer; INL, inner nuclear layer; IPL, inner plexiform layer. Scale bars: 10µm (A-J).

**Contributed by Sivaraman Natarajan**

There was no interaction signal present in the OPL if both primary antibodies were omitted or if only one primary antibody was applied (followed by incubation with the two oligonucleotide-conjugated secondary antibodies) demonstrating the specificity of the detection assay. As a further negative control RIBEYE and opsin were tested for interaction by PLA and did not produce any signal in the OPL further demonstrating specificity of the PLA interaction assays (Fig. 28J). In contrast, a mixture of rabbit polyclonal RIBEYE (U2656) and mouse monoclonal CtBP2 antibodies (positive control) gave a strong PLA interaction system in the OPL (Fig. 28L). Remarkably, RIBEYE and mGluR6 did not produce a PLA interaction signal in the OPL (Fig. 28M). RIBEYE at the synaptic ribbon and mGluR6 at the tips of invaginating ON bipolar cells of the ribbon synapse obviously are not close enough to produce a PLA interaction signal further emphasizing the very close proximity of GCAP2 and synaptic ribbons in the presynaptic terminal *in-situ* (see discussion).

### **3.20. Characterization of RIBEYE(B)-GCAP2 binding**

In order to further characterize binding of GCAP2 to RIBEYE we analyzed why the presence of 1mM  $\beta$ ME is essential for RIBEYE-GCAP2 interaction in the fusion protein pull-down experiments. If  $\beta$ ME was absent from the incubation buffer, RIBEYE(B) did not bind to GCAP2-GST in the fusion protein pull-down assays (Fig. 17A; Fig. 30A,B). It is well known that  $\beta$ ME can cleave disulfide bridges (for review, see Berg et al., 2007). rRIBEYE(B)-domain contains 8 cysteine residues: RIBEYE(B)C587; RIBEYE(B)C603; RIBEYE(B)C667; RIBEYE(B)C683; RIBEYE(B)C781; RIBEYE(B)C786; RIBEYE(B)C861 and RIBEYE(B)C899. From these cysteines only cysteine C667 and cysteine C899 in the SBD of RIBEYE are predicted to be close enough to form disulfide bridges in monomeric RIBEYE (Fig. 29A,B). RIBEYE(B)C667 is located in SBDa spatially close to RIBEYE(B)899C in the SBDb and a disulfide bridge between these residues would thus link the two different parts of the SBD with each other. We analyzed RIBEYE(B)C899S for its capability to interact with GCAP2 and tested whether this RIBEYE point mutant needs  $\beta$ ME to interact with GCAP2 in pull-down assays. Most interestingly, RIBEYE(B)C899S interacted with GCAP2 in the absence of  $\beta$ ME (Fig. 30B) demonstrating that RIBEYE(B)C899S does not need  $\beta$ ME to bind to GCAP2.

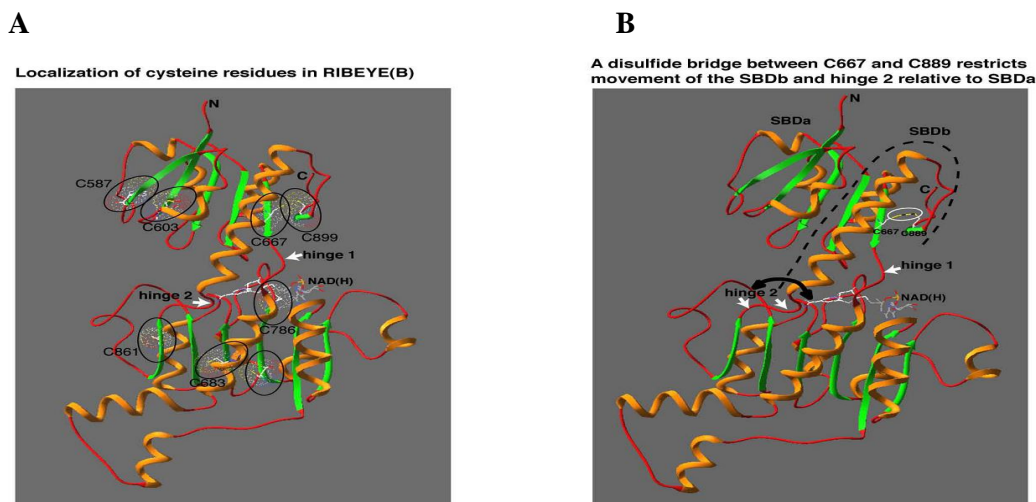


**Figure 29.** (A) Localization of cysteine residues in RIBEYE(B): Only cysteine C667 and cysteine C899 are located within a distance of  $\sim 4\text{\AA}$  to form a disulfide bridge. (B) A predicted disulfide bridge between C667 in SBDA and C889 in SBDb (indicated by a yellow-black dashed line) can be expected to limit the rotational freedom of the hinge 2 region and the movement of the SBDb relative to SBDA. The structure model in (A,B) starts at amino acid P575 and ends at amino acid F905 of RIBEYE and is based on the crystal structure of tCTBP1 (Kumar et al., 2002; Nardini et al., 2003; see also Magupalli et al., 2008; Alpadi et al., 2008).

RIBEYE(B)C899S stimulates GCAP2 binding to RIBEYE whereas RIBEYE(B)C683S does not

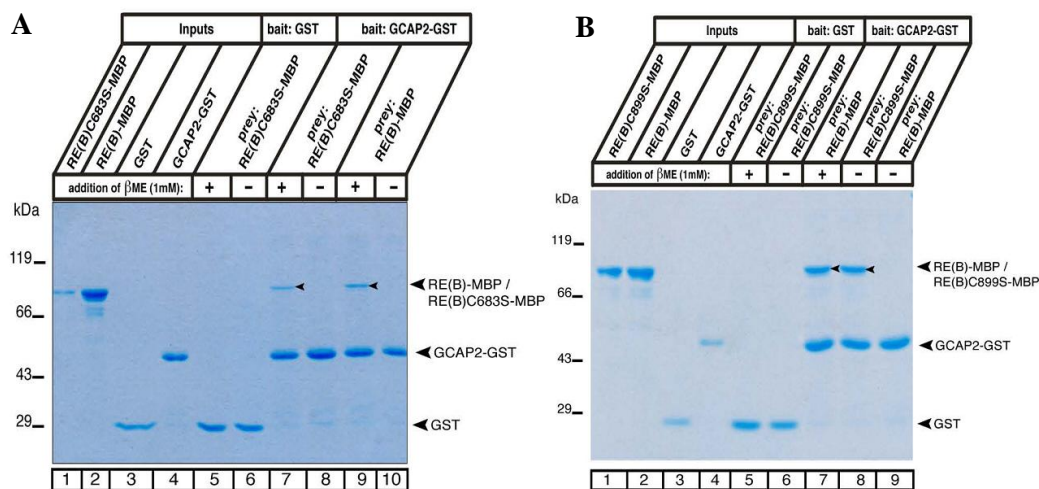


**Figure 30.** The binding of GCAP2 to the hinge 2 region of RIBEYE(B) is modulated by the substrate-binding subdomain (SBD) of RIBEYE(B). (A, B) Fusion protein pull-down assays analyzed by SDS-PAGE (10% acrylamide gels). (A) GCAP2 does not pull-down both wild type RE(B) as well as RE(B)C683S in the absence  $\beta$ ME (lanes 8,10) but only in the presence of  $\beta$ ME (lanes 7,9; arrowheads). (B) In contrast, GCAP2 pulls down RIBEYE(B)C899S in the absence of  $\beta$ ME lane 8 (arrowhead).

The binding of RIBEYE(B)C899S to GCAP2 in the absence of  $\beta$ ME indicates that cysteine C899 is part of the “ $\beta$ -mercaptoethanol effect” that promotes GCAP2/RIBEYE interaction. Mutating RIBEYE(B)C683 (which is located in the homo-dimerization interface of the NBD (Fig. 30A) into RIBEYE(B)C683S did not change the dependency of GCAP2/RIBEYE binding from the presence of  $\beta$ ME (Fig.

30A, lane 7-8). RIBEYE(B)C683S did not interact with GCAP2 in the absence of  $\beta$ ME (Fig. 30A, lane 8) demonstrating that only specific cysteine mutations of RIBEYE(B) lead to an independence from  $\beta$ ME for GCAP2 binding. RIBEYE(B)C899S which was shown to be important in modulating GCAP2/RIBEYE interaction (Fig. 30B, Fig. 29A,B) is located in the SBD of RIBEYE(B).

### 3.21. Mutations in SBD of RIBEYE influence the binding of GCAP2 to RIBEYE(B)

I also tested non-cysteine mutants of the SBD, namely RIBEYE(B)F904W and RIBEYE(B) $\Delta$ CTR, for their capability to interact with GCAP2. RIBEYE(B)F904 is located in the SBD<sub>b</sub> at the end of the modelled structure (Fig. 9B; Fig. 10A,B; Fig. 29A,B). RIBEYE(B) $\Delta$ CTR lacks the hydrophobic carboxyterminal region (CTR; aa912-918 of RIBEYE); the structure of the CTR has not yet been resolved (Kumar et al., 2002; Nardini et al., 2003). RIBEYE(B)F904W and RIBEYE(B) $\Delta$ CTR did not interact with GCAP2 in the YTH system although these mutants are not within the proper binding region of RIBEYE for GCAP2 (Fig. 29A,B). We interpret these data that the latter mutants of the SBD are likely not relevant for a direct physical interaction with GCAP2 but are less well capable to stabilize a conformation of the hinge 2 region that can bind GCAP2.

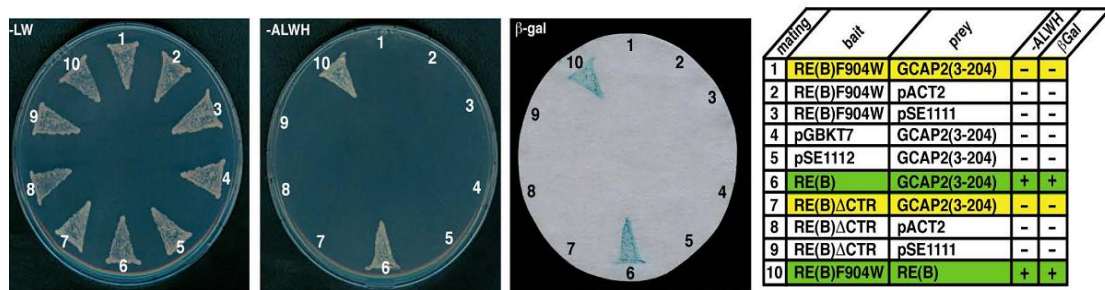


**Figure 31. Mutations in SBD of RIBEYE influence the binding of GCAP2 to RIBEYE(B):** Point mutating F904 in RIBEYE(B) to RE(B)F904W abolishes RIBEYE(B)-GCAP2 interaction in the YTH system (mating #1). Similarly, deleting the hydrophobic carboxyterminal region (CTR) of RIBEYE(B) results in a lack of interaction between RIBEYE and GCAP2 in the YTH system (mating #7).

### 3.2.2. RIBEYE(B)-GCAP2 interaction is NAD(H)-dependent

I tested whether the reducing power of  $\beta$ ME is important in promoting RIBEYE-GCAP2 interaction. RIBEYE(B) efficiently binds reduced NAD(H) (Schmitz et al., 2000; Alpadi et al., 2008) Therefore, we analyzed whether NADH could replace  $\beta$ ME in promoting RIBEYE-GCAP2 interaction. Indeed, GCAP2 bound to RIBEYE(B) in the absence of  $\beta$ ME if NADH was present in the incubation buffer (Fig. 32A,B). Surprisingly, also the oxidized form of NAD(H),  $\text{NAD}^+$ , induced RIBEYE(B)-GCAP2 interaction in the absence of  $\beta$ ME (Fig. 32B) demonstrating that the reducing power of NADH does not play a major role in promoting GCAP2-RIBEYE interaction. Both the oxidized as well as the reduced form of NAD(H) ( $\text{NAD}^+$  and NADH, respectively) stimulate RIBEYE-GCAP2 interaction.

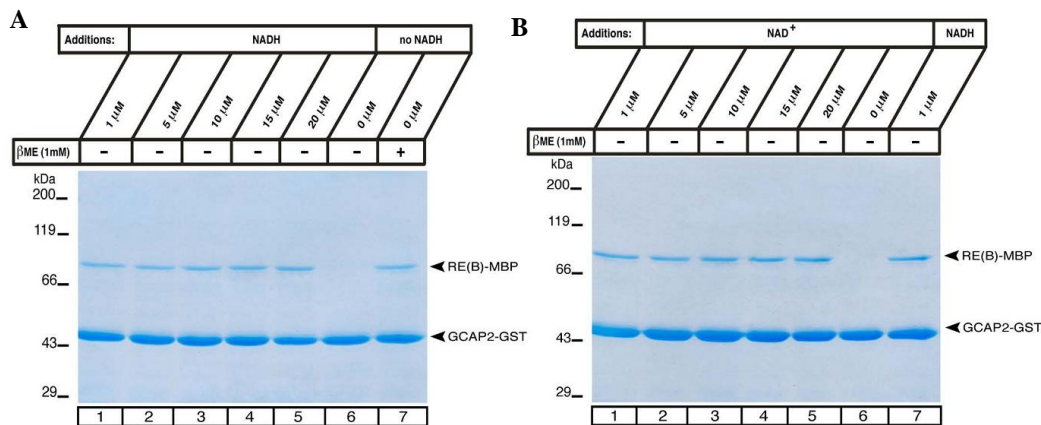


**Figure 32. NADH and  $\text{NAD}^+$  are essential co-factors for the binding between RIBEYE and GCAP2 in the absence of  $\beta$ -mercaptoethanol ( $\beta$ -ME).** Fusion protein pull-down assays were analyzed by SDS-PAGE (10% acrylamide gels). RIBEYE(B) binds NAD(H) with high affinity (Schmitz et al., 2000). (**A,B**) In fusion protein pull-down assays, GCAP2-RIBEYE(B) interaction requires the presence of  $\beta$ -mercaptoethanol ( $\beta$ -ME). If  $\beta$ ME is absent GCAP2 does not bind to RIBEYE(B) unless NADH or  $\text{NAD}^+$  is added to the incubation buffer. Both the reduced form (NADH) (Fig. 22A) as well as the oxidized form ( $\text{NAD}^+$ ) (Fig. 22B) promote RIBEYE(B)-GCAP2 interaction.

### 3.2.3. Low concentrations of NAD(H) promote RIBEYE/GCAP2 interaction

In the fusion protein pull-down analyses the fusion proteins were used at an equimolar concentration of  $0.8 \mu\text{M}$ . We tested whether low concentrations of  $\text{NAD}^+$  (**A**) or NADH (**B**) (ranging from  $0.1$  to  $0.8 \mu\text{M}$ ) were able to stimulate binding of RIBEYE to GCAP2. Even the lowest concentration of  $\text{NAD}^+$  or NADH ( $0.1 \mu\text{M}$ ) stimulated binding of RIBEYE(B)-MBP to GCAP2-GST (lanes 3-6); without addition of  $\text{NAD}^+$  or NADH no binding was observed between GCAP2-GST and RE(B)-MBP in the absence of  $\beta$ ME (lane 1). The addition of  $\beta$ ME replaced the need for either  $\text{NAD}^+$  or NADH in promoting GCAP2-RIBEYE(B) interaction: even in the

absence of  $\text{NAD}^+$ /NADH GCAP2 bound to RIBEYE(B) if  $\beta\text{ME}$  was present (lane 2). In (C) and (D) even lower concentrations of  $\text{NAD}^+$  (C) or NADH (D) were tested.  $\text{NAD}^+$ /NADH promoted RIBEYE(B)/GCAP2 binding already at concentrations as low as 10nM (lane 4). If still lower concentrations of NAD(H) were used, i.e. 1nM and 5nM (lanes 2,3) interaction was no longer observed, similar to the absence of interaction in the absence of any  $\text{NAD}^+$  (lane 1; Fig. 33C)/ or NADH (lane 1; Fig. 33D). The incubation buffer in the experiments shown in Fig. 33C,D did not contain any  $\beta\text{ME}$ .

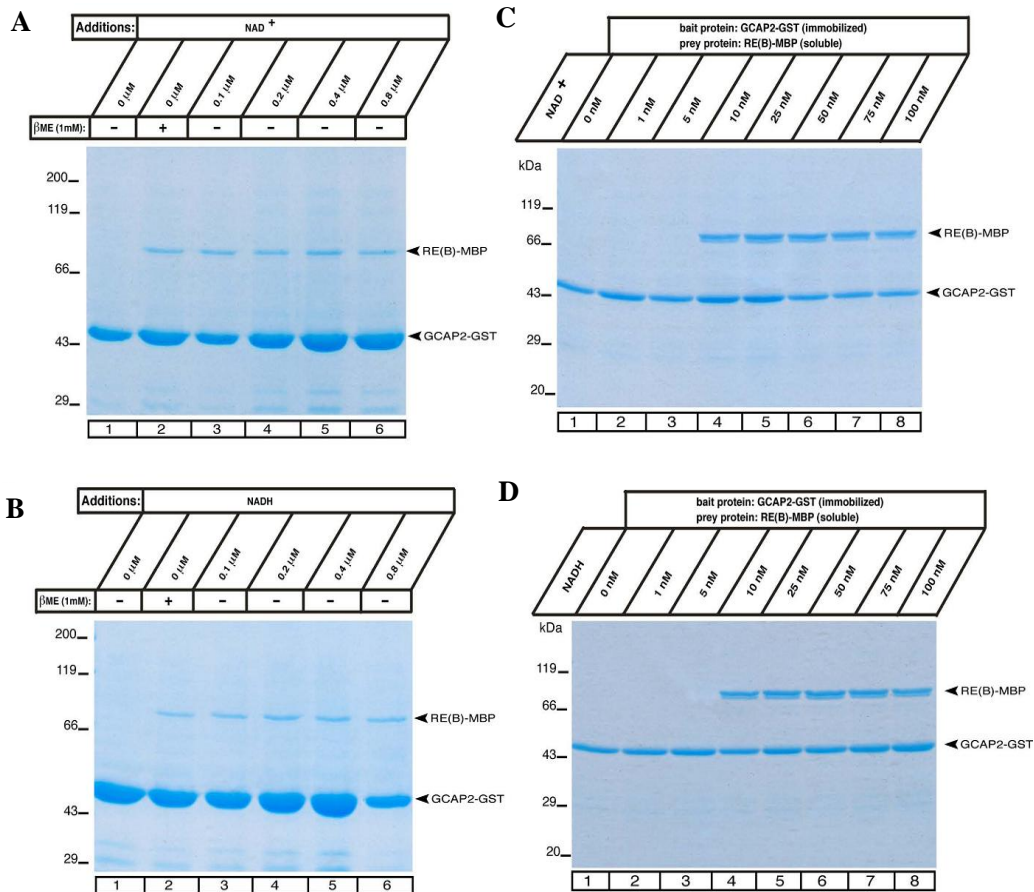


**Figure 33. Low concentrations of NAD(H) promote RIBEYE/GCAP2 interaction.**

The binding of RIBEYE(B)-MBP (0.8  $\mu\text{M}$ ) to GST-GCAP2 (0.8  $\mu\text{M}$ ) was analyzed in the presence of increasing concentrations of  $\text{NAD}^+$  (A,C) or NADH (B,D). In A and B we tested low concentration of  $\text{NAD}^+$  and NADH ranging from 0.1  $\mu\text{M}$  to 0.8  $\mu\text{M}$  (lane 3 to lane 6) were stimulating binding of RE(B)MBP to GCAP2-GST. In C and D we tested even lower concentration of  $\text{NAD}^+$  and NADH ranging from 1nM to 100nM. At the concentration of 10nM (lane 4) both  $\text{NAD}^+$  and NADH promotes GCAP2/RIBEYE(B) binding but if we used lower concentration i.e., 1nM and 5nM of  $\text{NAD}^+$  and NADH interaction was no longer observed (lane 2,3).

### 3.24. NAD(H) binding-deficient RIBEYE(B)G730A mutant

I analyzed the NAD(H)-binding-deficient RIBEYE point mutant, RIBEYE(B)G730A, (Magupalli et al., 2008; Alpadi et al., 2008) in the YTH system for interaction with GCAP2. In agreement with the essential requirement of NAD(H) in promoting RIBEYE/GCAP2 interaction in fusion protein pull-down analyses, GCAP2 did not interact with this NAD(H) binding-deficient RIBEYE point mutant in the YTH system (Fig. 34) although this RIBEYE point mutant was able to efficiently hetero-dimerize with RIBEYE(B) wildtype protein .

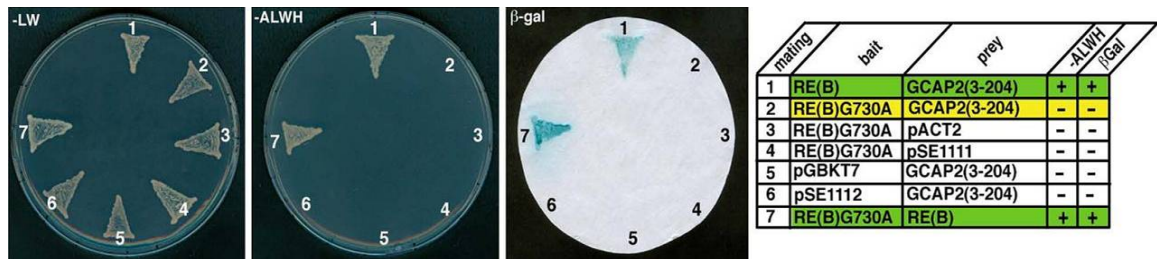


**Figure 34. NAD(H) binding-deficient RIBEYE(B)G730A mutant.** GCAP2 did not bind to the NAD(H)-binding-deficient RIBEYE point mutant RIBEYE(B)G730A in the YTH system as judged by the lack of growth on –ALWH selective medium and lack of β-galactosidase expression (mating #2). Mating #1 indicates a positive control (RIBEYE(B) mated with GCAP2). Matings #3-6 show the respective auto-activation controls. RIBEYE(B)G730A is still able to homo-dimerize with wildtype RIBEYE(B) demonstrating that RIBEYE(B)G730A is not misfolded (mating #7). For convenience, experimental bait-prey pairs are underlayered in color (green in case of interacting bait-prey pairs; yellow in case of non-interacting bait-prey pairs); control matings are non-colored.

### 3.25. Viral overexpression of GCAP2 in presynaptic photoreceptor terminals promotes disassembly of photoreceptor synaptic ribbons.

We further tested whether synaptic GCAP2 expression could be related to the  $Ca^{2+}$ -dependent dynamic changes of synaptic ribbons. For this purpose, we generated recombinant GCAP2-EGFP expressing Semliki Forest (SLF) virus and used this recombinant virus for infecting retinal explants. EGFP-expressing SLF virus served as control virus. In organotypic retinal explant cultures the recombinant SLF viruses preferentially infected photoreceptors (Fig. 35A-D). Photoreceptors were infected at a high density with the SLF viruses (Fig. 35A,B) and showed expression of GCAP2-EGFP (Fig. 35C) or EGFP (Fig. 35D) throughout all photoreceptor cell compartments including the synaptic terminals (Fig. 35). Our organotypic cultures did no longer contain outer segments as also observed in other organotypic retinal cultures. Interestingly, photoreceptor terminals that were infected with GCAP2-EGFP virus typically displayed a loss of synaptic ribbons as analyzed by co-immunolabeling with RIBEYE antibodies (U2656) (Fig. 35E-L, Fig. 35R). Photoreceptor terminals infected with EGFP-virus (control virus) did not show loss of synaptic ribbons indicating that

the loss of synaptic ribbons in GCAP2-EGFP-infected photoreceptors is not due to a cytopathic effect of the virus infection itself (Fig. 35M-R).

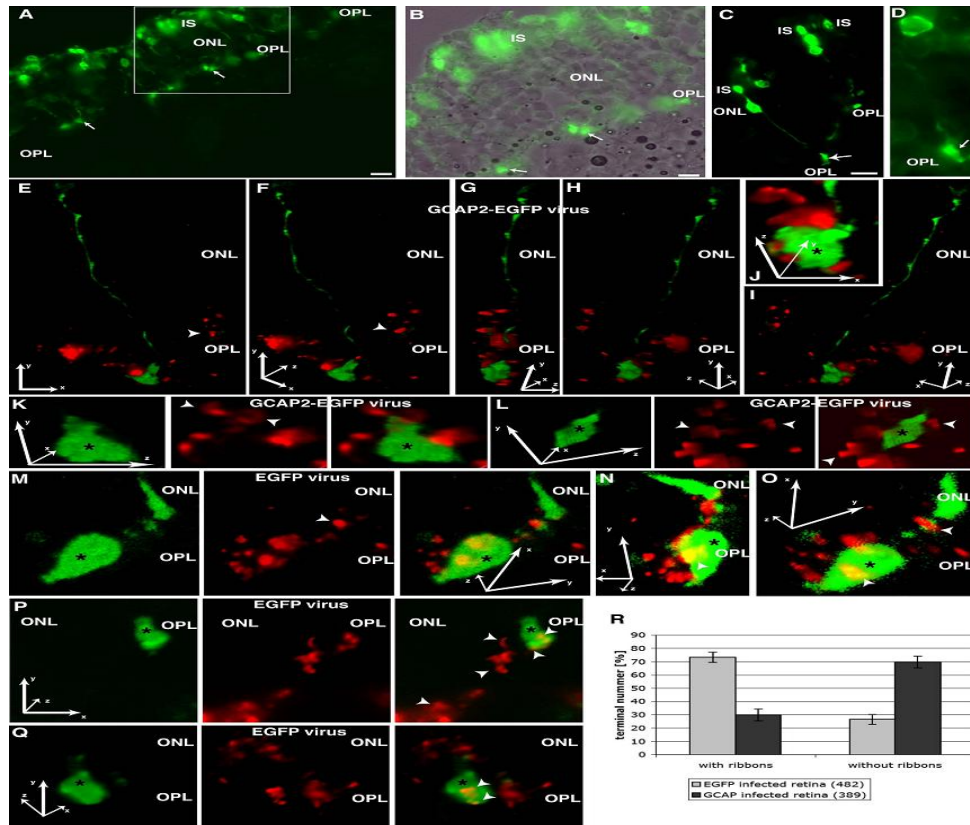


**Figure 35. Overexpression of GCAP in photoreceptor terminals disassembles synaptic ribbons**  
 Recombinant expression of either GCAP2-EGFP or EGFP in organotypic retina explant cultures (A-D). Simliki Forest (SLF) virus efficiently infects photoreceptors in organotypical explant cultures of the retina. SLF-mediated GCAP2-EGFP (A-C) heterologous expression labels the entire photoreceptor from the inner segments to the synaptic terminals (arrows) in the OPL. As generally observed by us and other groups, outer segments are absent from explant preparations. In analogy to GCAP2-EGFP expression also infection with EGFP-SLF virus leads to labelling of the entire photoreceptor (D) in retina explant culture. Scale bars in A-D represent 10µm. (E-Q) Three-dimensional reconstructions of individual optical stacks along the z-axis of SLF virus infected retina explant recorded with the apotome (Zeiss). (E-Q) In order to visualize synaptic ribbons in GCAP2-EGFP- and EGFP-infected retina explants, samples were immunolabeled with polyclonal RIBEYE antibody (U2656, red signals). Synaptic ribbons are abundantly present in the OPL of the organotypical retina cultures but absent from GCAP2-EGFP-expressing photoreceptor terminals (white arrows in E-I, asterisks in J-Q). (E-I) show lower magnifications of a three-dimensional reconstructed GCAP2-EGFP expressing photoreceptor from different angles to emphasise the lack of synaptic ribbons within the terminal (white arrows) without influencing the presence of synaptic ribbons (arrowhead in E) in the neighboring non-infected photoreceptors. The x,y and z labeled arrows indicate the coordinate axes in the three dimensions and are scaled to represent the distance of 5 µm in each spacial direction. (J-L) represent high magnifications of GCAP2-EGFP infected photoreceptor terminals. Although abundant ribbon labeling (red signals) can be detected next to the infected terminals (asterisks) no ribbon structures are present within the GCAP2 overexpressing terminals. (M-Q) Lack of ribbon structures within infected photoreceptor terminals is not due to viral infection as terminals overexpressing EGFP alone do contain ribbon structures (M-Q) visualized by the yellow color within the EGFP expressing synaptic terminals. (N) and (O) represent view of the same infected, EGFP-expressing terminal as in (M) but from different angles. (R) Statistical analysis of photoreceptor terminals infected with either EGFP-SLF virus or GCAP2-EGFP-SLF-virus. In contrast to EGFP overexpressing photoreceptor terminals 70% of synaptic terminals overexpressing GCAP2 lack synaptic ribbons. Error bars represent standard deviation, numbers in parenthesis indicate the number of counted terminals per construct. Abbreviations: OS, outer segments; IS, inner segments; ONL, outer nuclear layer; OPL, outer plexiform layer.

**Contributed by Karin Schwarz and Sivaraman Natarajan**

The same observation described above for the light microscopic analyses was also observed at the electron microscopic level using EM analyses of GCAP2-EGFP and EGFP (control)-infected retinas (Fig. 36). In GCAP2-EGFP-infected retinas we observed a dramatic reduction in the number of synaptic ribbons in comparison to EGFP-infected control retinas.

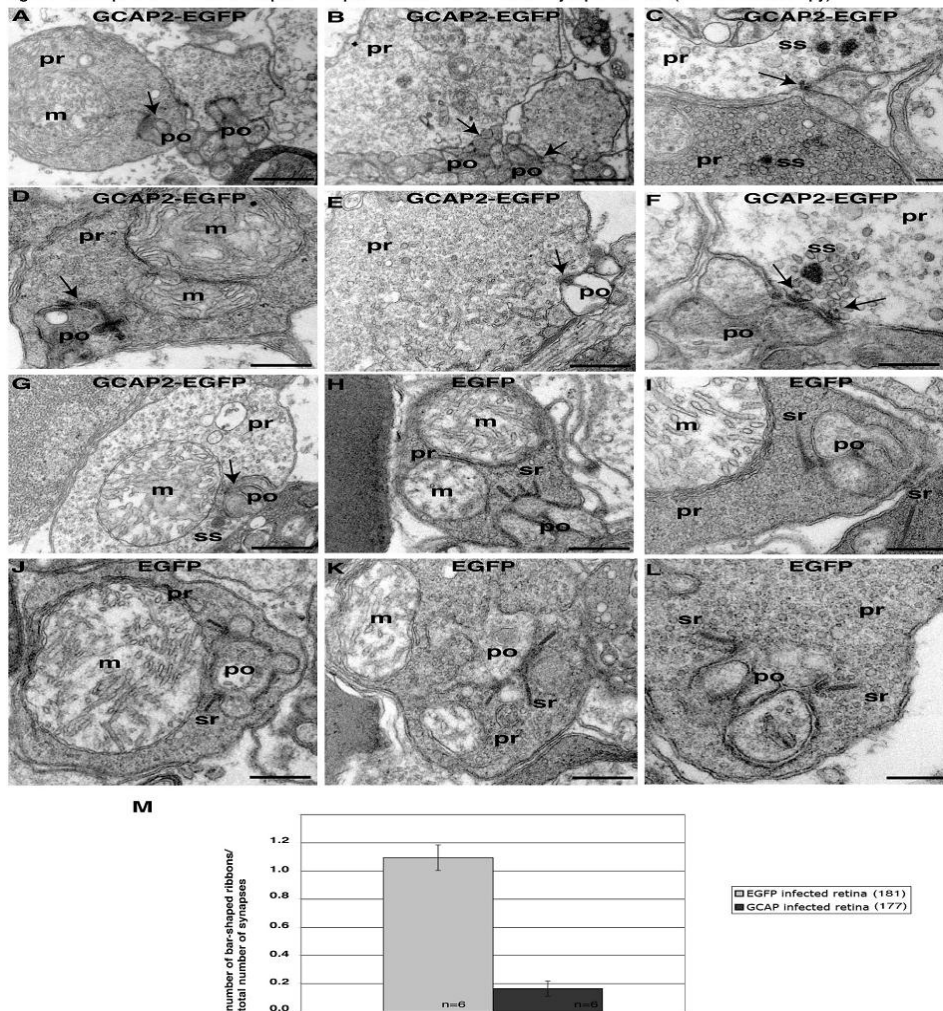


**Figure 36. Overexpression of GCAP2 in photoreceptor terminals disassembles synaptic ribbons: Electron microscopic analyses.** Recombinant expression of either GCAP2-EGFP (A-G) or EGFP in organotypic retina explant cultures (H-L), see also Fig. 35. Infection with GCAP-EGFP (A-G) leads to a loss of synaptic ribbons at the presynaptic active zones (labelled by arrows). In many cases, instead of bar-shaped anchored synaptic ribbons, floating, non-anchored spherical synaptic ribbons (ss) were observed which are considered as intermediate stages in the disassembly of synaptic ribbons. EGFP-transfected photoreceptors (control infections; H-L) displayed normally looking photoreceptor terminals with normal looking bar-shaped synaptic ribbons. **M:** semiquantitative evaluation: Approximately 180 randomly picked synapses were analyzed for the presence of bar-shaped synaptic ribbons (>150nm in length) at photoreceptor active zones (6 retinas for each construct). GCAP2-EGFP infected retinas show a dramatic reduction of bar-shaped synaptic ribbons in comparison to EGFP (control)-infected retinas. Abbreviations: pr, presynaptic terminal; po, postsynaptic dendrites; sr, synaptic ribbon; ss, spherical synaptic ribbon (synaptic sphere); m, mitochondrion. Scale bars: 1µm (A,B,D,E); 250nm (C), 500nm (F,G-L).

**Contributed by Karin Schwarz and Sivaraman Natarajan**

**CHAPTER 4**

---

**DISCUSSION**

GCAP2 is a photoreceptor-enriched neuronal  $\text{Ca}^{2+}$ -sensor protein. Its role as a  $\text{Ca}^{2+}$ -dependent modulator of the phototransduction cascade is well known (for review, see Palczewski et al., 2004). Previous studies have shown that GCAP2 is not restricted to photoreceptor outer and inner segments but also present in photoreceptor presynaptic terminals (Otto-Bruc et al., 1997; Duda et al., 2002, Pennesi et al., 2003; Makino et al., 2008). The function of GCAP2 in photoreceptor synapses is not known. The analyses of GCAP2 knockout mice suggested a synaptic function of GCAPs based on ERG analyses that showed a defect in the b-wave of the electroretinogram (Pennesi et al., 2003). But the mechanism how GCAPs might work in the synapse remained unclear. In the present study, we provide first evidence how GCAP2 works in the synapse. We showed with many different, independent approaches that RIBEYE, the major component of synaptic ribbons in the active zone of photoreceptor synapses, binds to GCAP2.

#### **4.1. RIBEYE-GCAP2 interaction requires structural rearrangements of RIBEYE(B)-domain**

The hinge 2 region of RIBEYE(B) is responsible for the interaction with the carboxyterminal region of GCAP2 as shown by YTH analyses. This suggestion is further supported by the analysis of point mutants of the hinge 2 region that completely abolished RIBEYE-GCAP2 interaction. Therefore, the hinge 2 region of RIBEYE(B) represents the core docking region for GCAP2. The hinge 2 region serves as a flexible linker and its conformation is dependent on NAD(H) binding as judged by structural analyses obtained for members of D-isomer-specific hydroxyacid dehydrogenase family to which also RIBEYE belongs (Lamzin et al., 1994; Goldberg et al., 1994, Kumar et al., 2002, Nardini et al., 2003; for review, see Popov and Lamzin, 1994, Chinnadurai, 2002). NAD(H) binding results in a significant change in the overall conformation of the entire protein. NAD(H)-binding induces movement of the SBD towards to the NBD via rotation around the hinge regions (Lamzin et al., 1994) resulting in closure of the NAD(H) binding cleft (“closed” conformation). Additionally, binding of NAD(H) results in the structural organization of the carboxyterminal region (CTR) (Lamzin et al., 1994). The NAD(H)-induced creation of a new  $\beta$ -helix that interacts with NADH stabilizes the “closed” conformation (Lamzin et al., 1994). This event was shown for formate dehydrogenase (Lamzin et al., 1994) from which structures exist in both the apo- and holo-state. Since

RIBEYE(B) belongs into the same protein family, it is reasonable to assume similar structural changes also in RIBEYE(B) in response to NAD(H) binding (Lamzin et al, 1994; Goldberg et al., 1994; Kumar et al., 2002; Nardini et al., 2003).

Thus, we suggest that binding of GCAP2 to the hinge 2 region of RIBEYE(B) requires the NAD(H)-induced, closed conformation of RIBEYE(B). This hypothesis can explain the NAD(H)-induced stimulation of GCAP2 binding and provides an explanation for the observed modulatory role of the SBD: As discussed above, formation of the NAD(H)-induced closed conformation requires considerable structural rearrangements in the SBD and movement of both SBDa and SBDb. The predicted disulfide bridge between C667 and C899 locks SBDa to the SBDb and restricts the movements of the two portions of the SBD relative to each other (Fig. 8E). Therefore, the observed capability of RIBEYE(B)C899S to bind GCAP2 in the absence of  $\beta$ -ME could be attributed to an enhanced conformational flexibility of the SBD. In the cysteine mutant RIBEYE(B)C899S a disulfide bridge can no longer be formed between cysteines C667 and C899. We propose that this enhanced structural flexibility of the SBD in RE(B)C899S favors a conformation of the flexible hinge 2 region that is able to bind GCAP2 similar to the NAD(H)-bound conformation. The incapability of the RIBEYE(B) mutants RIBEYE(B)F904W and RIBEYE(B) $\Delta$ CTR to bind to GCAP2 can be explained by a decreased capability of these mutants to stabilize the closed conformation. RIBEYE(B) $\Delta$ CTR lacks the hydrophobic carboxyterminal region (CTR) of RIBEYE(B) which undergoes enormous structural re-arrangements upon NADH binding (Lamzin et al., 1994; Nardini et al., 2003). RIBEYE(B)F904 is located at the beginning of the CTR in the SBD of RIBEYE(B) (Magupalli et al., 2008). The CTR has an important role in stabilizing the closed conformation in the D-isomer-specific 2-hydroxyacid dehydrogenase protein family (Lamzin et al., 1994). We suggest that the incapability of the RIBEYE(B) $\Delta$ CTR mutant and of the RIBEYE(B)F904W mutant to bind to GCAP2 is based on the insufficient stabilization of the closed conformation. We propose that these mutants destabilize a conformation of the hinge 2 region of RIBEYE(B) that is compatible with GCAP2 binding. Further investigations will be necessary to understand the complex regulation of GCAP2-RIBEYE interaction and how it is mediated by structural changes in the protein.

## **4.2. GCAP2, a candidate to mediate Ca<sup>2+</sup>- and illumination-dependent synaptic ribbon dynamics**

RIBEYE is a major component of synaptic ribbons (Schmitz et al., 2000; Zenisek et al., 2004; Wan et al. 2005, Magupalli et al., 2008) and therefore synaptic ribbons can probably bind considerable amounts of GCAP2. Such a Ca<sup>2+</sup>-sensing- and buffering protein placed in the active zone will shape Ca<sup>2+</sup>-dependent synaptic vesicle trafficking in ribbon synapses (von Gersdorff and Matthews, 1994; Neves and Lagnado, 1999; Beutner et al., 2001; Thoreson et al., 2004; Innocenti and Heidelberger, 2007). The binding of GCAP2 to RIBEYE is regulated by NAD(H) and provides the synaptic ribbon with a dynamically adjustable Ca<sup>2+</sup>-sensing and Ca<sup>2+</sup>-buffering system. The NAD(H)-dependent, dynamic RIBEYE-GCAP2 interaction explains why most, but not all, of the synaptic ribbons contain GCAP2 (Figs. 17,18,19). Since GCAP2 needs to be recruited to synaptic ribbons the physiological processes targeted by GCAP2 are likely not extremely fast. More likely, slower Ca<sup>2+</sup>-dependent processes will be affected. We propose that GCAP2 mediates the known Ca<sup>2+</sup>-dependent structural changes of synaptic ribbons during light- and darkness. A variety of studies have shown that synaptic ribbons (e.g. number and shape of synaptic ribbons) are important determinants of synaptic performance that adjust the synaptic machinery to transmit a broad range of stimulus intensities (Hull et al., 2006; Johnson et al., 2008; Meyer et al., 2009). The structure of synaptic ribbons is dynamically regulated. Spiwoks-Becker et al. (2004) demonstrated disassembly of synaptic ribbons in photoreceptor terminals during illumination when exocytosis is low. Illumination of photoreceptors also reduces the presynaptic Ca<sup>2+</sup> concentration in photoreceptor ribbon terminals (Jackman et al., 2009). Interestingly, the tendency of synaptic ribbons to disassemble during environmental illumination could be mimicked by removing (chelating) extracellular Ca<sup>2+</sup> indicating that Ca<sup>2+</sup> is an important mediator of synaptic ribbon dynamics and that Ca<sup>2+</sup> stabilizes the synaptic ribbon. GCAP2 could mediate these Ca<sup>2+</sup>-dependent effects by chelating Ca<sup>2+</sup> at the synaptic ribbon. Chelating Ca<sup>2+</sup> by GCAP2 which has been recruited to RIBEYE via a NAD(H)-dependent mechanism at the synaptic ribbon thus would result in a reduction in the number of synaptic ribbons. The hypothesis that GCAP2 is important for the stability of synaptic ribbons is supported by our finding that viral overexpression of GCAP2 in photoreceptors reduces the number of synaptic ribbons; GCAP2 overexpression in the synapse works similar on ribbon dynamics as chelating

Ca<sup>2+</sup>. Both procedures lead to a preferential disassembly of synaptic ribbons although the size of the responses is bigger in the virus-induced disassembly of synaptic ribbons. This is probably due to intracellular overexpression of the Ca<sup>2+</sup> chelating protein which can be expected to induce a stronger effect than the indirect manipulation of intracellular Ca<sup>2+</sup> through the chelation of extracellular Ca<sup>2+</sup>.

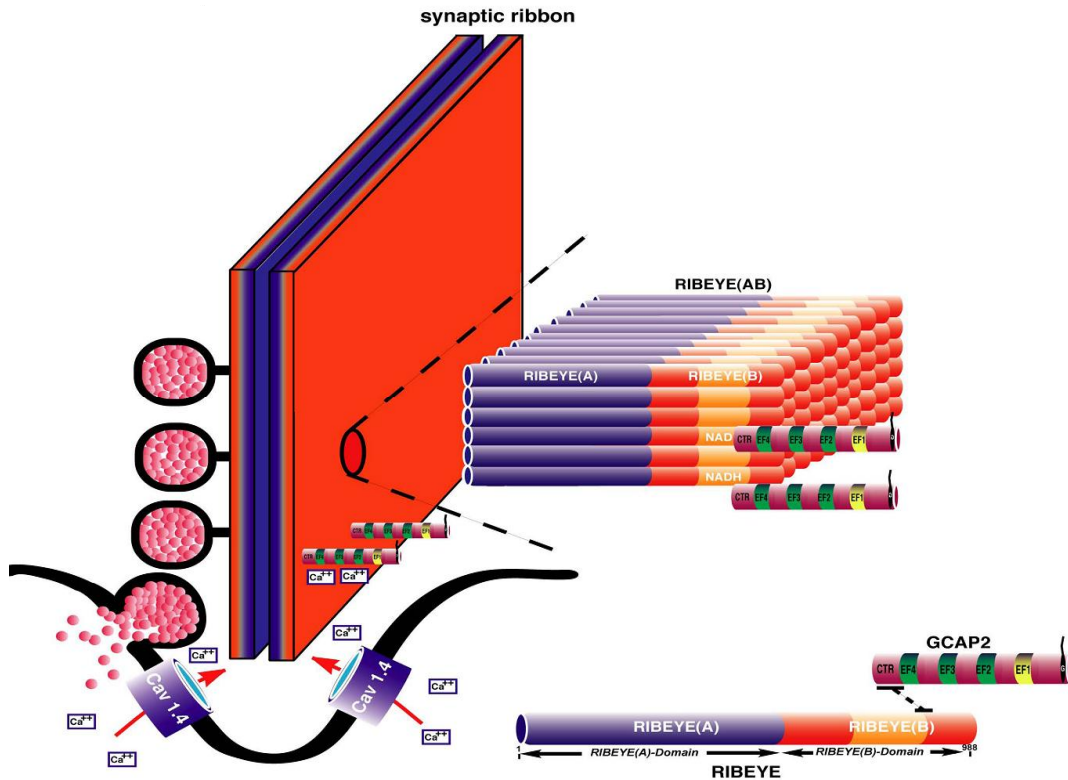


**Figure 37.** Schematic, simplified working model of RIBEYE-GCAP2 interaction in the photoreceptor ribbon synapse. The synaptic ribbon is anchored at the active zone of photoreceptor ribbon synapses and located close to L-type, voltage-gated presynaptic Ca<sup>2+</sup>-channels (Cav1.4). RIBEYE, a major component of synaptic ribbons, forms the scaffold of the synaptic ribbon via RIBEYE-RIBEYE interactions. RIBEYE consists of a unique A-domain with mainly structural functions and a B-domain that specifically binds NAD(H). Based on currently available data (Schmitz et al., 2000; Alpadi et al., 2008), the B-domain of RIBEYE probably points to the cytoplasmic face of synaptic ribbons. GCAP2 binds to RIBEYE(B) in a NAD(H)-dependent manner. We suggest that binding of NAD(H) to RIBEYE recruits GCAP2 to synaptic ribbons. The dynamic, NAD(H)-dependent nature of RIBEYE/GCAP2 interaction could explain why most, but not all, synaptic ribbons co-localize with GCAP2 (Fig. 26).

Photoreceptor terminals also contain guanylate cyclases (Liu et al., 1994, Cooper et al., 1995; Duda et al., 2002; Venkataraman et al., 2003) that might be targeted by GCAP2. The regulation of intracellular cGMP levels is important for various aspects of structural and functional plasticity of photoreceptor terminals (Spiwoxks Becker et al., 2004; Zhang et al., 2005). cGMP-gated Ca<sup>2+</sup>-channels have been reported in photoreceptor synapses which could be targeted by GCAP2-regulated cGMP levels to

adjust synaptic transmission (Rieke and Schwartz, 1994, Savchenko et al., 1997; Müller et al., 2003). Which synaptic mechanisms are targeted by RIBEYE-GCAP2 interaction, the characterization of GCAP2 effector proteins, how GCAP2- effector interaction is affected by intracellular  $\text{Ca}^{2+}$  concentrations and how the recruitment of NADH to RIBEYE is regulated remains to be elucidated by future analyses.

The selective association of GCAP2 with photoreceptor synaptic ribbons but not with bipolar cell synaptic ribbons can contribute to known physiological differences between different types of retinal ribbon synapses (e.g. Heidelberger et al., 1994; Thoreson et al. 2004; Sheng et al., 2007). We suggest that the disturbance of synaptic transmission in GCAP2 knockout mice (Pennesi et al. 2003) as measured by reduced b-waves in ERG analyses is due to a defect in synaptic transmission at photoreceptor ribbon synapses.

**CHAPTER 5**

---

**BIBLIOGRAPHY**

Alpadi K, Magupalli VG, Käppel, S, Köblitz, L, Seigel GM, Sung CH, Schmitz F (2008) RIBEYE recruits Munc119, a mammalian ortholog of the *Caenorhabditis elegans* protein unc119, to synaptic ribbons of photoreceptor synapses. *J Biol Chem* 283: 2641-26467.

Ames JB, Dizhoor AM, Ikura M, Palczewski K, Stryer L (1999) Three-dimensional structure of guanylyl cyclase activating protein-2, a calcium-sensitive modulator of photoreceptor guanylyl cyclases. *J Biol Chem* 274: 19329-19337.

Ashery U, Betz A, Xu T, Brose N, Rettig J (1999) An efficient method for the infection of adrenal chromaffin cells using the Semliki Forest virus gene expression system. *Eur J Cell Biol* 78: 525-532.

Berg JM, Tymoczko JL, Stryer L (2007) *Biochemistry*, Sixth Ed. (WH Freeman).

Beutner D, Voets T, Neher E, Moser T (2001) Calcium dependence of exocytosis and endocytosis at the cochlear inner hair cell afferent synapse. *Neuron* 29: 681-690.

Chinnadurai G (2002) CtBP, an unconventional transcriptional corepressor in development and oncogenesis. *Mol Cell* 9: 213-224.

Cooper N, Liu L, Yoshida A, Pozdnyakiv N, Margulis A, Sitaramaya A (1995) The bovine rod outer segment guanylate cyclase, ROS-GC, is present in both outer segments and synaptic layers of the retina. *J Mol Neurosci* 6: 211-222.

Cuenca N, Lopez S, Howes K, Kolb H (1998) The localization of guanylyl cyclase-activating proteins in the mammalian retina. *Invest Ophthalmol Vis Sci* 39, 1243-1250.

Duda T, Koch KW, Venkataraman V, Lange C, Beyermann M, Sharma RK (2002)  $Ca^{2+}$  sensor S100beta-modulated sites of membrane guanylate cyclase in the photoreceptor–bipolar synapse. *EMBO J* 21: 2547-2556.

Fischer F, Kneussel M, Tintrup H, Haverkamp S, Rauen T, Betz H, Wässle H (2000) Reduced synaptic clustering of GABA and glycine receptors in the retina of the gephyrin null mutant mouse. *J. Comp Neurol* 42: 634-648.

Fjeld CC, Birdsong WT, Goodman RH (2003) Differential binding of NAD<sup>+</sup> and NADH allows the transcriptional corepressor carboxyl-terminal binding protein to serve as a metabolic sensor. *Proc Natl Acad Sci USA* 100: 9202-9207.

Goldberg JD, Yoshida T, Brick P (1994) Crystal structure of a NAD-dependent D-glycerate dehydrogenase at 2.4Å resolution. *J Mol Biol* 236: 1123-1140.

Gustafsdottir SM, Schallmeiner E, Fredriksson S, Gullberg M, Söderberg O, Jarvius M, Jarvisu J, Howell M, Landegren U (2005) Proximity ligation assays for sensitive and specific protein analyses. *Anal, Biochem*: 345, 2-9.

Heidelberger R, Heinemann C, Neher E, Matthews G (1994) Calcium dependence of the rate of exocytosis in a synaptic terminal. *Nature* 371: 513-515.

Heidelberger R, Thoreson WB, Witkovsky P (2005) Synaptic transmission at retinal ribbon synapses. *Prog Ret Eye Res* 24: 682-720.

Hull C, Studholme K, Yazulla S, von Gersdorff H (2006) Diurnal changes in exocytosis and the number of synaptic ribbons at active zones of an ON-type bipolar cell terminal. *J. Neurophysiol* 96: 2025-2033.

Imanishi Y, Li N, Sokal I, Sowa ME, Lichtarge O, Wensel TG, Saperstein DA, Baehr W, Palczewski K (2002) Characterization of retinal guanylate cyclase-activating protein 3 (GCAP3) from zebrafish to man. *Eur J Neurosci* 15: 63-78.

Innocenti B, Heidelberger R (2007) Mechanisms contributing to tonic release at the cone photoreceptor ribbon synapse. *J Neurophysiol* 99: 25-36.

Jackman SL, Choi S-Y, Thoreson WB, Rabl K, Bartoletti TM, Kramer RH (2009) Role of the synaptic ribbon in transmitting the cone light response. *Nature Neurosci* 12: 303-310.

Johnson SL, Forge A, Knipper M, Münkner S, Marcotti W (2008) Tonotopic variation in the calcium dependence of neurotransmitter release and vesicle pool replenishment at mammalian auditory ribbon synapses. *J Neurosci* 28: 7670-7678.

Kachi S, Nishizawa Y, Olshevskaya E, Yamazaki A, Miyake Y, Wakabayashi T, Dizhoor AM, Usukura J (1999) Detailed localization of photoreceptor guanylate cyclase activating protein-1 and -2 in mammalian retinas using light and electron microscopy. *Exp Eye Res* 68: 465-473.

Koch K-W, Duda T, Sharma RK (2002) Photoreceptor specific guanylate cyclases in vertebrate phototransduction. *Mol Cell Biochem* 230: 97-106.

Kumar V, Carlson JE, Ohgi KA, Edwards TA, Rose DW, Escalante CR, Rosenfeld MG, Aggarwal AK (2002) Transcription corepressor CtBP is an NAD<sup>+</sup>-regulated dehydrogenase. *Mol Cell* 10: 857-869.

Lamzin VS, Dauter Z, Popov VO, Harutyunyan EH, Wilson KS (1994) High resolution structures of holo and apo formate dehydrogenase. *J Mol Biol* 236: 759-785.

Liu X, Seno K, Nishizawa Y, Hayashi F, Yamazaki A, Matsumoto H, Wakabayashi T, Usukura J (1994) Ultrastructural localization of retinal guanylate cyclase in human and monkey retinas. *Exp Eye Res* 59: 761-768.

Magupalli VG, Schwarz K, Alpadi K, Natarajan S, Seigel GM, Schmitz F (2008) Multiple RIBEYE-RIBEYE interactions create a dynamic scaffold for the formation of the synaptic ribbons. *J Neurosci* 28: 7954-7967.

Makino CL, Peshenko IV, Wen X-H, Olshevskaya EV, Barrett R, Dizhoor AM (2008) A role for GCAP2 in regulating the photoresponse: guanylyl cyclase activation and rod electrophysiology in GUCA1B knockout mice. *J Biol Chem* 283: 29135-29143.

Meyer AC, Frank T, Khimich D, Hoch G, Riedel D, Chapochnikow NM, Yarin YM, Harke B, Hell SW, Egnér A, Moser T (2009) Tuning of synapse number, structure and function in the cochlea. *Nature Neurosci* 4: 444-453.

Müller F, Schotten A, Ivanova E, Haverkamp S, Kremmer E, Kaupp UB (2003) HCN channels are expressed differentially in retinal bipolar cells and concentrated at synaptic terminals. *Eur J Neurosci* 17: 2084-2096.

Nardini M, Spano S, Cericola C, Pesce A, Massaro A, Millo E, Luini A, Corda D, Bolognesi M (2003) CtBP/BARS: a dual function protein involved in transcription co-repression and Golgi membrane fission. *EMBO J* 22: 3122-3130.

Neves G, Lagnado L (1999) The kinetics of exocytosis and endocytosis in the synaptic terminal of goldfish retinal bipolar cells. *J Physiol* 515: 181-202.

Otto-Bruc A, Fariss RN, Haeseleer F, Huang J, Buczylo J, Surgocheva I, Baehr W, Milam AH, Palczewski K (1997) Localization of guanylate cyclase-activating protein 2 in mammalian retina. *Proc Natl Acad Sci USA* 94: 4727-4732.

Olshevskaya EV, Hughes RE, Hurley JB, Dizhoor AM (1997) Calcium binding, but not a calcium-myristoyl switch, controls the ability of guanylyl cyclase-activating protein GCAP2 to regulate photoreceptor guanylyl cyclase. *J Biol Chem* 272: 14327-14333.

Palczewski K, Sokal I, Baehr W (2004) Guanylate cyclase-activating proteins: structure, function and diversity. *Biochem Biophys Res Comm* 7: 161-164.

Pennesi ME, Howes KA, Baehr W, Wu, SM (2003) Guanylate cyclase-activating protein (GCAP) 1 rescues cone recovery kinetics in GCAP1/GCAP2 knockout mice. *Proc Natl Acad Sci USA* 100: 6783-6788.

Pérez-León J, Frech MJ, Schröder JE, Fischer F, Kneussel M, Wässle H, Backus KH (2003) Spontaneous synaptic activity in an organotypic culture of the mouse retina. *Invest Ophthalmol Vis Sci* 44: 1376-1387.

Purves, D., Augustine, G.J., Fitzpatrick, D., Katz, L.C., La Mantia, A.S., McNamara, J.O and Williams, SM (2001). *Neuroscience*. Second edition.

Popov VO, Lamzin VS (1994) NAD<sup>+</sup>-dependent formate dehydrogenase. *Biochem J* 301: 625-643.

Rieke F, Schwartz EA (1994) A cGMP-gated current can control exocytosis in cone synapses. *Neuron* 13: 863-879.

Schmitz F, Bechmann M, Drenckhahn D (1996) Purification of synaptic ribbons, structural components of the photoreceptor active zone complex. *J Neurosci* 16: 7109-7116.

Schmitz F, Königstorfer A, Südhof TC (2000) RIBEYE, a component of synaptic ribbons. A proteins journey through evolution provides insight into synaptic ribbon function. *Neuron* 28: 857-872.

Schmitz F, Tabares L, Khimich D, Strenzke N, de la Villa-Polo P, Castellano-Munoz M, Bulankina A, Moser T, Fernandez-Chacon R, Südhof TC (2006) CSPalpha deficiency causes massive and rapid photoreceptor degeneration. *Proc Natl Acad Sci USA* 103: 2926-2931.

Schmitz F (2009) the Making of Synaptic Ribbons: How They Are Built and What They Do. *The Neuroscientist* 15(6): 611-624.

Schoch S, Mittelstaedt T, Kaeser P, Padgett D, Feldmann N, Chevaleyre V, Castillo PE, Hammer RE, Han W, Schmitz F, Lin W, Südhof TC (2006) Redundant functions of RIM1alpha and RIM2 alpha in Ca<sup>2+</sup>-triggered neurotransmitter release. *EMBO J* 25: 5852-5863.

Savchenko A, Barnes S, Kramer RH (1997) Cyclic-nucleotide-gated channels mediate synaptic feedback by nitric oxide. *Nature* 390: 694-698.

Sheng Z, Choi S, Dharia A, Li L, Sterling P, Kramer RH (2007) Synaptic Ca<sup>2+</sup> is lower in rods than cones, causing slower tonic release of vesicles. *J Neurosci* 27: 5033-5042.

Söderberg O, Gullberg M, Jarvis M, Ridderstrale K, Leuchowius KJ, Jarvius I, Wester K, Hydbrig P, Bahram F, Larsson L-G, Landegren U (2006) Direct observation of individual endogenous protein complexes in situ by proximity ligation. *Nature Methods* 3: 995-1000.

Söderberg O, Leuchowius K-J, Gullberg M, Jarvius M, Weibrecht I, Larsson L-G, Landegren (2008) Characterizing proteins and their interactions in cells and tissues using the in situ proximity ligation assay. *Methods* 45: 227-232.

Spiwoks-Becker I, Glas M, Lasarzik I, Vollrath L (2004) Mouse photoreceptor synaptic ribbons lose and regain material in response to illumination changes. *Eur J Neurosci* 19: 1559-1571.

Sterling P, Matthews G (2005) Structure and function of ribbon synapses. *Trends Neurosci* 28: 20-29.

Tachibana, M. (1999). Regulation of transmitter release from retinal bipolar cells. *Prog. Biophys. Mol.Biol.* 72, 109-133.

Thoreson WB, Rabl K, Townes-Anderson E, Heidelberger R (2004) A highly Ca<sup>2+</sup>-sensitive pool of vesicles contributes to linearity at the rod photoreceptor ribbon synapse. *Neuron* 42: 595-605.

tom Dieck S, Brandstätter JH (2006) Ribbon synapses of the retina. *Cell Tiss Res* 326: 339-346.

Venkataraman V, Duda T, Vardi N, Koch K-W, Sharma RK (2003) Calcium-modulated guanylate cyclase transduction machinery in the photoreceptor bipolar synaptic region. *Biochemistry* 42: 5640-5648.

Von Gersdorff H, Matthews G (1994) Inhibition of endocytosis by elevated internal calcium in a synaptic terminal. *Nature* 370: 652-655.

Wan L, Almers W, Chen W (2005) Two ribeye genes in teleosts: the role of ribeye in ribbon formation and bipolar cell development. *J Neurosci* 25: 941-949.

Zenisek D, Horst NK, Merrifield C, Sterling P, Matthews G (2004) Visualizing synaptic ribbons in the living Cell. *J Neurosci* 24: 9752-9759.

Zhang Q, Piston DW, Goodman RH (2002) Regulation of corepressor function by nuclear NADH. *Science* 295: 1895-1897.

Zhang M, Marshall B, Atherton SS (2008) Murine cytomegalovirus infection and apoptosis in organotypic retinal cultures. *Invest Ophthalmol Vis Sci* 49: 295-303.

Zhang N, Beuve A, Townes-Anderson E (2005) The nitric oxide – cGMP signaling pathway differentially regulates presynaptic structural plasticity in cone and rod cells. *J Neurosci* 25: 2761-2770

## LIST OF FIGURES

Figure 1.	Ribbon synapses of mammalian retina	18
Figure 2.	Electron Micrograph of a photoreceptor ribbon synapse	20
Figure 3.	3D representation of synaptic ribbons	22
Figure 4.	Schematic domain structure of RIBEYE	23
Figure 5.	Predicted RIBEYE(B) domain structure using homology modelling with CtBP1.	24
Figure 6.	Binding of NAD <sup>+</sup> to the B-Domain of RIBEYE/CtBP2	26
Figure 7.	The schematic drawing of GCAP2(aa1-204)	28
Figure 8.	Domain structure of Guanylate Cyclase and their interaction with GCAP Proteins.	30
Figure 9.	RIBEYE interacts with GCAP2 in the YTH system	76
Figure 10.	RIBEYE interacts with myristoylation-deficient full-length GCAP2	77
Figure 11.	Mutations of the carboxyterminal region(CTR) of GCAP2 abolish interaction with RIBEYE	78
Figure 12A.	Structure model of the B-domain of RIBEYE based on the crystal Structure of CtBP1.	78
Figure 12B.	GCAP2 not interact with the NBD and SBD of RIBEYE(B)	79
Figure 13A.	Structure model of the B-domain of RIBEYE	79
Figure 13B.	GCAP2 interacts with the hinge2 region of RIBEYE(B)	80
Figure 14A.	Structure model of RIBEYE(B)-domain in which the interface between NBD and SBD	81
Figure 14B.	Point mutants of the hinge2 region of RIBEYE(B) disrupt interaction with GCAP2	81
Figure 15.	The A-domain of RIBEYE does not prevent GCAP2/RIBEYE(B) interaction	82
Figure 16.	GCAP2 binds to monomeric RIBEYE(B)	83
Figure 17A.	RIBEYE(B) interacts with GCAP2 in protein pull-down analyses	84
Figure 17B.	RIBEYE(B) interacts with GCAP2 in protein pull-down analyses (Western blot)	84
Figure 18.	Expression of GST-GCAP2 fusion protein	85

Figure 19. Polyclonal GCAP2 antiserum cross-reacts with GCAP1	85
Figure 20. Detection of GCAP2 in bovine retina can be blocked by GCAP2-GST but not by GST preabsorbption.	86
Figure 21A. Schematic depiction of the domain structure of RIBEYE, GCAP2 and GCAP1	87
Figure 21B. RIBEYE interacts with GCAP2 but not with GCAP1	87
Figure 22. The monoclonal GCAP2 antibody is specific for GCAP2 and does not react with GCAP1	88
Figure 23. Co-immunoprecipitation of RIBEYE and GCAP2 from the bovine retina	89
Figure 24. GCAP2 is present on purified synaptic ribbons	90
Figure 25. GCAP2 co-localizes with synaptic ribbons in photoreceptor ribbon Synapses	91
Figure 26. GCAP2 is weekly expressed in cone photoreceptor ribbon synapses	93
Figure 27. Labeling of presynaptic GCAP2 immunosignals can be blocked by GCAP2-GST but not by GST preabsorption	94
Figure 28. Co-localization of RIBEYE and GCAP2 as analyzed by In-situ Proximity Ligation Assays(PLA)	96
Figure 29. Localization of cysteine residues in RIBEYE(B)	98
Figure 30. The binding of GCAP2 to the hinge2 region of RIBEYE(B) is modulated by the substrate-binding domain(SBD)	98
Figure 31. Mutations in SBD of RIBEYE influence the binding of GCAP2 to RIBEYE(B)	99
Figure 32. NADH and NAD <sup>+</sup> are essential co-factor for the binding between RIBEYE and GCAP2 in the absence of $\beta$ -mercaptoethanol	100
Figure 33. Low concentrations of NAD(H) promote RIBEYE/GCAP2 interaction	101
Figure 34. NAD(H) binding-deficient RIBEYE(B)G730A mutant	102
Figure 35. Overexpression of GCAP in photoreceptor terminals disassembles synaptic Ribbons	103
Figure 36. Overexpression of GCAP2 in photoreceptor terminals disassembles synaptic ribbons: Electron microscopic	104
Figure 37. Schematic, simplified working model of RIBEYE-GCAP2 interaction in the photoreceptor ribbon synapse	109

## List of abbreviations

µg	microgram
µl	microlitre
ΔHDL	Deletion of dimerisation loop
A	Adenine
A260 nm	Absorbance at 260 nm
A280 nm	Absorbance at 280 nm
aa	Amino acids
AD	Activation Domain
-ALWH	Drop out medium lacking Adenine, Leucine, Tryptophan and Histidine
Amp	Ampicillin
BARS	brefeldin A-ADP ribosylated substrate
bc	Bipolar cell
BD	Binding Domain
bp	base pair
BSA	Bovine serum albumin
C	Celsius
cDNA	complementary DNA
CtBP1	C-terminal Binding Protein 1
CtBP2	C-terminal Binding Protein 2
Cy2	Carbocyanin
Cy3	Indocarbocyanin
ddH <sub>2</sub> O	double distilled water
DEAE	dextran Diethylaminoethyl dextran
DMEM	Dulbecco's Modified Eagle's Medium
DNA	Deoxyribonucleic acid
dNTP	deoxyribonucleotides
DTT	Dithiothreitol
ECL	Enhanced chemiluminescence

<i>E. coli</i>	<i>Escherichia coli</i>
EGFP	Enhanced Green Fluorescent Protein
EDTA	Ethylenediaminetetrachloroacetic acid
EM	Electron microscopy
F1	Forward
For. Primer	Forward primer
Gal	Galactose
GCAP	Guanylate cyclase activating protein
GCL	Ganglion cell layer
GFP	Green Fluorescent Protein
GST	Glutathione S-transferase
H	Histidine
Hc	Horizontal cell
INL	Inner nuclear layer
IPTG	Isopropyl- $\beta$ -D-Thiogalactopyranoside
IPL	Inner plexiform layer
IS	Inner segments
Kb	Kilobases
kDa	kilo Dalton
-L	Yeast selection medium lacking Leucine
LB	Luria-Bertani medium
-LW	Yeast selection medium lacking Leucine and Tryptophan
MBP	Maltose binding protein
MCS	Multiple cloning site
min(s)	minute(s)
ml	millilitre
MW	Molecular weight
NAD <sup>+</sup>	oxidised Nicotinamide adenine dinucleotide
NADH	reduced Nicotinamide adenine dinucleotide
NBD	NADH binding sub-domain
ng	nanogram
nm	nanometer
NLS	Nuclear localization signal

OD	Optical density
OLM	Outer Limiting Membrane
ONL	Outer nuclear layer
ONPG	o-Nitrophenyl- $\beta$ -D-galactoside
OPL	Outer plexiform layer
OS	Outer segments
P	Primer
PBS	Phosphate Buffered Saline
PCR	Polymerase Chain Reaction
PFA	Paraformaldehyde
PMSF	Phenylmethanesulphonylfluoride
R, rev	Reverse
RE(A)	RIBEYE(A)-Domain
RE(B)	RIBEYE(B)-Domain
Rev. primer	Reverse primer
rpm	revolutions per minute
RT	Room temperature
RT-PCR	Reverse transcription-PCR
SBD	Substrate binding sub-domain
SD	Synthetic Drop out medium
SDS	Sodiumdodecylsulfate
SDS-PAGE	SDS Polyacrylamide gel electrophoresis
s.e.m	Standard error of mean
TAE	Tris Acetate EDTA
TE	Tris EDTA
Tris	Trishydroxymethylaminomethane
U	Unit
V	Volts
V/V	volume/volume
-W	Yeast selection medium lacking Tryptophan
X-Gal	5-Bromo-4-chloro-3-indolyl- $\beta$ -D-galactopyranoside
YPD	Yeast extract, peptone, and dextrose
YTH	Yeast two-hybrid

## Curriculum Vitae

### JAGADEESH KUMAR VENKATESAN

---

Graduate student,  
Department of Neuroanatomy,  
Institute for Anatomy and Cell Biology,  
Faculty of Medicine, Saarland University,  
Building, 61, Kirrberger Strasse,  
Homburg-66421, Saarland, Germany.  
Tel: 0049-17627587080  
E-mail: [jegadish.venki@gmail.com](mailto:jegadish.venki@gmail.com)

### Personal Details

---

First name: Jagadeesh Kumar  
Family name: Venkatesan  
Date of Birth: 24.07.1983  
Sex: Male  
Place of Birth: Kanchipuram, India  
Nationality: Indian

### Academic Education

---

Ph.D. Neuroscience (2006-present)  
University of Saarland, Germany

M.Sc. Biochemical Technology (2005)  
Madurai Kamaraj University, India First Class

B.Sc. Biochemistry (2003)  
University of Madras, India. First Class

### Research Experience

---

#### **Ph.D. thesis (Thesis submission expected in February, 2010)**

“Molecular and functional characterization of RIBEYE interaction with GCAP2 in photoreceptor ribbon synapse”

Advisor: **Prof. Dr. Frank Schmitz MD**, Department of Neuroanatomy, Institute for Anatomy and Cell Biology, Faculty of Medicine, Saarland University, Germany

#### **Master's degree thesis (2005)**

“Identification of sex specific molecular marker in molly *Poecilia sphenops*”  
Department of Immunology, School of Biological Science, Madurai Kamaraj University, India.

Advisor: **Prof. T.J.Pandian**, Head, Department of Genetics, Madurai Kamaraj University, Centre for Excellence in Genomics, School of Biological Science, Madurai Kamaraj University, India

## Publication:

---

1. NAD(H)-dependent binding of the neuronal Ca<sup>2+</sup> sensor protein GCAP2 to photoreceptor synaptic ribbons. Jagadeesh Kumar Venkatesan, Sivaraman Natarajan, Karin Schwarz, Sabine I. Mayer, Kannan Alpadi, Venkat Giri Magupalli, Ching-Hwa Sung and Frank Schmitz. **J Neuroscience (Accepted for publication, in press)**

## Technical expertise

---

- Recombinant DNA technology
- Recombinant protein expression and purification
- Site-directed Mutagenesis
- GST pull-down assay, Coimmunoprecipitation
- Yeast Two Hybrid Assays
- Cell culture and Transfection
- Immunocytochemistry
- Fluorescence Resonance Energy Transfer (FRET)
- Fluorescence microscopy
- Electron microscopy
- Generation of recombinant viruses

## References

---

Prof. Dr. Frank Schmitz MD  
Department of Neuroanatomy,  
Institute for Anatomy and Cell Biology,  
Faculty of Medicine,  
Saarland University,  
Homburg-66421, Saarland, Germany.  
Tel: +49-6841162 6012  
E-mail: frank.schmitz@uniklinik-saarland.de

Prof. Dr. G.S. Selvam  
Department of Biochemistry,  
Center for Excellence in Genomic Sciences,  
School of Biological Sciences,  
Madurai Kamaraj University, Madurai 625 021  
Phone: 0452-2458213/2458223  
Email: drselvamgsbiochem@yahoo.com